Modification of the SWAT Model to Simulate Hydrologic Processes in a Karst-influenced Watershed

by

Guido A. Yactayo Echegaray

Thesis submitted to the faculty of Virginia Polytechnic Institute and State University in partial fulfillment of the requirements for the degree of

Master of Science

In

Biological Systems Engineering

Mary Leigh Wolfe (Co-chair)

Conrad Heatwole (Co-chair)

Madeline Schreiber

August 12, 2009

Blacksburg, Virginia

Keywords: watershed modeling, SWAT, karst, sinkholes, sinking streams, nitrate

Modification of the SWAT Model to Simulate Hydrologic Processes in a Karst-influenced Watershed

Guido A. Yactayo Echegaray

Abstract

In the United States, karst ecosystems cover approximately 20 percent of the country and karst aquifers provide 40 percent of the water used for drinking. In karst-influenced watersheds, karst features such as sinkholes and sinking streams act as rapid pathways for carrying water and pollutants into streams and groundwater. Human activities on karst landscapes can present some special problems such as alterations to hydrologic regime, contamination of groundwater, ground subsidence, and damage to cave ecosystems. Modeling a karst-influenced watershed can provide a better understanding of the interactions between surface and ground water and how water quality is affected by human activities.

Several models were evaluated to determine their ability to model both discharge and nutrient transport in karst watersheds. The Soil Water Assessment Tool (SWAT) model was found to be appropriate due to its capability to represent almost all of the hydrological processes, its user-friendliness, and its ability to generate most of the parameters from available data. Moreover, SWAT can represent nitrogen transformations and transport processes and calculate nitrogen loadings, which is critical for karst watersheds. While SWAT has been widely used and found to be an appropriate prediction tool, it does not explicitly include the capacity to represent specific features characteristic of karst-influenced basins. Baffaut and Benson (2008) modified the SWAT 2005 code to simulate faster aquifer recharge in karst environments, and this version was further modified here in the SWAT-karst to represent karst environments at the HRU scale. A new parameter *sink* allows simulating the hydrology and nitrate transport in a sinkhole representing its unique landuse and soil characteristics, and a new parameter *ss* partitions nitrate transported with water that is lost from sinking streams.

The SWAT-karst model was used to simulate discharge and nitrogen loadings within the Opequon Creek karst-influenced watershed, located in the Potomac and Shenandoah River basin in Virginia and West Virginia. In the Opequon Creek watershed, SWAT-karst using the HRU to represent sinkholes had a more notable impact in the watershed hydrology than SWAT Baffaut and Benson (2008) version using a pond to represent sinkholes.

Results of statistical evaluation show that SWAT-karst and SWAT Baffaut and Benson (2008) version performed better than SWAT in predicting streamflow in a karst-influenced watershed. Although SWAT-karst showed almost the same performance as SWAT Baffaut and Benson (2008) version, SWAT-karst model offers the flexibility to represent the unique relationship between surface and ground water in karst features in an HRU.

Using an HRU to represent sinkholes can depict the associated variability of a karst landscape. The new variables *sink* and *ss* provide a mechanism to represent the nutrient transport through sinkholes and sinking streams. Sensitivity analysis showed that SWAT-karst was sensitive to the new parameter *sink* which can be used for model calibration and to represent water recharge and nutrient transport to aquifers outside the watershed boundary.

Dedication

Dedicated to my parents: Alberto and Gladys, and to my sister Lorena.

Acknowledgments

I would like to thank my committee members Drs. Wolfe, Heatwole, and Schreiber, and all the Biological Systems Engineering Staff that made my experience at Virginia Tech memorable.

TABLE OF CONTENTS

List of Figures

List of Tables

Chapter 1: Introduction

A karst landscape results from the weathering of bedrock types that are soluble in water and development of efficient underground drainage. Karst landscapes include features such as sinking streams, caves, sinkholes, and large springs. Springs and groundwater are important sources of water supply and they can be vulnerable to increased concentrations of pollutants associated with human activities. Karst topography is a fragile ecosystem that can provide rapid transport of contaminants without natural filtering.

Fissures in the ground in karst basins provide rapid infiltration of pollutants in streams and groundwater. Some of the pollutants include nutrients from manure and fertilizers, pathogens from manure, herbicides, insecticides, and sediment. Development activities on karst landscapes can present some special problems such as ground subsidence, contamination of groundwater, and damage to cave ecosystems. Furthermore, population growth in rural areas and cities leads to a growing demand on both surface and ground water resources.

According to the Karst Water Institute (2009), approximately 25% of the world's population either resides on or obtains water from aquifers in karst regions. In the United States, karst ecosystems cover approximately 20% the country and karst aquifers provide 40% of the water used for drinking. Modeling pollutant transport on a watershed scale can provide a better understanding of the interactions between surface and ground water and how water quality is affected by human activities to protect water resources and public health.

The Opequon Creek watershed is located in Virginia's Frederick and Clarke Counties and West Virginia's Berkeley and Jefferson Counties. It is a landscape dominated by karst terrain, and surface and ground water resources are closely related in this watershed. Groundwater is the major contributor to flow in many streams and rivers in the Opequon Creek watershed and has a strong influence on river and wetland habitats for plants and animals (USGS, 2008). Agriculture represents about 50% of the total area in this watershed, which is also an area of rapid population growth. Forest and farmland environments have been rapidly converted into new residential construction and other urban development areas.

1.1 Objectives

The overall goal of this research was to develop a watershed model that explicitly represents karst features and to simulate the hydrology and nitrogen transport in a karst basin. Specific objectives were to:

1. Determine the appropriateness of existing models for quantifying nitrogen concentrations in surface and ground water in karst-influenced watersheds;
2. Modify an existing model to simulate the hydrologic processes that drive nitrogen transport and to quantify nitrate concentrations in a karst basin accurately; and
3. Use the model to examine the major hydrologic contributor of nitrate (NO_3^-) to the stream in the Opequon Creek watershed.

Chapter 2: Literature Review

2.1 Karst environments

Karst aquifers are distinguished from aquifers in non-karstic rocks by the presence of conduits that act as rapid pathways for carrying water and pollutants from sinking streams and sinkholes to springs (Harmon and Wicks, 2006). Karst is associated primarily with limestone, but also forms in other carbonates and other soluble rocks (Waltham et al., 2005). Karst areas are fragile ecosystems and they are home to features such as sinking streams, caves, sinkholes, and large springs (Sasowsky and Wicks, 2000). Karst topography can allow rapid recharge of flow through fractures in rock, providing little opportunity for natural filtering to occur (USGS, 2002). Human activities on karst landscapes can present some environmental problems such as alterations to hydrologic regime, ground subsidence, contamination of groundwater, and damage to cave ecosystems.

2.2 Karst types

Karst landscapes are composed of a repetitive set of karst landforms and the dominant landform is usually used to describe the karst landscape (White 1988). Fluviokarst is a landscape that consists of springs, closed depressions, and caves, and occurs in areas where soluble and nonsoluble rocks appear in the same basin. Doline karst is a landscape karst type that is characterized by the existence of sinkholes. In the United States, most of the karst regions of the central and eastern areas of the country are fluviokarst with some limited areas of doline karst.

2.3 Hydrogeology in karst

In non-karstic regions, there is a clear distinction between surface and ground water, and between surface drainage basins and groundwater aquifers. Streams are fed by groundwater discharge and by overland flow from the land surface that slopes down into the channels. However, that concept cannot be applied in karst environments. In karstic regions, surface water

becomes groundwater when it sinks into the streambed and sinkholes and then karst groundwater becomes surface water when it emerges from springs (White, 1988).

In a karst landscape, surface water and groundwater flow function as one continuous unit and all water is circulating through the soil matrix, fissures and conduits (Weight, 2008). White (1988; 2002) describes two ways in which precipitation can recharge carbonate aquifers: allogenic recharge and autogenic recharge. Allogenic recharge refers to surface water that flows from non-karst areas of the basin to karst areas and enters carbonate aquifers through sinking streams. Streams sink into karst areas and become part of the subsurface drainage system (Q_a).

Autogenic recharge is divided into two components: diffuse infiltration and internal runoff. Diffuse infiltration (Q_d) is the rainfall distributed directly onto the karst surface, and from there enters the aquifer as infiltration through the soil and fractures. Internal runoff (Q_I) refers to the water that enters the subsurface through conduits. Internal runoff is overland flow captured by sinkholes. The change in water stored in the aquifer (ΔQ_S) can be positive or negative depending on whether the aquifer has a net gain or net loss during the time period considered.

Karst aquifers usually discharge groundwater back to the surface through springs (Q_B). Springs have a wide variety of physical forms and rates of discharge. Equation [1] defines a basic input-output budget for a fluviokarst basin:

$$\boldsymbol{Q_B = Q_a + Q_d + Q_I - \Delta Q_S} \qquad \textbf{[1]}$$

Where, $\boldsymbol{Q_B}$ is the spring discharge, $\boldsymbol{Q_a}$ are the losses from sinking streams**,** $\boldsymbol{Q_d}$ is diffuse infiltration **,**$\boldsymbol{Q_I}$ is internal runoff, and $\Delta\boldsymbol{Q_S}$ is the change in water stored in the aquifer.

2.4 Karst features

2.4.1 Sinkholes

Sinkholes are one of the most identifiable surface karst landforms. Sinkholes are circular or enclosed depressions and they differ in size. Sinkholes can be broad or barely noticeable, they can have a diameter from three to hundreds of meters, and depths can range from a few meters to several hundred of meters. Sinkholes can be identified using aerial photographs and topographic maps (Weight, 2008).

2.4.2 Sinking streams

Sinking streams are also called losing or disappearing streams. In sinking streams, at or near the contact of karst and non-karst rocks and sinkholes, water sinks through the streambed and/or along the stream bank through openings into the aquifer. Aquifer recharge from sinking streams is vital to the development of caves and springs in karst environments (Weight, 2008).

2.4.3 Springs

Springs are found in mature karst regions and they are the location where baseflow appears at the surface. Springs provide important quantities of water for human consumption and commercial enterprises. There are two types of springs: diffuse flow and conduit flow (Weight, 2008). Diffuse flow springs discharge from fractures and highly permeable areas and they are recharged by diffuse recharge. Diffuse flow springs have nearly constant chemical characteristics regardless of season and storm events and they are considered highly variable and baseflow can take months to travel short distances (Weight, 2008). Conduit flow springs are recharged by sinkholes. Springs discharge from conduits are known to be flashy. In conduit flow springs, baseflow can travel up to a 1.6 km per day (Weight, 2008).

2.5 Sources of nitrogen

Sources of groundwater contamination can be grouped into two major categories: naturally occurring and artificial (human-made). Almost every human activity has a potential to impact groundwater to some extent. Sources of nitrogen in groundwater are primarily derived from the biological activity of plants and microorganisms in the environment, from animal waste, and from many anthropogenic activities such as agriculture and animal feeding operations, sewage disposal, atmospheric deposition due to combustion of fossil fuels, and urban runoff (Kresic, 2007).

2.6 Nitrogen transformation and transport in karst

Excessive nitrogen from fertilizer applications in agriculture and from septic tanks leaches into the groundwater and consequently into the surface water impairing water bodies. Nitrogen pollution is a worldwide issue, with severe consequences such as the impairment of drinking water supply and eutrophication (Novotny, 2002). Karst features act as rapid pathways for transport pollutants.

Nitrogen occurs in groundwater as uncharged ammonia (NH_3), which is the most reduced inorganic form, nitrite and nitrate (NO_2^- and NO_3^-, respectively), in cationic form as ammonium (NH_4^+), and at intermediate oxidation states as a part of organic solutes (Kresic, 2007). Nitrogen can undergo numerous reactions that can lead to storage in the subsurface or conversion to gaseous forms that can remain in the soil for periods of minutes to many years. The main reactions include immobilization and mineralization, nitrification, denitrification, and plant uptake (Kresic, 2007).

Nitrite and organic forms are unstable in aerated water and easily oxidized, and they are considered indicators of pollution by sewage or organic waste. Ammonium is strongly adsorbed by mineral surfaces, and nitrate is easily transported by groundwater and stable over a considerable range of conditions (Kresic, 2007).

2.7 Watershed modeling

Mathematical modeling has become a primary tool for addressing questions about land use effects on hydrologic response and analyzing nonpoint source pollution and its spatial distribution. Watershed models can represent every phase of the water cycle and can calculate water and pollutant movement through a watershed via overland flow, through unsaturated and saturated soils, and flow down streams and rivers (Westervelt, 2001). The Soil Water Assessment Tool (SWAT) is a basin-scale, continuous-time model that operates on a daily time step and is designed to predict the impact of management on water, sediment, and agricultural chemical yields in watersheds (Neitsch et al., 2005). Major model components include weather, hydrology, soil temperature, plant growth, nutrients, pesticides, and land management (Gassman et al., 2007).

The ability of a model to accurately simulate field observations must be evaluated using quantitative methods. For watershed models such ad SWAT, the general model evaluation guidelines developed by Moriasi et al. (2007) are often used to judge model performance. Moriasi et al. (2007) described model evauation statistics such as the percent bias (PBIAS), the NSE, and RMSE-observations standard deviation ratio (RSR) to assess the model performance in watershed simulations (Table 1). The PBIAS statistic is a measurement of the average tendency of the simulated data to be larger or smaller than the observed data. The optimal value is zero and positive and negative values indicate underestimation and overestimation, respectively. The Nash-Sutcliffe efficiency (NSE) is a statistic that estimates the relative magnitude of the residual variance compared to the observed data variance. NSE optimal value is 1, and values lower than 0 indicate that the mean observed value is a better predictor than the simulated value. The RMSE is an error index statistic. The RSR standardizes RMSE using the observations standard deviation. RSR optimal value is zero and the lower the RSR the better the model simulation performance.

Spruill et al. (2000) evaluated the performance of the SWAT model for simulating daily and monthly discharge in small watersheds in the karst region of central Kentucky that are susceptible to lateral subsurface flow and deep groundwater flow, typical of karst topography.

Daily streamflow data from 1996 were used for the calibration and sensitivity analysis and data from 1995 were used for the validation. The sensitivity analysis showed that the model was sensitive to the drainage area in this particular watershed. The average absolute deviation between the observed and simulated streamflow was the lowest when the drainage area suggested from the dye trace studies was used, rather than the drainage area calculated using topographic data. Those analyses confirmed the results of previous dye trace studies of the surrounding sinkholes, indicating that a much larger area contributes to streamflow than the area defined by topographic boundaries. Result of model evaluation show that the Nash-Sutcliffe efficiency (NSE) coefficients for daily simulated streamflow for the calibration and validation phases indicate a poor correlation; they were 0.19 and -0.04, respectively. The NSE values for monthly simulated flow for the calibration and validation phases were 0.89 and 0.58, respectively.

Afinowicz et al. (2005) used SWAT to evaluate the influence of woody plants on water budgets of semiarid rangelands in karst terrain in Texas. The SWAT model was modified to calculate water that could recharge directly to the underlying confined aquifer instead of calculating baseflow using the total amount of water infiltrating through the soil. Calibration was performed using five years of streamflow data on a daily basis from January 1, 1992 to December 31, 1996. Validation was performed from January 1, 1997 to September 30, 2003. Unexpected NSE values for monthly simulated flow were 0.29 for calibration and 0.5 for validation phases. It was unexpected that the NSE value would be higher for the validation phase than for the calibration phase. The NSE values for daily simulated flow were 0.4 for the calibration and 0.09 for the validation phases.

Benham et al. (2006) reported that SWAT was used in a fecal coliform total maximum daily load (TMDL) study in a karst watershed in southwest Missouri. Daily NSE and correlation coefficients were lower than the calibration criteria; although the validation period, the calibration criteria were met. However, according to the authors, a visual comparison of the simulated and observed hydrographs indicated that the model was simulating the system satisfactorily, and one of the reasons why the SWAT model performance did not meet the criteria

is that the model did not adequately represent a very dry year combined with flows sustained by karst features.

The modular finite-difference groundwater flow model (MODFLOW) is a computer program that predicts three-dimensional groundwater flow in a porous media using a finite-difference method (Harbaugh et al, 2000). MODFLOW and similar models are commonly used for assessing and predicting groundwater flow in the United States. According to Palmer (2006), MODFLOW is the most popular and widely accepted model to simulate groundwater; however, it does not have a robust fit to karst. Bacchus (2006) found that MODFLOW is not appropriate to perform localized site-scale evaluations in karst environments because the cell size used to construct the groundwater model is too large to represent small features. Sasowsky and Wicks (2000) stated that MODFLOW has been adapted with varying levels of success for use in some karst scenarios, but did not provide detailed information. Galbiati et al. (2005) assessed surface and subsurface water quality and quantity as affected by anthropogenic activities in the Bonello watershed (Italy) using a linkage of SWAT and MODFLOW. The linkage of a groundwater and a surface hydrologic model provide the flexibility of exchanging a component of one model with an appropriate component from another model (Cho, 2007).
Bouraoui and Grizzetti (2007) presented a tiered approach for addressing nutrient fate at various scales in non-karst watersheds. The SWAT model was used in two large basins in France in a region that is one of the most intensive agricultural areas in the country, with two-thirds of the national livestock and half of the cereal production. The main objective of the modeling study was to identify the major processes and pathways controlling nutrient losses in those basins. It was shown that groundwater is the major contributor to total nitrate load in the streams and that mitigation measures should focus on primarily reducing nitrate leaching.

The Hydrological Simulation Program-FORTRAN (HSPF) is a set of computer codes that can simulate the nonpoint source pollutant loads, hydrology, and associated aggregate water quality, based on describing processes on pervious and impervious land surfaces, streams, and well-mixed impoundments (Bicknell et al., 1997). Tzoraki and Nikolaidis (2007) developed a karstic spring flow model that was used with the HSPF model to simulate the hydrology, sediment transport, and nutrient loads of a Greek river basin. They reported an NSE value of 0.86 for daily

flow. This study found that almost fifty percent of the flow came from the springs and that the concentration of nutrients had a seasonal variability in that region.

The general model evaluation guidelines developed by Moriasi et al. (2007) are used to judge model performance. Moriasi et al. (2007) described model evauation statistics such as the percent bias (PBIAS), the NSE, and RMSE-observations standard deviation ratio (RSR) to assess the model performance in watershed simulations (Table 1). The PBIAS statistic is a measurement of the average tendency of the simulated data to be larger or smaller than the observed data. The optimal value is zero and positive and negative values indicate underestimation and overestimation, respectively. The Nash-Sutcliffe efficiency (NSE) is a statistic that estimates the relative magnitude of the residual variance compared to the observed data variance. NSE optimal value is 1, and values lower than 0 indicate that the mean observed value is a better predictor than the simulated value. The RMSE is an error index statistic. The RSR standardizes RMSE using the observations standard deviation. RSR optimal value is zero and the lower the RSR the better the model simulation performance.

Table 1. General performance ratings for recommended statistics for a monthly time step (Moriasi et al., 2007).

Performance Rating	RMSE-observations standard deviation ratio (RSR)	Nash-Sutcliffe efficiency (NSE)	PBIAS (%)	
			Streamflow	N, P
Very good	0.00 ≤RSR≤0.50	0.75 <NSE≤1.0	PBIAS < ±10	PBIAS < ±25
Good	0.50 <RSR≤0.60	0.65 <NSE≤0.75	±10≤ PBIAS <±15	±25≤ PBIAS <±40
Satisfactory	0.60 <RSR≤0.70	0.50 <NSE≤0.65	±15≤ PBIAS <±25	±40≤ PBIAS <±70
Unsatisfactory	RSR>0.70	NSE≤0.50	PBIAS ≥±25	PBIAS ≥±70

Baffaut and Benson (2008) calibrated the SWAT model for the James River Basin, a karst basin in southwest Missouri. Sinking streams were simulated using high soil conductivities in channels, and sinkholes were represented using ponds. The code was modified to simulate faster percolation in karst environments. Five USGS flow gauges provided flow and water quality data for the calibration and validation periods from 1971 to 1980 and from 2001 to 2007,

respectively. Subbasin outlets were matched with the flow gauges. Nutrient loadings of septic tanks and wastewater treatment plants were considered in the model configuration. The general model evaluation guidelines developed by Moriasi et al. (2007) were used to judge model performance, and the calibration indicators were the PBIAS and the NSE (Table 1). During the calibration and validation periods, values of PBIAS for simulated flow were satisfactory for all of the flow gauges (PBIAS<25%), and the NSE values were satisfactory for three flow gauges (NSE≈0.5). The values of NSE for total phosphorous concentrations, total phosphorous loads, and coliform concentrations were unsatisfactory (NSE<0.3). According to the authors, routing of phosphorous and bacteria through the soil profile, groundwater, and the unconfined aquifer must be included in the model to obtain accurate water quality results.

Fleury et al. (2008) developed an empirical reservoir model to simulate the discharge of a karst aquifer through a spring and to estimate water volumes in the different parts of the aquifer. The study is located in Fontaine de Vaucluse, which is the largest karstic outlet in France with a mean flow rate over 20 m3/s. The model represented the rapid infiltration from sinkholes or open fractures (runoff), and the slow infiltration through the carbonate matrix (diffuse infiltration). Daily flow rates from 1995 to 1996 were used for the model calibration and the authors reported a Nash Sutcliffe value of 95.7%. Daily flow rates from 1996 to 2004 were used for the model validation, which resulted in a NSE value of 92.3%.

Chapter 3: Evaluation of existing hydrologic models to be used in karst-influenced watersheds.

Several existing models were evaluated to determine their appropriateness for use in a karst basin. Each model's appropriateness was determined based on whether the model includes the hydrology and nutrient transport components to represent karst features at a watershed scale. The evaluation determined if and how the models represent hydrologic processes such as surface and ground water flow, nutrient transport, and karst features such as allogenic recharge (sinking streams), internal runoff (sinkholes), and diffuse infiltration (Figure 1). Each model's components were reviewed using model manuals and journal publications.

3.1 Hydrologic components of existing models

The watershed-scale models evaluated were the Soil Water Assessment Tool (SWAT), the Hydrological Simulation Program-FORTRAN (HSPF), and the Generalized Watershed Loading Function (GWLF). The hydrologic processes included in the models, and the descriptions of the algorithms that the models use to simulate those processes are compiled in Tables 2 and 3, respectively. The SWAT and HSPF models are long-term, continuous simulation, watershed-scale models that have been used in karst watersheds to simulate flow and pollutant transport (Bicknell et al.,1992; Neitsch et al., 2005). In the last years, their performance has improved slightly due to model modifications and model linkages with other models (Spruill et al., 2000; Afinowicz et al., 2005; Benham et al., 2006; Tzoraki and Nikolaidis, 2007; Baffaut and Benson, 2008). The Generalized Watershed Loading Function (GWLF) model is used for the simulation of mixed landuse watersheds to assess the effect of land use practices on long term loadings of sediment and nutrients downstream (Haith, 2008). Even though GWLF has not been used in a karst basin, the model was selected for the comparison. Groundwater models such as MODFLOW are commonly used in the United States to simulate groundwater flow, and according to Sasowsky and Wicks (2000), MODFLOW has been adapted with varying success for use in karst environments.

Simulation of runoff and infiltration processes differ among the watershed models (table 2). The main differences in the infiltration and surface runoff algorithms among the watershed models

are the empirical Curve Number (CN) and Green & Ampt or physical (Philip's methods) methods used and the simulation time step. Green & Ampt and Philip's (SWAT and HSPF, respectively) methods require sub-daily inputs, which are more complex than the daily data needed for the CN method (SWAT and GWLF). Inclusion and simulation of subsurface components (such as interflow, unconfined aquifer, and confined aquifer) differ among the selected watershed models. HSPF uses a set of relationships that includes infiltration characteristics to calculate interflow and SWAT uses a kinematic approach (tables 2 and 3). HSPF simulates water flux from the unconfined aquifer storage to baseflow and to the confined aquifer. SWAT also accounts for multiple fluxes of water from the unconfined aquifer, including groundwater to streams, evapotranspiration in the capillary fringe, deep percolation, and pumping activities.

SWAT and HSPF simulate stream routing (Bicknell et al.,1992; Neitsch et al., 2005), whereas GWLF calculates streamflow by summing the total watershed runoff from all source areas plus groundwater discharge from the unconfined aquifer (Haith et al., 1992). SWAT is the only model that can simulate stream transmission losses; this component was used by Baffaut and Benson (2008) to represent sinking streams. Finally, the three models do not include the components to simulate sinkholes and springs.

The USGS finite difference model MODFLOW simulates groundwater in a three-dimensional environment and aquifer systems in which saturated flow conditions and Darcy's law apply (Harbaugh et al, 2000). Processes such as water routing in the stream is simulated using the SFR1 package, and, according to USGS (1997), the model also can represent springs.

Table 2. Hydrologic processes included in the four models.

Hydrologic component	HSPF	MODFLOW	SWAT	GWLF
Runoff	✓		✓	✓
Infiltration	✓		✓	✓
Percolation	✓		✓	✓
Interflow/ lateral flow	✓		✓	
Groundwater	✓	✓	✓	✓
Unconfined aquifer/ Confined aquifer	✓	✓	✓	✓
Water routing in stream	✓	✓	✓	✓
Channel transmission losses (sinking streams)			✓	
Sinkholes				
Springs		✓		

Table 3. Model algorithms used to represent hydrologic processes.

Hydrologic component	HSPF	MODFLOW	SWAT	GWLF
Runoff	*Subroutine PROUTE* The model uses the Chezy-Manning equation to determine surface runoff. *Output*: SURO = surface outflow (in/interval)		Empirical methods: 1. SCS curve number (SCS, 1972) *Output:* Daily runoff (mm) 2. The Green & Ampt infiltration method (1911) *Output:* Cumulative infiltration for a given time step (mm). The water that does not infiltrate into the soil becomes surface runoff.	Rural and urban runoff is calculated using SCS curve number (Ogrosky and Mockus, 1964) *Output:* runoff from source area for a day (cm)
Infiltration	*Subroutine SURFAC* Infiltration is computed using Philip's equation (1957). Physically based algorithm separates moisture inputs into infiltrating and non infiltrating fractions *Output:* mean infiltration capacity over the land segment (in/interval)		Water balance equation. $SW_t = SW_0 + \sum(R_{day} - Q_{surf} - E_a - W_{seep} - Q_{gw})$ Where, SW_0 is the initial soil water content (mm), *Rday* is the precipitation (mm), *Qsurf* is the surface runoff (mm), *Ea* is the evapotranspiration (mm), *Wseep* is water entering the vadose zone from the soil profile (mm), and *Qgw* is baseflow (mm). *Output:* Soil water content (mm).	Infiltration equals the excess, if any, of rainfall and snowmelt less runoff and evapotranspiration. *Output:* infiltration (cm)
Percolation	*Subroutine UZONE*		Percolation occurs if the soil	Percolation occurs when

	Percolation occurs when the upper zone moisture ratio is bigger than the lower zone moisture ratio, and it is calculated using an empirical equation. *Output:* percolation from the upper zone (in/interval)		water content exceeds the field capacity. Percolation is calculated using storage routing methodology. $W_{perc} = SW_{excess}[1-exp[-\Delta t/TT_{perc}]]$ *Output:* water percolating to the underlying soil layer on a day (mm).	unsaturated zone water exceeds field capacity. $PC_t = Max\ (0;U_t+R_t+M_t-Q_t-E_t-U)$ *Output:* Percolation (cm)
Interflow/ lateral flow	*Subroutine INTFLW* The amount of interflow and storage updating is calculated assuming a set of relationships that includes infiltration characteristics. *Output:* interflow outflow (in/interval)		Kinematic storage model for subsurface flow (Sloan and Moore, 1984). This model simulates subsurface flow in a two-dimensional cross-section along a flow path down a steep hillslope. $Q_{lat} = 0.024 \times \frac{2 \times SW \times K \times slp}{\theta \times L}$ *Output:* water discharged from the hillslope outlet (mm/day).	
Groundwater	*Subroutine GWATER* The model assumes that the discharge of an aquifer is proportional to the product of the cross-sectional area and the energy gradient of the flow. Active groundwater outflow is calculated using: *AGWO=KGW*(1+KVARY*GWVS)*AGWS* *Output:* active groundwater outflow (in/interval)	MODFLOW simulates groundwater flow in the aquifer using a finite difference method, and divides the aquifer into rectangular cells by a grid. The model calculates groundwater levels at every cell at a time step.	Groundwater flow into the main channel is allowed to enter the reach only if the amount of water stored in the shallow aquifer exceeds a threshold value specified by the user. Groundwater is calculated using: $Q_{gw}=Q_{gw-i}*exp[-\alpha_{gw}*\Delta t]+W_{rchrg}(1-exp[-\alpha_{gw}*\Delta t])$ *Output:* groundwater flow into the main channel (mm)	Groundwater discharge is calculated by a lumped parameter model. $G_t = r*S_t$ *Output:* Groundwater discharge (cm)

Unconfined aquifer/ Confined aquifer	*Subroutine GWATER* Inflow to the aquifer is calculated summing the amount of infiltration and percolation. The amount of water in the active (unconfined aquifer) and inactive groundwater (confined aquifer) is specified by the user by the parameter DEEPFR. DEEPFR is the fraction of the groundwater inflow which goes to the confined aquifer.		The amount of water stored in the unconfined aquifer is calculated using: $aq_{sh}=aq_{sh-i}+W_{rchrg}-Q_{gw}-W_{revap}-W_{pump}$ *Output:* amount of water stored in the shallow aquifer on day (mm) The amount of water that percolates to the confined aquifer is calculated with the following equation: $W_{deep}=\beta_{deep} * W_{rchrg}$ *Output:* amount of water stored in the unconfined aquifer on day (mm)	Unsaturated and unconfined aquifer daily water balance are calculated using: $U_{t+1} = U_t+R_t+M_t-Q_t-E_t-PC_t$ $S_{t+1} = S_t+PC_t- G_t- D_t$ Seepage to the confined aquifer is calculated with the following equation: $D_t = s\ S_t$ *Output:*Unsaturated and unconfined aquifer moisture at the beginning of the day (cm)
Water routing in stream	*Subroutine ROUTE* This subroutine calculates rates and volumes of outflows using hydraulic routing. *(VOL - V1)/(ROD - ROD1) = (V2 - V1)/(ROD2 - ROD1)* S*ubroutine NOROUT* This subroutine calculates rates and volumes of outflows without using hydraulic routing; and outflow is a function of time only.	*SFR1 PACKAGE* MODFLOW SFR1 package routes streamflow through rivers, streams, canals, and ditches. Streamflow is always in the same direction along the channels, and is constant for each time step used in the ground-water flow model. Calculations are based on the continuity equation and assumption of piecewise steady (nonchanging in discrete time periods), uniform (nonchanging in location), and constant-	1. Variable storage routing method *qout=SC[qin+Vstored/Δt]* *Output:*Outflow rate at the end of the time step (m^3/s) $V_{out}=SC(V_{in}+V_{stored})$ *Output:* Volume of outflow during the time step (m^3). 2. Muskingum river routing method $q_{out=C_1*}\ q_{in2+}\ _{C_2*}\ q_{in1+}\ _{C_3*}q_{out1}$	Streamflow is calculated by summing the total watershed runoff from all source areas plus groundwater discharge from the unconfined aquifer.

		density streamflow.	$V_{out=C1*} V_{in2+} C_{2*} V_{in1+} C_{3*} V_{out1}$	
Channel transmission losses (sinking streams)			During periods when a stream receives no groundwater contributions, SWAT calculates water that is lost from the channel via transmission through the side and bottom of the channel. $t_{loss}=k_{ch}*TT*P_{ch}*L_{ch}$ *Output:* channel transmission losses (m3)	
Sinkholes				
Springs				

3.2 Nitrogen transformations and transport

The same group of models was evaluated to determine their appropriateness to represent nitrogen transformations and nitrate transport in a karst basin. The nitrogen transformations and nitrate transport components included in the models and the description of the algorithms that the models use to simulate those components are compiled in Tables 4 and 5, respectively.

Only SWAT and HSPF simulate nitrogen transformations in the soil profile. They simulate nitrogen transformations such as immobilization, mineralization, nitrification, denitrification, plant uptake, and nitrogen fixation (Bicknell et al., 2007; Neitsch et al., 2005). All of the models evaluated simulate the amount of nitrate transported with runoff and groundwater from land areas into streams. Only SWAT and HSPF simulate nitrate loadings from lateral flow and percolation. HSPF calculates the amount of nitrate transported with all the hydrologic components using a fraction parameter (Bicknell et al., 2007), while SWAT uses a loading function, except when it calculates the amount of nitrate transported with groundwater. SWAT calculates the amount of nitrate in the aquifer recharge using an exponential decay function, and then the model calculates the amount of nitrate transported with groundwater as a function of the amount of nitrate present in the aquifer (Neitsch et al., 2005). GWLF calculates the groundwater nitrate load using loading functions (Haith et al., 1992). The MT3D model was developed for use in any finite difference flow model such as MODFLOW. MT3D is a transport model that simulates advection, dispersion, and chemical reactions of contaminants in groundwater (Zheng and Wang, 1999).

SWAT and HSPF simulate the increase and decrease in the amount of nitrate in the stream due to the oxidation of nitrite and by the uptake of nitrate by algae, respectively. However, the manuals (Bicknell et al., 2007; Neitsch et al., 2005) do not specify how the models calculate the amount of nitrate in the stream. GWLF calculates the amount of nutrients in the stream summing point source, runoff, groundwater, and septic system dissolved nutrient loads.

Table 4. Nitrogen transformations and nitrate transport components included in the models.

Nitrogen components	HSPF	MODFLOW	SWAT	GWLF
Immobilization and mineralization	✓		✓	
Nitrification	✓		✓	
Denitrification	✓		✓	
Plant uptake	✓		✓	
Nitrogen fixation	✓		✓	
NO_3^- in runoff	✓		✓	✓
NO_3^- in lateral flow	✓		✓	
NO_3^- in percolation	✓		✓	
NO_3^- in groundwater	✓	✓	✓	✓
NO_3^- in the stream	✓		✓	✓
NO_3^- in the channel transmission losses				

Table 5. Model algorithms used to represent nitrogen transformations and nitrate transport.

Nitrogen components	HSPF	MODFLOW	SWAT	GWLF
Immobilization and mineralization	*Subroutine NITRXN* The model simulates immobilization, converting nitrate and ammonia to organic N, and mineralization converting organic N to ammonia. Two methods are available to simulate immobilization: 1. first-order kinetics 2. Michaelis-Menten - saturation kinetics method		A general relationship between C:N ratio and mineralization /immobilization is used to determine if mineralization occurs. • C:N > 30:1 immobilization occurs, a net decrease in soil NH_4^+ and NH_3 • C:N < 20:1 mineralization occurs, a net gain in soil NH_4^+ and NH_3. The algorithms were adapted from the PAPRAN mineralization model (Seligman and van Keulen, 1981), and two sources are considered: 1. *Humus mineralization* $N = \beta_{min} (\gamma_{tmp} * \gamma_{sw})^{1/2} * orgN_{act}$ *Output: nitrogen mineralized from the humus active organic N pool (kg N/ha)* 2. *Residue mineralization* Mineralization is controlled by a decay rate constant that is updated daily. The decay rate constant is calculated as a function of the C:N ratio. $N = 0.8 * \delta_{ntr} * orgN_{frsh}$ *Output:* nitrogen mineralized from the fresh organic N pool (kg N/ha)	

Nitrification	*Subroutine NITRIF* The model simulates oxidation of nitrate and ammonium by bacteria (nitrobacter). The model uses a first order equation where nitrification is directly proportional to the quantity of nitrate or ammonium. *Output:* amount of NH_3 oxidation (mg N/L)		Nitrification is simulated using a combination of the methods developed by Reddy et al. (1979) and Godwin et al. (1984). Nitrogen removed from the ammonium pool by nitrification is calculated using: $N = \frac{frn}{frn + frv} N_{nitvol}$ *Output:* the amount of nitrogen converted from NH_4^+ to NO_3 in layer (kg N/ha)	
Volatilization	*subroutine NH3VOL* The amount of total ammonia lost due to volatilization is calculated by a model of mass transfer based on Henry's Law. *Output:* Volatilization loss during the interval (mg N/L)		Volatilization is simulated using a combination of the methods developed by Reddy et al. (1979) and Godwin et al. (1984). The nitrogen removed from the ammonium pool by volatilization is calculated using: $N = \frac{frv}{frn + frv} N_{nitvol}$ *Output:* the amount of nitrogen converted from NH_4^+ to NH_3 in layer (kg N/ha).	

Denitrification	*Subroutine DENIT* The model simulates the reduction of nitrate by anaerobic bacteria. The process occurs if the amount of dissolved oxygen concentration is below the concentration specified by the user. The model uses a first-order equation and is a function of nitrate concentration. *Output:* Amount of NO_3 denitrified (mg N/L per interval)		Denitrification is a function of water content, temperature, presence of a carbon source, and nitrate. $N_{denit}=NO_3(1-\exp[-\beta_{denit}*\gamma_{tmp}*orgC])$ *Output:* the amount of nitrogen lost to denitrification (kg N/ha)	
Plant uptake	*Subroutine NITRXN* There are three methods: 1. The default method is a first-order equation. This method is sensitive to soil nutrient levels and nutrient application rates. 2. The second method uses a yield base algorithm. This method is less sensitive to soil nutrient levels and nutrient application rates. The third method uses Michaelis-Menten equation or saturation kinetics method. It is primarily used to simulate forest areas.*Output:* Plant uptake target for current crop (lb N/ac or kg N/ha)		Plant nitrogen uptake is controlled by the plant nitrogen equation. The depth distribution of nitrogen uptake is calculated with the function: $Nup = \frac{N}{[1-\exp(-\beta)][1-\exp(-\beta+root)]}$ *Output:* the potential nitrogen uptake from the soil surface to depth *z* (kg N/ha)	

Nitrogen fixation	*Subroutine NITRXN* Fixation occurs if the available soil nitrate and ammonium is insufficient to satisfy the plant uptake.		Nitrogen fixation is calculated as a function of soil water, soil nitrate content and growth stage of the plant. $N_{fix} = N_{demand} * f_{gr} * min(f_{sw}, f_{NO3}, 1)$ *Output:* the amount of nitrogen added to the plant biomass by fixation (kg N/ha)	
NO_3^- in runoff	*Subroutine PEST* Nutrient is simulated in the soil and runoff in three forms: dissolved, adsorbed, and crystallized. Nutrients are taken from their respective surface layer storages in proportion to the fraction of the surface soil layer removed by overland flow.		To calculate the amount of nitrate moved with the water, the concentration of nitrate in the mobile water is calculated. $concNO_3 = \frac{NO_3\left(1-\exp\left[\frac{-W_{mobile}}{(1-\theta)SAT}\right]\right)}{W_{mobile}}$ This concentration is then multiplied by the volume of surface runoff to obtain the mass of nitrate lost from the soil layer. $NO_{3surf} = \beta_{NO3} * conc_{NO3} * Q_{surf}$ *Output:* Nitrate removed in surface runoff (kg N/ha)	Rural nutrient loads are transported by runoff water and eroded soil. Rural nutrient loads are calculated by using loading functions, multiplying runoff by the nutrient concentrations from the source area. $LDm = 0.1\sum_{k}\sum_{t=1}^{dm} Cd_k Q_{kt} AR_k$ Runoff nutrient loads from urban areas are calculated using an exponential accumulation and wash off function. $W_{kt} = W[N_{kt} * e^{-0.12} + (n_k/0.12)(1-e^{-0.12})]$
NO_3^- in lateral flow	*Subroutine TOPMOV* Calculation of the fluxes and change in storage in the unsaturated zone is simulated by the subroutine TOPMOV using a fraction parameter.		$NO_{3lat} = \beta_{NO3} * conc_{NO3} * Q_{lat}$ *Output:* nitrate removed in lateral flow from a layer (kg N/ha)	

NO_3^- in percolation	*Subroutine TOPMOV* Calculation of the fluxes and change in storage in the unsaturated zone is simulated by the subroutine TOPMOV using a fraction parameter.		$NO_{3perc} = conc_{NO3} * W_{perc}$ *Output:* nitrate moved to the underlying layer by percolation (kg N/ha)	
NO_3^- in groundwater	*Subroutine SUBMOV* This subroutine calculates the fluxes and change in storage in the saturated zone and unconfined aquifer using a fraction parameter.	*MT3DMS PACKAGE* *MT3DMS* is a three-dimensional transport model for simulation of advection–dispersion and chemical reaction of contaminants in the groundwater. Eulerian–lagrangian equation or the finite difference methods are used to calculate nutrients reaching the channels through groundwater flow.	• Nitrate in water recharge to both unconfined and confined aquifers is calculated using an exponential decay weighting function proposed by Venetis (1969) $NO_{3\ rchrg} = (1 - exp[-1/\delta_{gw}] * NO3_{perc} + exp[-1/\delta_{gw}] * NO_{3rchg\ i}$ *Output:* amount of nitrate in recharge entering the aquifers (kg N/ha). • Nitrate in the unconfined aquifer may remain in the aquifer, move with recharge to the confined aquifer, or move with groundwater flow into the main channel. $NO_{3gw} = (NO_{3sh} + NO_{3rchrg}) Q_{gw} / (aq_{sh} + Q_{gw} + W_{revap} + W_{rchrg})$ *Output:* nitrate in groundwater flow from the unconfined aquifer (kg N/ha).	Monthly groundwater nutrient load to the stream is calculated using: $$DGm = 0.1 \times C_g \times AT \sum_{t=1}^{dm} Gt$$

NO_3^- in the stream	*Subroutine NUTRX* NO_3 and NH_3 from upstream reaches, tributary land areas, and atmospheric deposition (deposition of NO2 is not considered) is summed *Output:* total input of dissolved nutrient to reach The *subroutine ADVECT* calculates the total outflow of nitrate over the time interval.		SWAT calculates the amount of nutrient entering the main channel summing the runoff, lateral flow and groundwater nitrate loadings. Then the amount of nitrogen entering the stream may be increased by the oxidation of nitrite or decreased by the uptake of nitrate by algae.	Stream flow contains dissolved nutrients associated with runoff, point sources and groundwater, and solid-phase nutrients associated with point sources, rural soil erosion and wash off material from urban areas. Monthly loads of dissolved nutrient in streamflow is calculated using: $LD_m = DP_m + DR_m + DG_m + DS_m$
NO_3^- in the channel transmission losses				

It is important to assess the impact of human activities in karst regions. Activities such as water consumption, agriculture, industry, etc. affect the hydrology and water quality of the watershed. The human activities components included in the models are compiled in Table 6.

Table 6. Human activities included in the models.

Human Activities	HSPF	MODFLOW	SWAT	GWLF
Agricultural and animal feeding operations	✓		✓	✓
Urban runoff	✓		✓	✓
Sewage disposal	✓		✓	
Septic systems	✓		✓	
Water treatment plants	✓		✓	✓
Wells		✓	✓	

3.3 Model's suitability for modeling karst-influenced watersheds

GWLF and MODFLOW were not found appropriate for application in karst-influenced watersheds because they are not able to simulate most of the required hydrologic processes. Moreover, GWLF calculates only monthly outputs due to the lack of detail in predictions and stream routing. HSPF and SWAT can represent almost all of the hydrologic processes and nutrient transformations and transport processes; whereas SWAT is the only model that can simulate sinking streams and none of the models can represent other karst features.

According to Migliaccio and Srivastava (2007), to simulate a watershed where stream flow is dominated by groundwater recharge, SWAT would be a better choice because it has more groundwater components than other existing models. In non-karst regions, based on statistical and graphical comparisons, previous studies showed that the characteristics of simulated flows from both SWAT and HSPF models are similar to each other and to the observed flows (Singh et al., 2005). However, HSPF performed better when calculating temporal variations of daily flow and sediment (Saleh and Du, 2004; Sangjun et al., 2007). HSPF is less user-friendly than SWAT and requires more effort due to the large number of parameters. Also, the calibration process is

more demanding and time-consuming. On the other hand, most of the SWAT parameters are automatically generated using GIS data or other information and are relatively easy to adjust (Singh et al., 2005; Sangjun et al., 2007; Saleh and Du, 2004).

According to Borah et al. (2006), SWAT simulates the transfers and internal cycling of the major forms of nitrogen and phosphorous. SWAT is an especially strong nitrogen model because it is based on the accumulated expertise acquired in agricultural systems. According to Saleh and Du (2004), in the Upper North Bosque River watershed in central Texas, nitrogen loadings were underpredicted due to the inability of HSPF to integrate detailed farm management practices. The authors suggest that SWAT is a much better predictor of daily and monthly nitrogen loadings than HSPF.

Finally, the SWAT model is considered the most appropriate model among the evaluated models due to its capability to represent almost all of the hydrological processes, its user-friendliness, and its ability to generate most of the parameters from available data. Moreover, the most important reason to select SWAT is not only for its capability to represent all of the nitrogen transformations and transport processes, but also because its strength in calculating nitrogen loadings among other models.

Chapter 4: Modification of the SWAT model for a karst-influenced watershed

The purpose of building a modeling framework is to simulate the rapid transport of water and pollutants through karst features and the interactions between surface and ground water. The SWAT model was selected to represent the hydrologic processes that drive nitrogen transport in a karst-influenced watershed.

4.1 SWAT model component and parameter evaluation

SWAT 2005 code and SWAT user's manuals (Neitsch et al., 2005) were reviewed to determine the model algorithms that control the hydrologic processes and the transport of nutrient. The equations given in the rest of this chapter are from those two sources, unless otherwise cited. The code was downloaded on 3/10/2009 at http://www.brc.tamus.edu/swat/soft_model_2005soft.html. SWAT divides the watershed into subunits. In SWAT the first level of subdivision is the subbasin. Subbasins have a geographic location in the watershed and are spatially linked to one another. A subbasin will contain:

- Unlimited number of hydrologic response units (HRU) (described below)
- A tributary channel (1 per subbasin)
- A main channel (1 per subbasin)
- A pond and/or a wetland (1 per subbasin, optional)
- Point sources (optional)

The next level of subdivision is the Hydrologic Response Unit (HRU). HRUs have unique landuse/management/soil attributes. Unlike subbasins, HRUs are conceptual units not physical ones, and do not interact among each other. Loadings for each HRU in a subbasin are calculated separately and then summed for all HRUs to determine the total loadings from the subbasin. HRU size is the modeler's choice. Theoretically, the minimum HRU size can be a cell; however, it is suggested by the developers that a subbasin should have 1-10 HRUs (Neitsch et al., 2005). If more complexity is desired, it is recommended the user increase the number of subbasins in the

watershed rather than the number of HRUs within a few subbasins. The SWAT model divides the hydrologic cycle into land and routing phases.

4.1.1 The land phase

The land phase of the hydrologic cycle controls the amount of water, sediment, nutrient and pesticide loadings to the main channel in each subbasin. The land phase of the hydrologic cycle of the SWAT model, computed for each HRU, is presented in Figure 1.

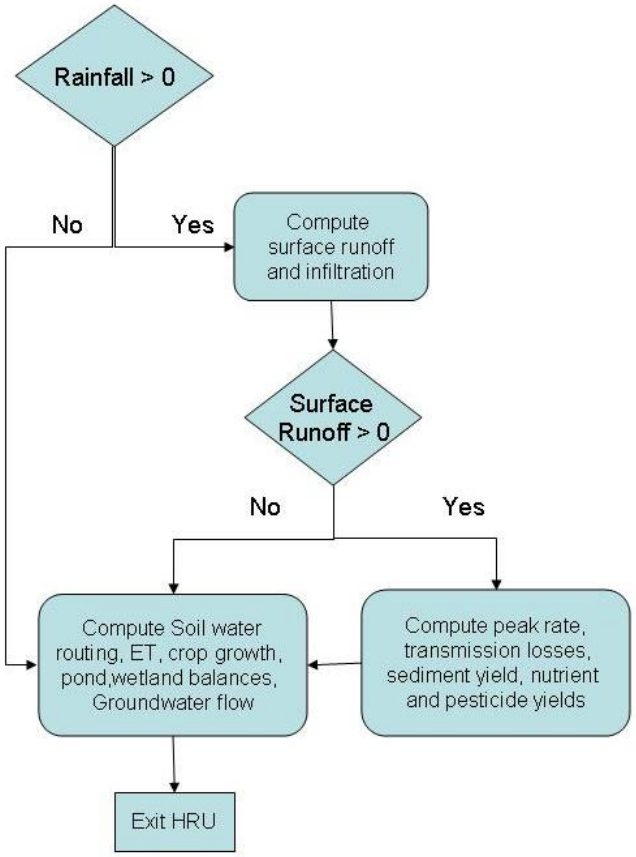

Figure 1. Sequence of processes used by SWAT to model the land phase of the hydrologic cycle for each HRU.

4.1.1.1 Runoff

SWAT simulates surface runoff for each HRU using the SCS curve number equation (SCS, 1972). Daily precipitation (mm) and CN2 – moisture condition II curve number (0-100) are used during the calculations. The peak runoff rate is the maximum runoff flow rate that occurs with a

certain rainfall event in an HRU. The peak runoff rate is an indicator of the erosive power of a storm and is used to predict sediment loss. SWAT calculates the peak runoff rate with a modified rational method. The following variables are used to calculate peak runoff rate:

- Area of the HRU (km^2)
- Fraction of the subbasin area contained in the HRU
- Average slope length (m)
- Average slope steepness
- Manning value for overland flow
- Tributary channel length in subbasin
- Average slope of tributary channel (m/m)
- Manning value for tributary channel

In the model, runoff and peak runoff rate calculations are performed at the HRU level. Both runoff and peak rate are adjusted when transmission losses occur in tributary channels. Transmission losses from surface runoff percolate into the unconfined aquifer (Figure 2).

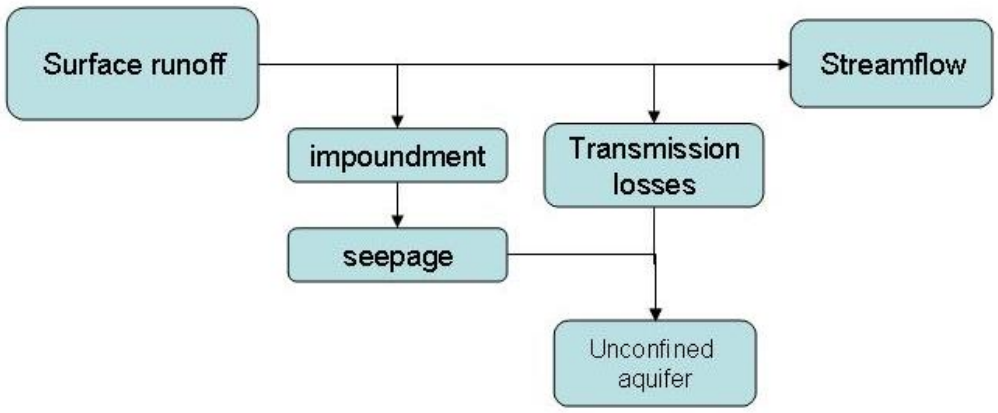

Figure 2. Schematic pathways for runoff water movement in SWAT.

4.1.1.2 Percolation

The vertical movement of water through micropores in the unsaturated zone is simulated by SWAT. Percolation occurs when field capacity of a soil layer is exceeded (Figure 3). Soil water excess is calculated using:

$SW_{excess} = SW - FC$ if $SW > FC$ **[2]**

$SW_{excess} = 0$ if $SW \leq FC$ **[3]**

Where, SW_{excess} is the drainable volume of water in the soil layer for the day from the HRU (mm), SW is the water content of the soil layer for the day (mm), and FC is the water content of the soil layer at field capacity (mm). Percolation is governed by the saturated hydraulic conductivity (mm/hr) of the soil layer and is calculated as:

$$W_{perc} = SW_{excess}\left[1 - \exp\left(\frac{-\Delta t}{TT_{perc}}\right)\right] \quad \textbf{[4]}$$

Where, W_{perc} is the amount of water percolating to the underlying soil layer for the day from the HRU (mm), Δt is the length of the time step (hrs), and $TTperc$ is the travel time for percolation (hrs), calculated as:

$$TTperc = (SAT - FC) / K_{sat} \quad \textbf{[5]}$$

Where, SAT is the amount of water in the soil layer when completely saturated (mm) and K_{sat} is the saturated hydraulic conductivity of the soil layer (mm/hr).

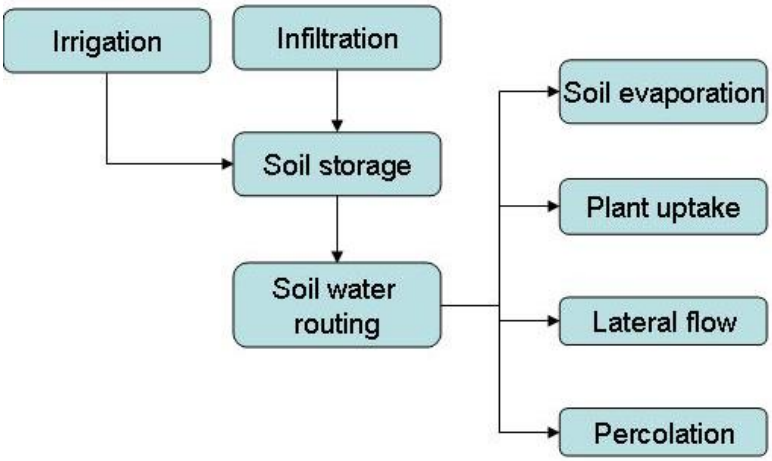

Figure 3. Schematic pathways for soil water movement in SWAT.

Bypass flow, often called macropore or preferential flow, is simulated by SWAT. Bypass flow is the vertical movement of water through macropores through the soil horizons in the unsaturated zone. This process occurs in soils that shrink when dried and swell when moistened forming large cracks at the soil surface. Runoff is calculated and a calculated fraction is considered to enter through cracks. Surface runoff in excess of the crack volume remains overland flow. The total amount of water percolating to the underlying soil layer from the HRU is calculated using:

$$sepbtm = Wperc + Wcrk \quad \textbf{[6]}$$

Where, *sepbtm* is the daily amount of water percolating from the HRU (mm), and *Wcrk* is the amount of water flow past the lower boundary of the soil profile due to bypass flow for the day from the HRU (mm).

4.1.1.3 Groundwater recharge

Groundwater recharge is calculated summing percolating water, bypass flow, seepage from ponds and wetlands, and stream transmission losses. Groundwater recharge is a function of the time it takes for water to flow through the vadose zone. The delay time is the number of days required for water to reach the underliying unconfined aquifer. All groundwater recharge is

assumed to travel vertically to the aquifer with the same delay time. Unconfined aquifer recharge is calculated using:

$$rchrg = (1- \exp[-1/delay]) * (sepbtm + rchrg\_imp) + \exp[-1/delay] * rchrg1 \quad [7]$$

Where, *rchrg* is the daily amount of recharge entering the unconfined aquifer from the HRU (mm), *delay* is the delay time (days), *sepbtm* is the daily amount of water percolating and flowing past the lower boundary of the soil profile due to bypass flow for the day from the HRU (mm), *rchrg_imp* is the daily seepage from ponds, wetlands and tributary channel transmission losses (mm), and *rchrg1* is the amount of recharge entering the aquifer on the previous day (mm).

A subbasin located in upstream Opequon Creek watershed was simulated in SWAT to evaluate the groundwater aquifer recharge component. The default delay time (delay = 31 days) allows simulating a sustained aquifer recharge during drought periods. Shorter delay times produce a more rapid recharge during storm events (Figures 4 and 5).

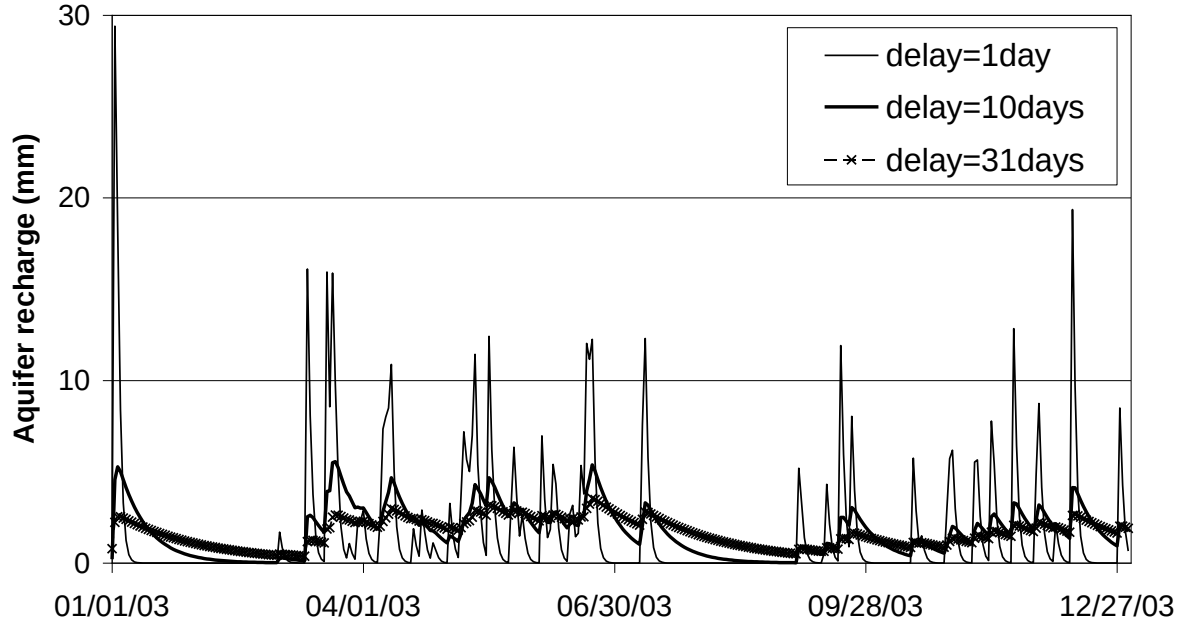

Figure 4. Example daily aquifer recharge in SWAT for different delay times.

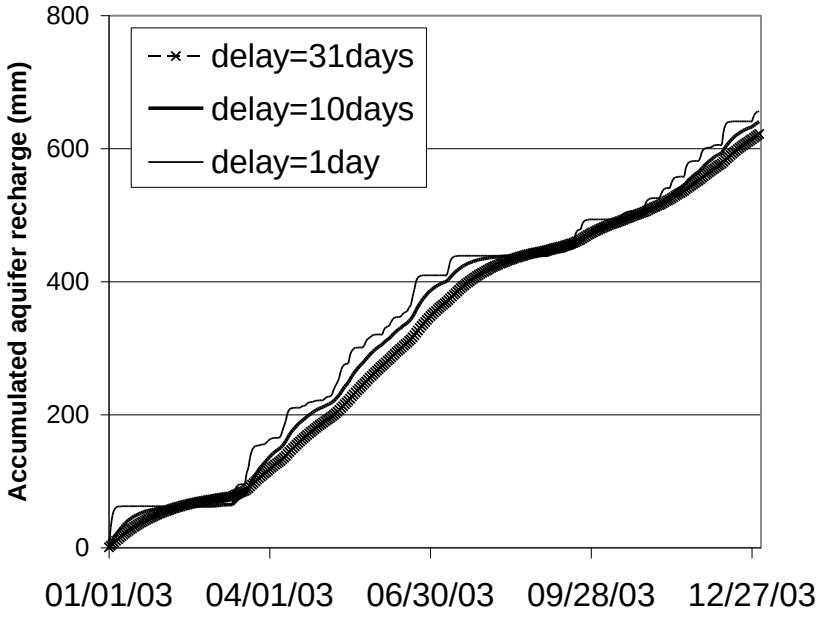

Figure 5. Example accumulated aquifer recharge in SWAT for different delay times.

In karst regions, where water enters the aquifer as diffuse infiltration, baseflow can take months to emerge from springs. In karst regions where water enters the aquifer through conduits (sinkholes and sinking streams), baseflow takes shorter periods of time to emerge from springs and it is considered to be more rapid. Base on the parameter evalation and the characteristics of karst regions, the delay time 10 days is used to simulate diffuse infiltration and the delay time 1 day is used to simulate the aquifer recharge through sinkholes and sinking streams. In non-karst regions, the default delay time 31days is used to simulate the aquifer recharge from percolation.

SWAT partitions aquifer recharge into unconfined aquifer recharge, which contributes return flow to streams within the watershed, and confined aquifer recharge, which contributes return flow to streams outside the watershed. Confined aquifer recharge is calculated using:

$$gwseep = \beta_{deep} * rchrg \quad \textbf{[8]}$$

Where, *gwseep* is the amount of water moving into the confined aquifer for the day from the HRU (mm), β_{deep} is deep aquifer percolation fraction, and *rchrg* is the amount of recharge entering both aquifers on the day (mm).

4.1.1.4 Baseflow

Baseflow is allowed to enter the reach only if the amount of water stored in the unconfined aquifer exceeds a threshold value specified by the user. The amount of baseflow is calculated using:

$$gw\_q = gw\_q\ 1 * \exp[-\alpha_{gw}*\Delta t] + (rchrg - gwseep) * (1-\exp[-\alpha_{gw}\ ]) \quad \text{if} \quad aq_{sh} > aq_{shthr} \quad \textbf{[9]}$$

$$gw\_q = 0 \quad \text{if} \quad aq_{sh} \leq aq_{shthr} \quad \textbf{[10]}$$

Where, *gw_q* is the groundwater flow into the main channel for the day from the HRU (mm), gw_q 1 is the groundwater flow into the main channel for the previous day (mm), α_{gw} is the baseflow alpha factor or baseflow recession constant, aq_{sh} is the amount of water stored in the unconfined aquifer at the beginning of day (mm), and aq_{shthr} is the threshold water level in the unconfined aquifer for baseflow contribution to the main channel to occur (mm).

Manguerra and Engel (1998) found that the SWAT model is sensitive to the baseflow alpha factor, or recession constant, that characterizes the rate at which baseflow is returned to the stream. The model developers recommend values from 0.9 to 1 for a region with rapid recharge. A subbasin located in upstream Opequon Creek watershed was simulated in SWAT to evaluate the baseflow component. The alpha factor default value in SWAT is equal to 0.048. Using the default alpha factor (alpha=0.048) and the default delay time (delay=31 days), baseflow calculations resulted close to the maximum baseflow (alpha=1) (Figures 6 and 7).

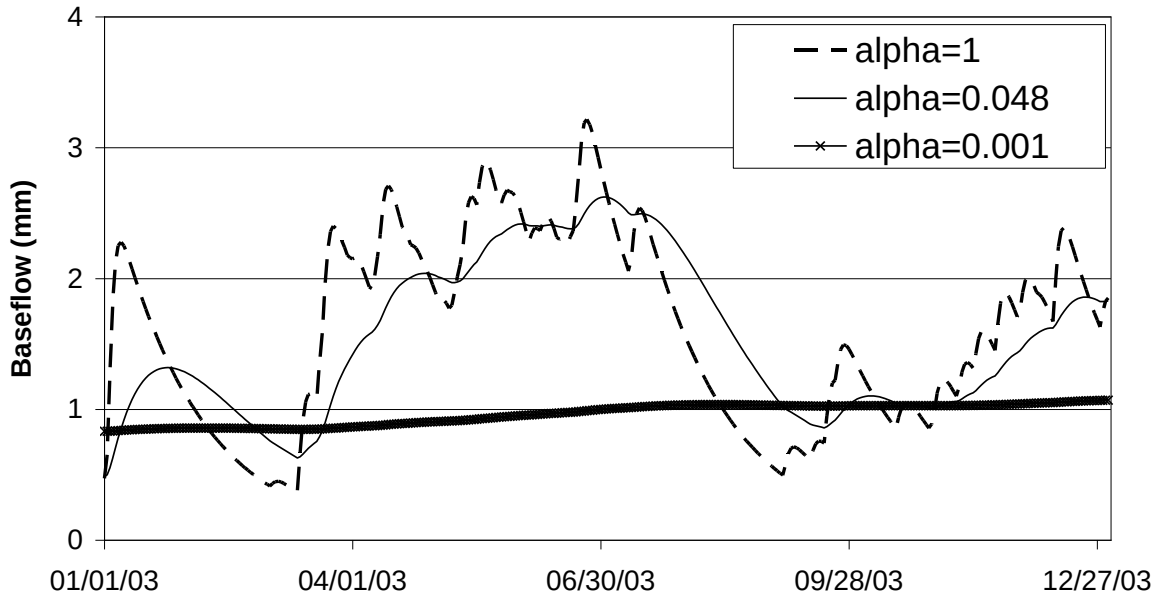

Figure 6. Example daily baseflow in SWAT for different alpha factors and the default delay time (31 days).

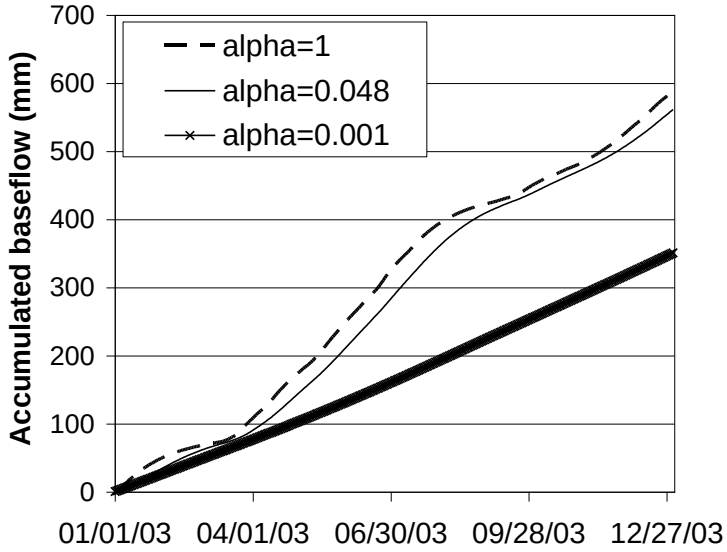

Figure 7. Example accumulated baseflow in SWAT for different alpha factors and the default delay time (31 days).

Using the default alpha factor (alpha=0.048) and the delay time recommended for a region with rapid recharge (delay=1 day), baseflow results were not close to the maximum baseflow (alpha=1). Baseflow calculated using alpha=1 resulted in higher baseflow peaks (Figures 8 and 9).

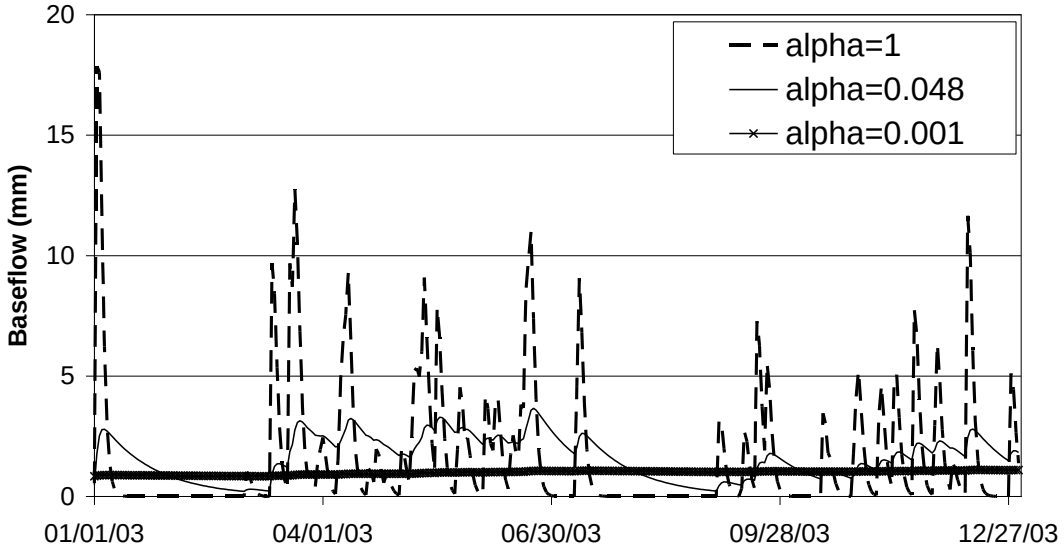

Figure 8. Example daily baseflow in SWAT for different alpha factors and delay time1day.

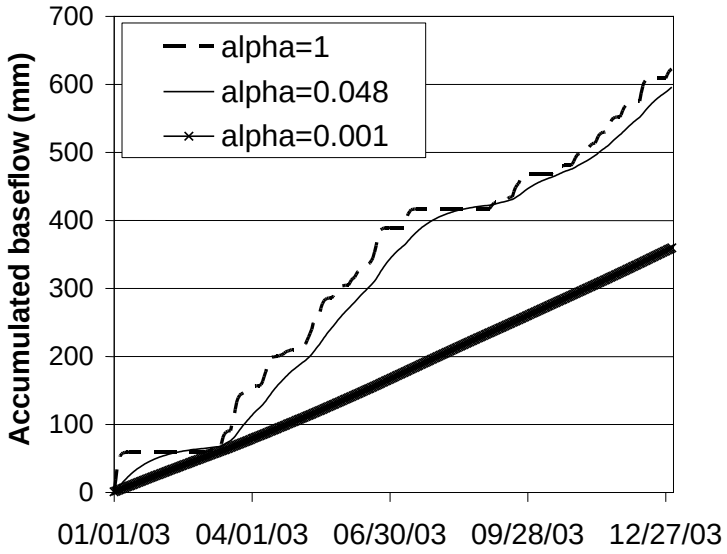

Figure 9. Example accumulated baseflow in SWAT for different alpha factors and delay time 1day.

Based on the parameter evaluation and the characteristics of non-karst and karst regions, baseflow in non-karst regions is calculated using the default alpha factor (alpha=0.048). In regions where water enters the aquifer through sinkholes and sinking streams (a region with rapid recharge), baseflow is calculated using the maximum alpha factor (alpha=1)

Water leaving the aquifer storage can also move upward into the capillary fringe (Figure 10). Capillary movement is computed only if the amount of water stored in the unconfined aquifer exceeds a threshold value specified by the user. Water in the aquifer can also be removed by pumping.

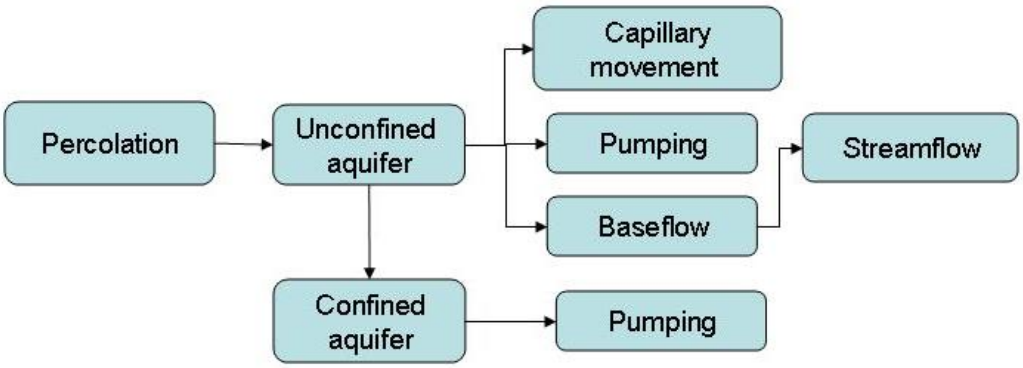

Figure 10. Schematic pathways for subsurface water movement in SWAT.

4.1.1.5 Tributary channels

A tributary channel is defined in SWAT as a lower order channel that drains only a part of the subbasin and does not receive groundwater contribution to its flow. All flow in the tributary channel is routed through the main channel of the subbasin. The tributary channel component defines the longest flow path in the subbasin. SWAT uses the attributes of tributary channels to determine the time of concentration for the subbasin and the transmission losses from runoff as it flows to the main channel.

4.1.1.6 Transmission losses from tributary channels

SWAT simulates water transmission through the bed of the channel. Transmission losses reduce runoff volume as water flows (flood wave travels) downstream contributing seepage to the unconfined aquifer (Figure 2). Water losses from the channel are a function of channel width and length and flow duration. Both runoff volume and peak rate are reduced when transmission

losses occur in tributary channels. Transmission losses from surface runoff are assumed to percolate into the unconfined aquifer. Surface runoff volume after transmission losses is calculated using:

$$volQsurf = 0 \quad \text{if} \quad volQsurf \leq vol_{thr} \qquad \textbf{[11]}$$

$$volQsurf = ax + bx * volQsurf_i \quad \text{if} \quad volQsurf > vol_{thr} \qquad \textbf{[12]}$$

Where, *volQsurf* is the volume of runoff after transmission losses, $volQsurf_i$ is the volume of runoff prior transmission losses, and vol_{thr} is the threshold volume for a channel of length L and width W. The threshold volume is calculated using the regression parameters for channels of differing lengths and widths:

$$vol_{thr} = - a_x/b_x \qquad \textbf{[13]}$$

Where, a_x and b_x (m^3) are the regression parameters intercept and slope, respectively, for a channel of length *L* and width *W*. The following variables are the inputs required to calculate a_x and b_x:

- Area of the subbasin (km^2)
- Fraction of the total subbasin area contained in the HRU
- Channel effective hydraulic conductivity (mm/hr)
- Average width of tributary channel (m)
- Longest tributary channel length in subbasin (km).

4.1.1.7 Impoundments

4.1.1.7.1 Ponds and wetlands

Ponds and wetlands are simulated in SWAT within a subbasin and cannot be simulated in the main channel. Ponds and wetlands do not receive water from upstream subbasins. Pond and wetland water storage is a function of daily inflows and outflows, including seepage and

evaporation (Figure 11). Ponds and wetlands receive inflow from a fraction of the subbasin, and the volume of water entering the water body is subtracted from the surface runoff, lateral flow, and groundwater loadings to the main channel.

Seepage is governed by the effective saturated hydraulic conductivity of the pond or wetland bottom and surface area of the water body. The algorithms used to simulate these water bodies differ only in the outflow calculation. Pond outflow is simulated as a function of storage and varies based on soil water content and flood season. The wetland outflow occurs whenever the water volume exceeds the storage volume. The following variables are used to calculate pond outflow:

- Surface area of the pond when filled to the emergency spillway (ha)
- Surface area of the pond when filled to the principal spillway (ha)
- Volume of water held in the pond when filled to the emergency spillway ($10^4 m^3$)
- Volume of water held in the pond when filled to the principal spillway ($10^4 m^3$)
- Fraction of the subbasin area draining into the pond
- Effective saturated hydraulic conductivity of the pond bottom (mm/hr).

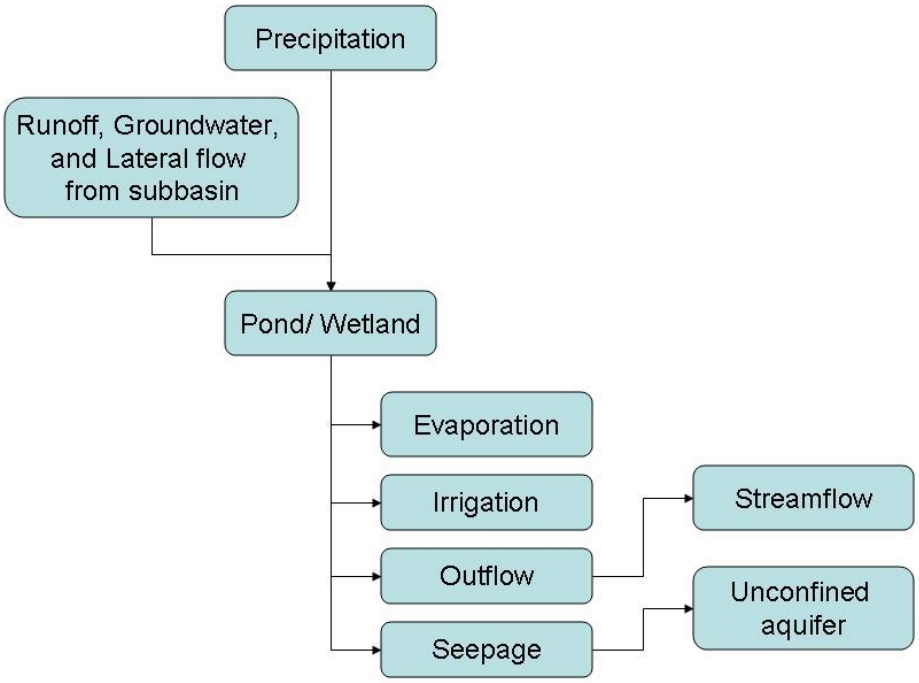

Figure 11. Schematic pathways for pond/wetland water movement in SWAT.

4.1.1.7.2 Potholes

Potholes are depression areas where runoff flows to the lowest part of the pothole rather than contributing to flow in the main channel (Figure 12). Potholes are simulated as an HRU unit. The following variables listed are used to simulate potholes:

- Timing of release/ impounding operation
- Slope of the HRU (m/m)
- Fraction of the HRU area draining into the pothole
- Leaf area index at which no evaporation occurs from the water surface
- Maximum amount of water that can be stored in the pothole (m^3).

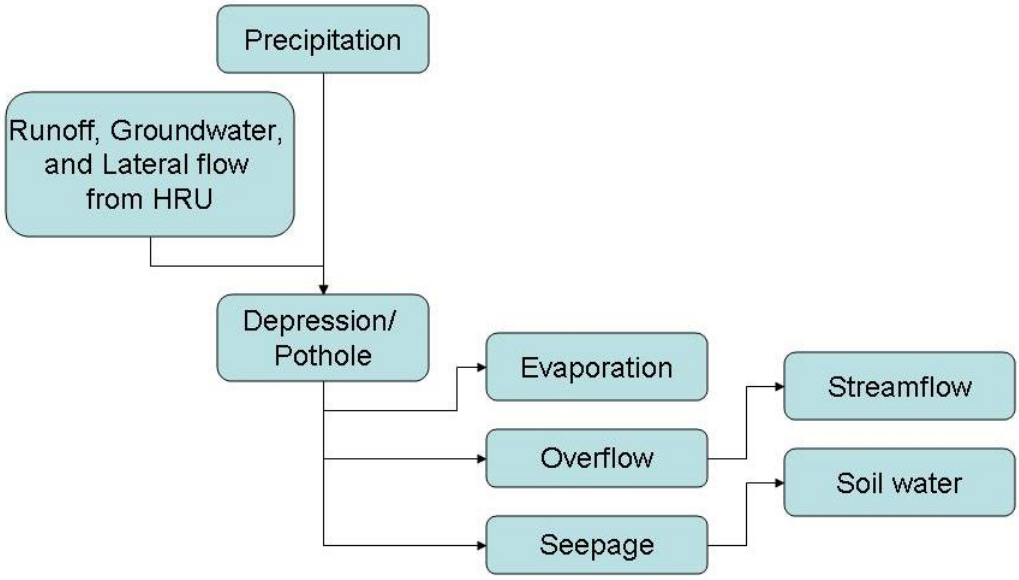

Figure 12. Schematic pathways for pothole water movement in SWAT.

4.1.2 The routing phase

4.1.2.1 Main channel

The routing phase of the hydrologic cycle is defined as the movement of water and pollutants through the channel network of the watershed to the outlet. The model uses Manning's equation to define the rate and velocity of open channel flow. Water is routed through the channel network using the variable storage routing method or the Muskingum routing method (Neitsch et al., 2005).

4.1.2.2 Transmission losses from main channels

Water may be lost due to evaporation and transmission through the bed of the channel. In SWAT, streams are classified as ephemeral, intermittent or perennial. This classification is a function of the amount of groundwater contribution received by the stream. Ephemeral streams contain water during and immediately after a storm event and are dry the rest of the year.

Intermittent streams are dry part of the year, but contain flow when the groundwater is high enough as well as during and after a storm event. Perennial streams receive continuous groundwater contributions and flow throughout the year.

Transmission losses in main channels occur when the stream does not receive groundwater contributions. Transmission losses from the main channel are assumed to enter bank storage or the deep aquifer. Effective hydraulic conductivity of the channel (mm/hr) and the channel length (km) are the variables required during the calculation.

4.1.3 Nitrogen transport

In this study it was assumed that nitrogen transformations in non-karst and in karst regions are the same in the soil matrix and nitrogen is not subject of transformations when it is transported with surface runoff, lateral flow, and baseflow.

4.1.3.1 Nitrogen movement

In SWAT, nitrate from land areas is transported into the stream network with surface runoff, lateral flow, and baseflow (Figure 14). The amount of mobile water is the total amount of water that transports nitrogen in the soil layer and is calculated using:

$w_{mobile} = surfq + latq + W_{perc}$ for top 10 mm **[14]**

$w_{mobile} = latq + W_{perc}$ for lower soil layers **[15]**

The concentration of nitrate in the mobile water is calculated using:

$$concNO3 = NO3 * (1 - \exp[-w_{mobile}/(1-\theta)*SAT])/ w_{mobile} \quad \textbf{[16]}$$

Where, *concNO3* is the concentration of nitrate in the mobile water for a layer (kg N/mm), *NO3* is the amount of nitrate in the layer (kg N/ha), w_{mobile} is the amount of mobile water in the layer (mm), θ is the fraction of porosity from which anions are excluded, and *SAT* is the saturated

water content of the soil layer (mm). Surface runoff removes nitrate from the top 10 mm of the soil. The amount of nitrate transported with runoff is calculated using:

surqno3 = nperco * concNO3 * surfq **[17]**

Where, *surqno3* is the amount of NO_3-N in surface runoff for the day from the HRU (kg N/ha), *nperco* is the nitrate percolation coefficient, *concNO3* is the concentration of nitrate in the mobile water for the top 10 mm of soil (kg N/mm), and *surfq* is the surface runoff generated for the day from the HRU (mm). The nitrate percolation coefficient allows the model user to set the surface runoff nitrate concentration to a fraction of the concentration in percolating water. Nitrate removed in lateral flow is calculated using:

latno3 = nperco * concNO3 * latq for top 10 mm **[18]**

latno3 = concNO3 * latq for lower soil layers **[19]**

Where, *latno3* is the amount of NO_3-N in lateral flow for the day from a layer from the HRU (kg N/ha), *nperco* is the nitrate percolation coefficient, *concNO3* is the concentration of nitrate in the mobile water for the layer (kg N/mm), and *latq* is the water discharged from the layer by lateral flow for the day from the HRU (mm). Nitrate moved to the underlying layer by percolation is calculated using:

percn = concNO3 * W_{perc} **[20]**

Where, *percn* is the amount of NO_3-N moved to the underlying layer by percolation for the day from the HRU (kg N/ha), *concNO3* is the concentration of nitrate in the mobile water for the layer (kg N/mm), and W_{perc} is the amount of water percolating to the underlying soil layer for the day (mm).

4.1.3.2 Nitrogen in the aquifer

In SWAT, it is assumed that there is no alteration in nitrate concentration as it moves through the vadose zone. Nitrate transported with percolating water is used to calculate the nitrate aquifer loading from recharge (Figure 13). The same approach used to simulate aquifer recharge is used to simulate nitrate movement from the soil profile to the aquifer.

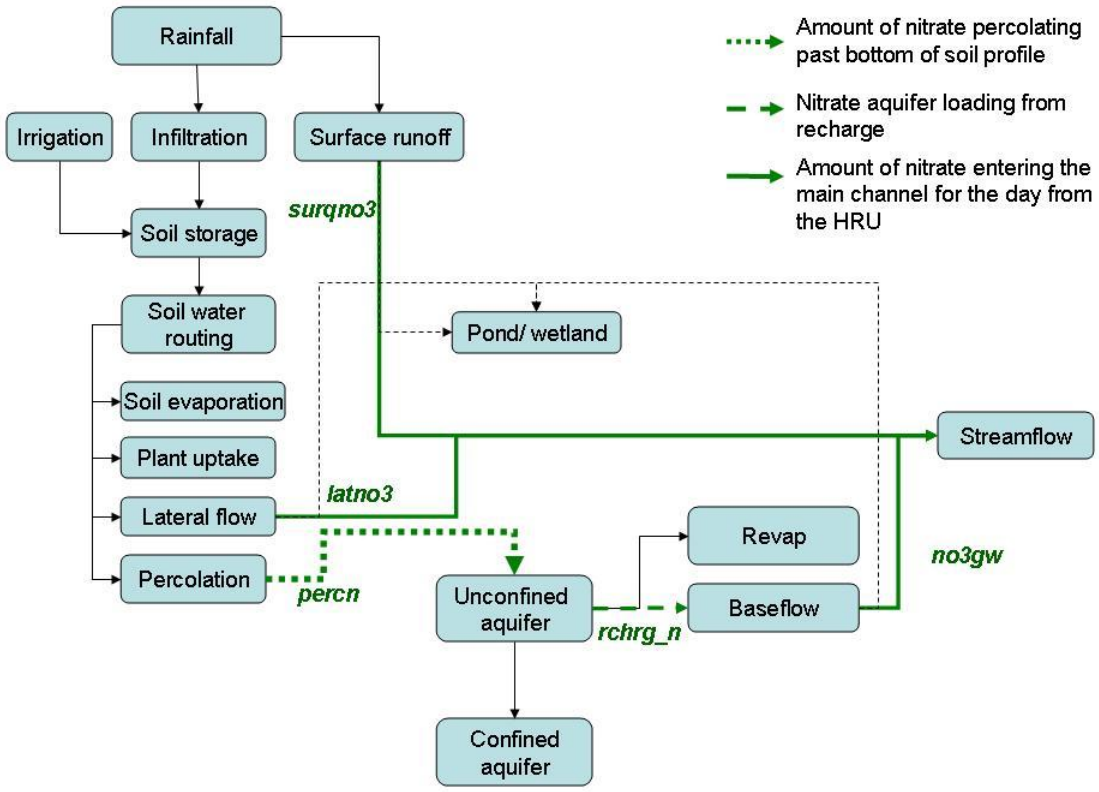

Figure 13. Schematic pathways for nitrate movement in SWAT in an HRU.

The nitrate in recharge to the aquifer is calculated using:

$$rchrg\_n = (1- \exp[-1/delay]) * percn + \exp[-1/delay] * rchrgn1 \quad \textbf{[21]}$$

where *rchrg_n* is the amount of nitrate in recharge entering the aquifer for the day from the HRU (kg N/ha), *delay* is the delay time (days), *percn* is the total amount of nitrate exiting the bottom

of the soil profile for the day from the HRU (kg N/ha), and *rchrgn1* is the amount of nitrate in recharge for the previous day.

Nitrate in the unconfined aquifer may remain in the aquifer, move with recharge to the deep aquifer, move with baseflow into the main channel, or be transported out of the unconfined aquifer with water moving into the soil zone in response to water deficiencies. The amount of nitrate moving with baseflow into the main channel is calculated using:

$$no3gw = (rchrg\_n) * gw\_q / (aq_{sh} + gw\_q + revapday + gwseep) \quad \textbf{[22]}$$

Where, *no3gw* is the amount of nitrate in baseflow from the unconfined aquifer for the day from the HRU (kg N/ha), *gw_q* is the groundwater flow into the main channel for the day from the HRU (mm), aq_{sh} is the amount of water stored in the unconfined aquifer at the beginning of the day (mm), *revapday* is the amount of water moving into the soil zone in response to water deficiencies for the day from the HRU (mm), and *gwseep* is the amount of water moving into the confined aquifer for the day from the HRU (mm).

4.2 Baffaut and Benson (2008) SWAT 2005 modifications

Baffaut and Benson (2008) modified the SWAT code (henceforth called SWAT-B&B) to simulate faster percolation in karst basins. They used transmission losses from tributary channels to represent sinking streams and ponds to represent sinkholes. The model was calibrated for flow, bacteria, and phosphorous. They used Moriasi et al. (2007) criteria to evaluate the performance of the model. They reported satisfactory performance for flow and unsatisfactory performance for pollutants during the calibration and validation periods.

Baffaut and Benson (2008) simulated sinking streams by specifying high saturated hydraulic conductivities in the tributary channels (10-50 mm/hr). Sinkholes were simulated as a pond with high hydraulic conductivity at the bottom (100 mm/hr) and using a fraction of the subbasin draining into the pond. When sinkholes are simulated as a pond, all sinkholes within each subbasin are lumped and represented by one pond, thus eliminating the possibility of

discriminating hydrologic processes among sinkholes. Moreover, simulating a pond requires a large number of parameters. Springs recharged by a region outside the watershed were represented as point sources. Springs recharged within a subbasin were calculated as a part of the return flow. The model does not allow transferring water from one subbasin to another.

Baffaut and Benson (2008) modified SWAT 2005 by dividing the aquifer recharge into two components: recharge from percolating water from the soil profile (small cracks but no direct conduits) and recharge from sinkholes and losing streams (via direct conduits). Aquifer recharge from karst regions and from non-karst regions are calculated separately using the same equation but different delay times. Aquifer recharge from percolating water from the soil profile is calculated using (Baffaut and Benson, 2008):

$$rchrg\_sepbtm = (1- \exp[-1/delay]) * sepbtm + \exp[-1/delay]* rchrg\_sepbtm1 \quad \textbf{[23]}$$

Where, *rchrg_sepbtm* is the recharge from percolation through the soil for the day from the HRU, *delay* is the delay time (days), *sepbtm* is the daily amount of water percolating and bypass flow for the day from the HRU (mm), and *rchrg_sepbtm1* is the amount of recharge entering the aquifer for the previous day. Seepage via direct conduits in karst regions is calculated using:

$$sep\_direct = tloss + twlpnd + twlwet \quad \textbf{[24]}$$

Where, *sep_direct* are the losses from sinking streams and ponds and wetlands for the day from the HRU, *tloss* is the water lost from a sinking stream, *twlpnd* is the seepage from ponds, and *twlwet* is the seepage from wetlands. Baffaut and Benson (2008) set the delay time for karst features to one-tenth that of percolating water, making the recharge from karst regions a faster process. Aquifer recharge in karst regions is calculated using:

$$rchrg\_direct = (1- \exp[-1/(delay/10)]) * sep\_direct + \exp[-1/(delay/10)]* rchrg\_krst1 \quad \textbf{[25]}$$

Where, *rchrg_direct* is the recharge from sinkholes and losing streams via direct conduits to the aquifer, *delay* is the delay time (days), *sep_direct* represents all losses from sinkholes and losing

streams via direct conduits, and *rchrg_krst1* is the amount of recharge from karst entering the aquifers for the previous day. The total unconfined aquifer recharge is calculated using:

$$rchrg = rchrg\_sepbtm + rchrg\_direct \quad \textbf{[26]}$$

Where, *rchrg* is the daily amount of recharge entering the aquifers for the day from the HRU (mm).

4.3 Modeling approach

SWAT-B&B was modified further for karst environments. Despite SWAT-B&B satisfactory performance to simulate flow, it still faces the limitation of representing karst features in a subbasin scale, not providing the possibility to differentiate karst features in a subbasin. Thus, for this project the SWAT model code was changed to simulate the sinkhole's hydrology and the transport of nutrients in karst features in an HRU scale. Code compilations and modifications were performed using Visual FORTRAN 5.0.

4.3.1 Sinkhole hydrology

Sinkholes can rapidly transfer water and pollutants directly to the underlying aquifer rather than going directly into streams. The water that goes through a sinkhole and recharges the aquifer should be, conceptually, equal to the depth of surface runoff of the area that sinks in the karst feature (Figure 14). Despite the fact that HRUs are not spatially linked in SWAT, their unique characteristics offer the possibility to discriminate hydrologic processes among sinkholes within a subbasin (Figure 15). In addition, HRUs offer the opportunity to describe multiple sinkholes within the subbasin.

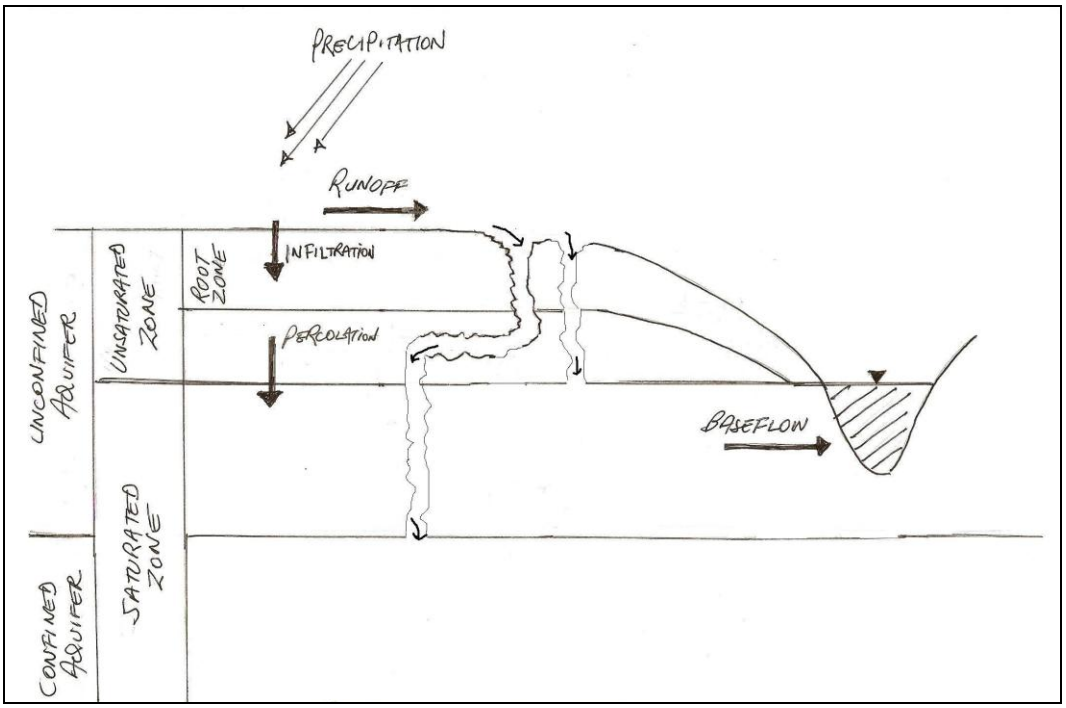

Figure 14. Hydrologic process in sinkholes.

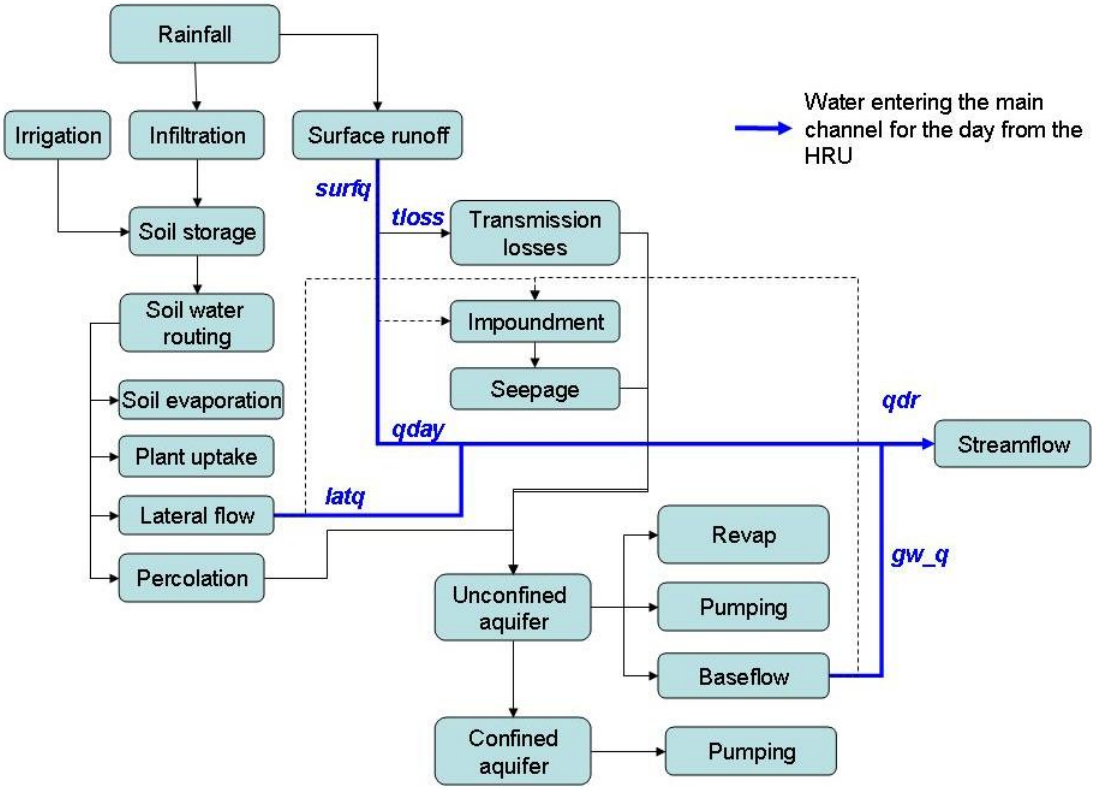

Figure 15. Schematic pathways for water movement in SWAT in an HRU.

For this project, a new parameter was created to allow simulating surface water that goes through a sinkhole and recharges the aquifer in an HRU. The new parameter is called *sink*, and it was allocated, defined, and initialized in the subroutines *allocate_parms, modparm, and zero0*, respectively. S*ink* is the sinkhole partitioning coefficient and it is the fraction of surface water that goes through a sinkhole and recharges the unconfined aquifer (Figure 16). Sink is included in the HRU groundwater input file (*.gw). When an HRU is not a sinkhole, the default value for *sink* has to be included in the groundwater input file (*sink* = 0).

The subroutine *readgw* reads information from the HRU groundwater input file (*.gw), and the subroutine *st2* writes that information in the standard input file (input.std). Those subroutines were modified in order to read the new parameter *sink*. The last step was to modify the subroutines that control surface water and groundwater calculations. The subroutine *subbasin* controls the simulation of the land phase of the hydrologic cycle. In this subroutine, the total amount of water entering the main channel for the day from each HRU is calculated using:

$$qdr = qday + latq + gw\_q + qtile \quad \textbf{[27]}$$

Where, *qdr* is the total amount of water entering the main channel for the day from the HRU, *qday* is surface runoff loading to main channel for the day from the HRU, *latq* is the total lateral flow in soil profile for the day from the HRU, *gw_q* is the groundwater contribution to streamflow for the day from the HRU, and *qtile* is the drainage tile flow in soil layer for the day. When a sinkhole is simulated as an HRU (when *sink>0*), *qday* and *latq* are not included in the calculations (Figure 16). The subroutine *tran* simulates tributary channel transmission losses. When a sinkhole is simulated as an HRU (when *sink>0*), HRU transmission losses from surface runoff are not simulated.

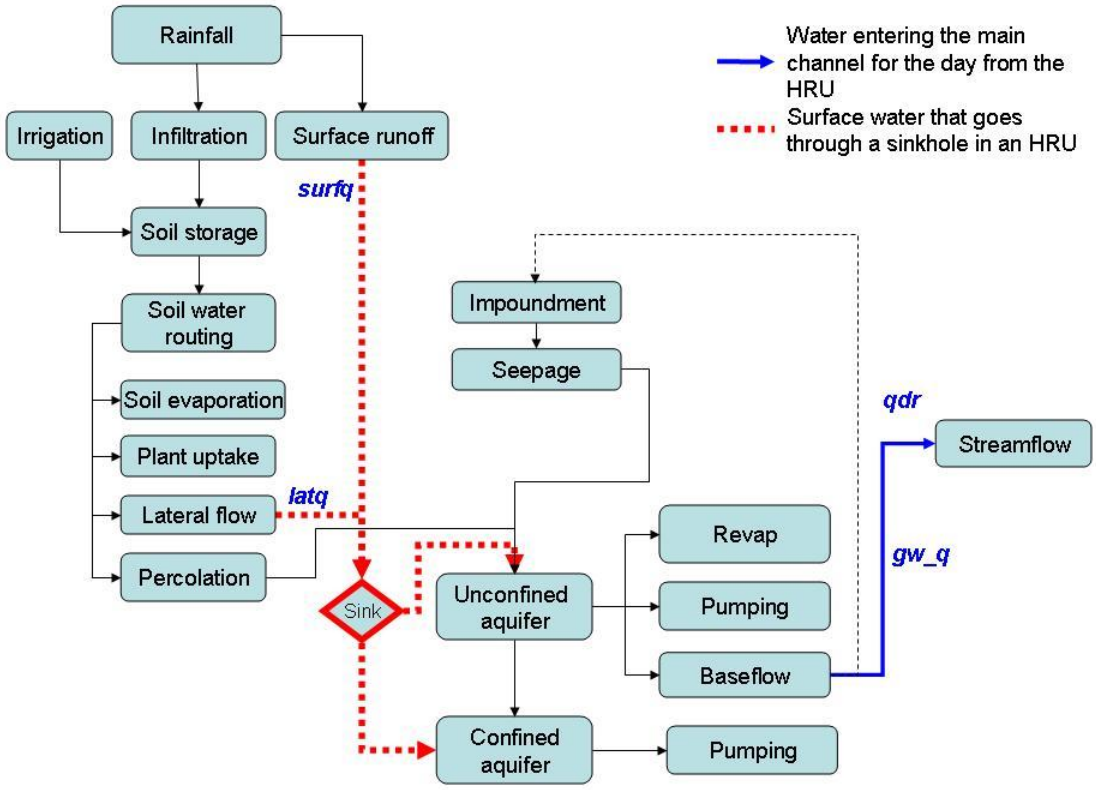

Figure 16. Schematic pathways for water movement in SWAT in a sinkhole.

The subroutine *gwmod* controls aquifer recharge and baseflow calculations. In non-karst regions, the unconfined aquifer recharge from percolating water and seepage from impoundments is calculated using:

$$rchrg\_sepbtm = (1- \exp[-1/delay]) * (sepbtm(j) + twlpnd + twlwet) + \exp[-1/delay] * rchrg\_sepbtm1 \quad \textbf{[28]}$$

Where, *rchrg_sepbtm* is the recharge from percolation through the soil for the day from the HRU, *delay* is the delay time (days), *sepbtm* is the daily amount of water percolating and bypass flow for the day from the HRU (mm), *twlpnd* is the seepage from ponds, *twlwet* is the seepage from wetlands, and *rchrg_sepbtm1* is the amount of recharge entering the aquifers for the previous day. When a sinkhole is simulated as an HRU (when s*ink* >0), surface runoff and lateral flow generated from the HRU are included in the seepage calculations in karst regions using the new equation:

sep_direct = sink * (surfq +latq) **[29]**

Where, *sep_direct* is the seepage from sinking streams and sinkholes for the day from the HRU, *sink* is the sinkhole partitioning coefficient, and (*surfq+ latq)* is the water that goes through a sinkhole generated for the day from the HRU. In karst regions, the unconfined aquifer recharge is calculated using Equation 25. The total aquifer recharge is the sum of recharge from percolating water and recharge from karst features.

When the water depth that goes through a sinkhole recharges another region outside the watershed (when *sink* ≈ 0.001), water is assumed to be lost from the system. When a sinkhole is simulated, the depth of water for the day from the HRU in the confined aquifer is calculated using:

deepst = gwseep + (1 - sink) * (surfq +latq) **[30]**

Where, *deepst* is the depth of water in the confined aquifer for the day from the HRU, *gwseep* is the amount of water recharging the deep aquifer for the day from the HRU, and (*surfq+ latq)* is the water that goes through a sinkhole generated for the day from the HRU.

4.3.1.1 Verification of model modifications

After *sink* was allocated, defined, and initialized in the new code and the new variable was specified in the groundwater input file, *sink* was read and printed in the input file successfully. The SWAT model and the new SWAT-karst were run in a monthly basis. The SWAT-karst was run to simulate a sinkhole as an HRU (sink=1). Surface runoff and lateral flow were included in aquifer recharge calculations and not included to calculate water entering to the main channel. The model output confirmed that the water that sinks through a sinkhole is included in baseflow calculations. The cumulative aquifer recharge and baseflow in a sinkhole increased in 40% in a year (Figures 17 and 18).

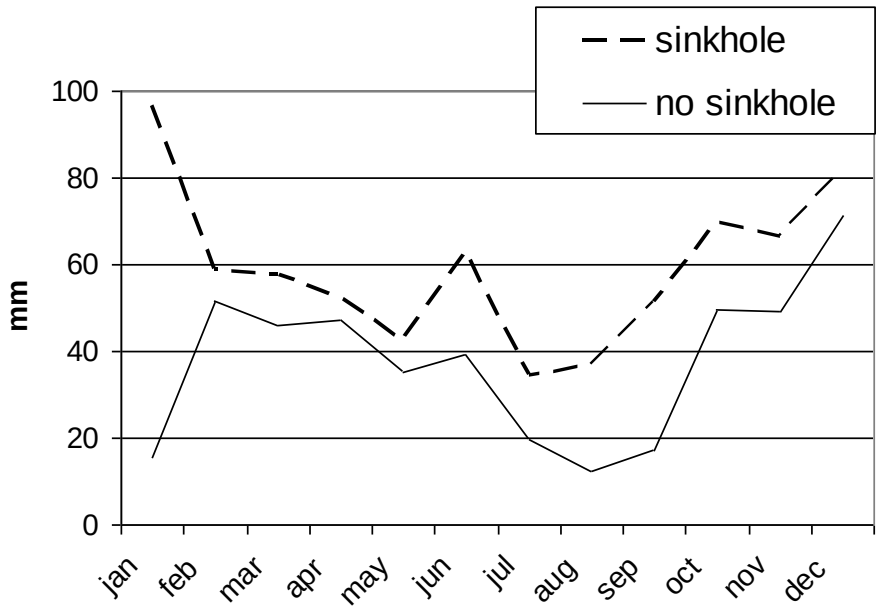

Figure 17. Monthly unconfined aquifer recharge when a sinkhole is simulated.

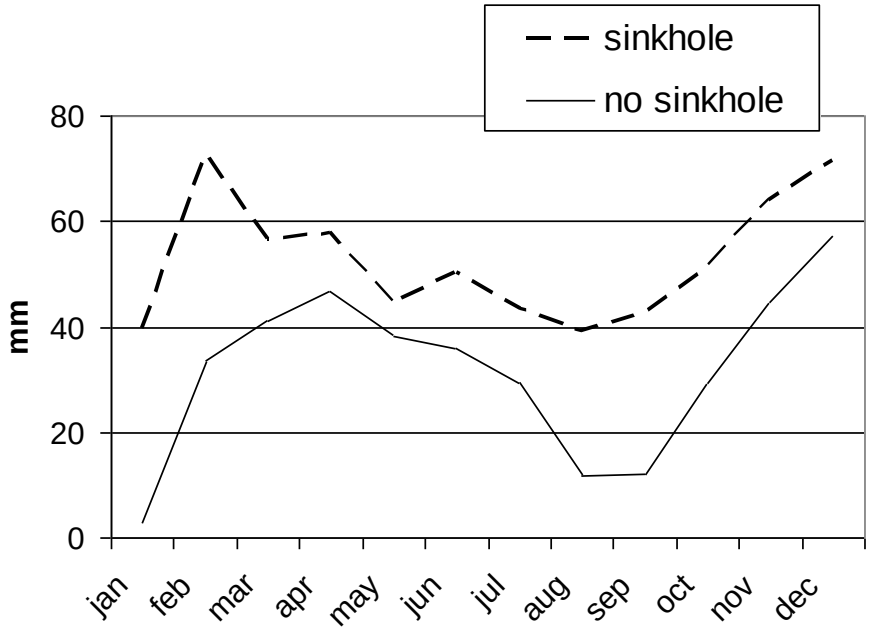

Figure 18. Monthly baseflow when a sinkhole is simulated.

4.3.2 Nitrogen transport in sinkholes

In karst environments, the amount of nitrate that goes through a sinkhole and recharges the unconfined aquifer should be, conceptually, equal to the amount of nitrate transported with surface water and lateral flow of the area that sinks into the sinkhole. The SWAT code was modified to represent the transport of nitrate through a sinkhole in an HRU. The subroutine *virtual* summarizes data, prints the daily output HRU file, and calculates the loading of nutrients into streams from a subbasin with multiple HRUs. When a sinkhole is simulated as an HRU (when *sink* >0), nitrate transported with surface runoff (*surqno3*) and lateral flow (*latno3*) generated from the HRU are not included in the calculation of nitrate loading entering the main channel from the subbasin (Figure 19).

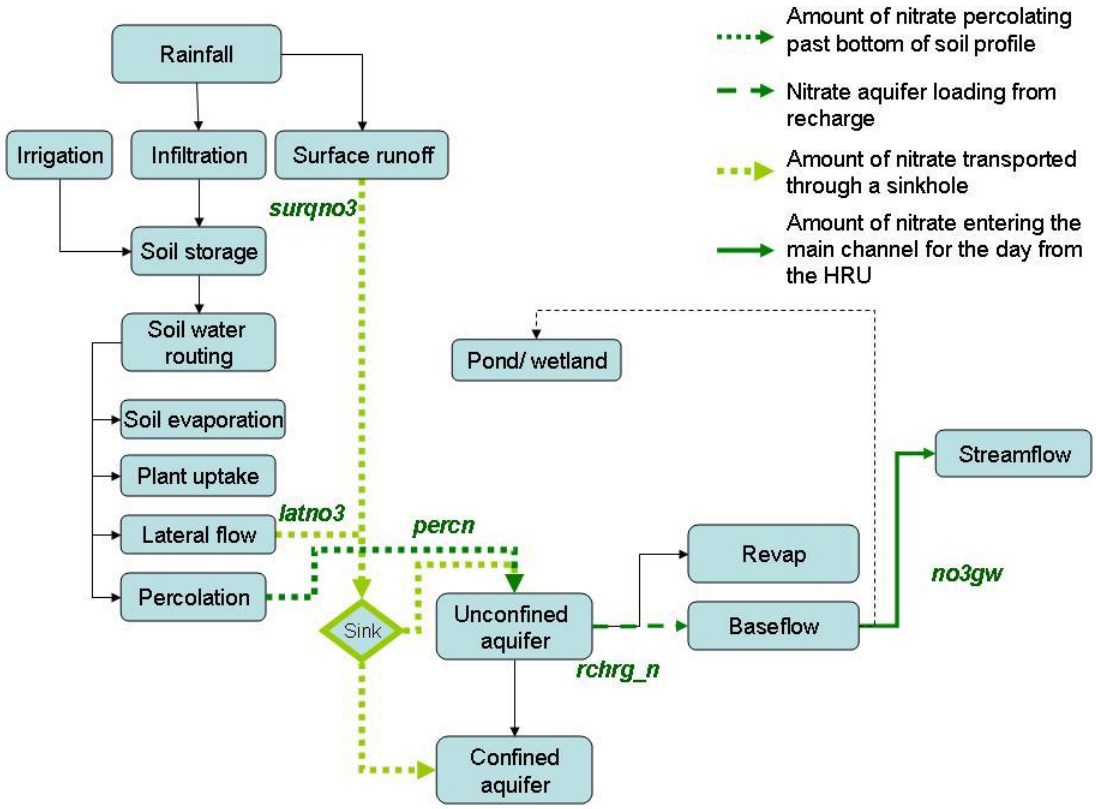

Figure 19. Schematic pathways for nitrate movement in SWAT in a sinkhole.

The subroutine *gw_no3* calculates the nitrate loading from aquifer recharge and nitrate baseflow contribution to streamflow in an HRU. Two new variables were created to allow simulating the nitrate loading that goes through a sinkhole and recharges the aquifer in an HRU. The new variables, *rchrg_nsepbtm* and *rchrg_ndirect*, were allocated, defined, and initialized in the subroutines *allocate_parms, modparm, and zero1,* respectively. In non-karst regions, the nitrate aquifer loading from recharge is calculated using:

rchrg_nsepbtm = (1 - exp [-1/delay]) * percn + exp [-1/delay] * rchrg_nsepbtm1 **[31]**

Where, *rchrg_nsepbtm* is the nitrate aquifer loading from recharge from percolating water through the soil for the day from the HRU, *delay* is the delay time (days), *percn* is the daily amount of nitrate transported with percolating water, and *rchrg_nsepbtm1* is the nitrate aquifer loading from recharge from percolating water for the previous day. The amount of nitrate transported through a sinkhole is calculated using:

sepn_direct = sink * (surqno3 + latno3) **[32]**

Where, *sepn_direct* is the nitrate loading that goes through karst features for the day from the HRU, *surqno3* is the nitrate transported with surface runoff generated from the HRU, *latno3* is the nitrate transported with lateral flow generated from the HRU, and *sink* is the sinkhole partitioning coefficient. Using the delay time for karst features (Equation 25), the nitrate loading to the unconfined aquifer from karst features is calculated using:

rchrg_ndirect = (1 - exp[-1/(delay/10)]) * sepn_direct +
exp[-1/(delay/10)] * rchrg_ndirect1 **[33]**

Where, *rchrg_ndirect* is the nitrate aquifer recharge loading from karst features for the day from the HRU, *delay* is the delay time (days), and *rchrg_ndirect1* is the nitrate aquifer recharge loading for the previous day.

The total nitrate aquifer loading from recharge for the day from the HRU is calculated using:

rchrg_n = rchrg_nsepbtm + rchrg_ndirect **[34]**

4.3.2.1 Verification of model modifications

After the new variables were allocated, defined, and initialized in the new code, the SWAT model and the new SWAT-karst were run in a monthly basis. The SWAT-karst was run to simulate the nutrient transport through a sinkhole as an HRU. The model output confirmed that nitrate transported through sinkholes is included in baseflow calculations (Figure 20). The cumulative nitrate transported with groundwater increased 1% in a year.

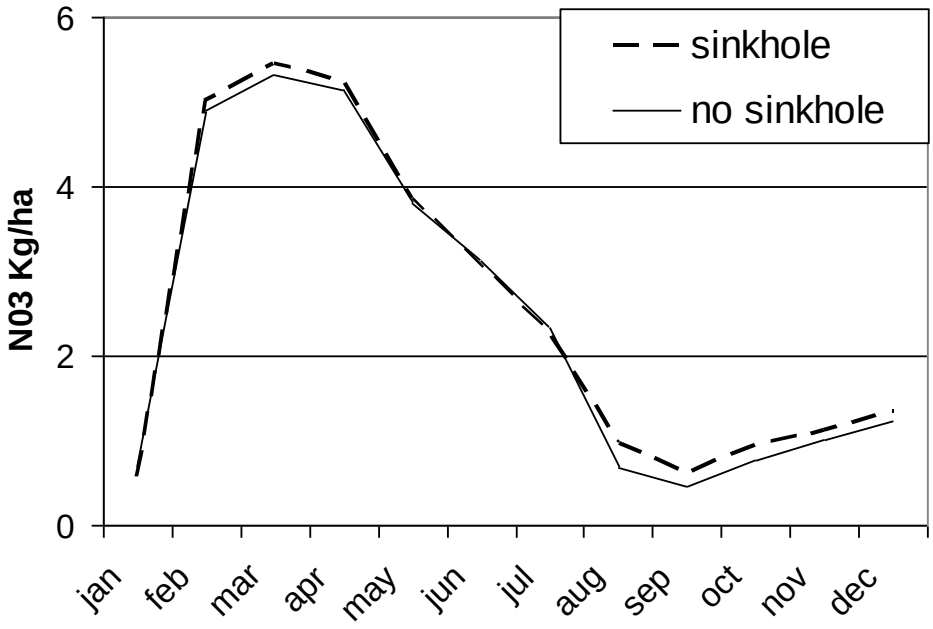

Figure 20. Monthly nitrate transported with baseflow when a sinkhole is simulated.

4.3.3 Sinking streams

In karst environments, surface streams from non-carbonate regions of the watershed sink in carbonate regions, and part of the surface water becomes groundwater. Sinking streams are simulated using the Baffaut and Benson (2008) approach. Specifically, sinking streams are

represented using tributary channels with a high hydraulic conductivity in the bed of the channel. Transmission losses contribute seepage to the unconfined aquifer. When simulating tributary channels, non-karst and sinking streams regions cannot be differentiated in a subbasin.

Nitrate transported with transmission losses from sinking streams is not simulated in SWAT. The sinking stream nutrient partitioning coefficient (*ss)* was introduced to the code to simulate nitrate transported with transmission losses in an HRU (Figure 21). *Ss* is the fraction resulting from dividing transmission losses by surface runoff. *Ss* is described only locally in the subroutines and is calculated using:

$$ss = tloss / surfq \quad \textbf{[35]}$$

Where, *ss* is the sinking stream nutrient partitioning coefficient from the HRU, *tloss* is the water lost from sinking streams (mm), and *surfq* is the surface runoff generated for the day from the HRU (mm).

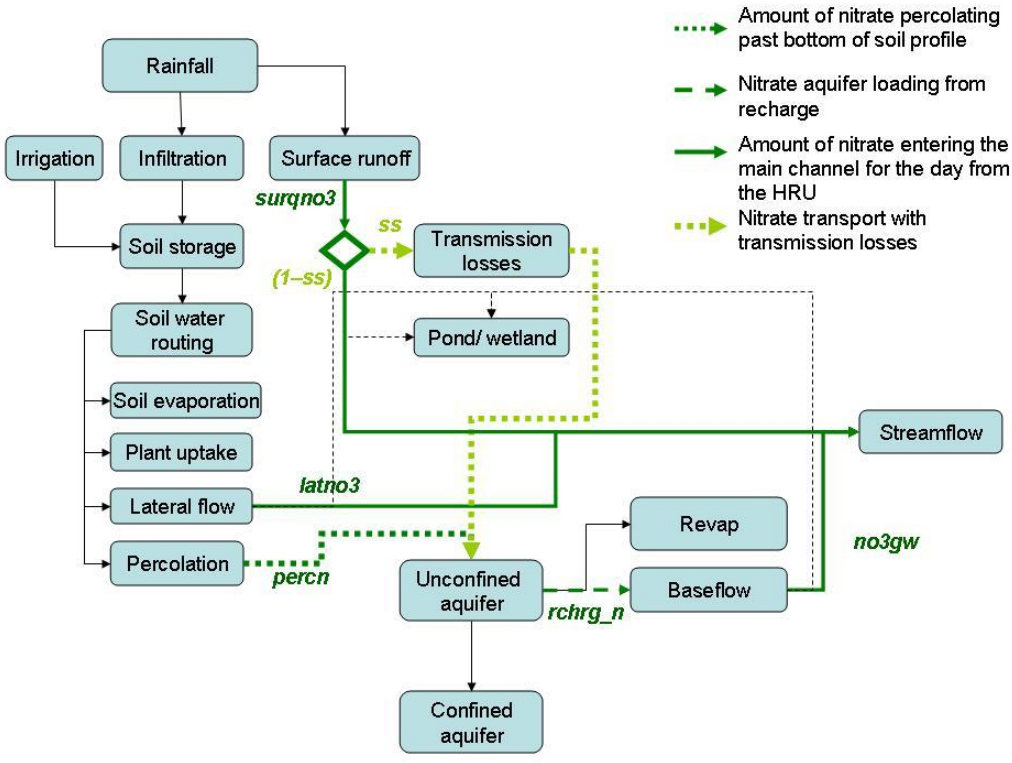

Figure 21. Schematic pathways for nitrate movement with transmission losses from a sinking stream in SWAT.

The subroutine *gw_no3* calculates the nitrate loading from aquifer recharge and nitrate baseflow contribution to streamflow in an HRU. Nitrate transported with surface runoff is partitioned to calculate sinking streams nitrate losses. The amount of nitrate lost from sinking streams is included in nitrate aquifer loading calculations. Nitrate lost from sinking streams is calculated using:

sepn_direct = ss * surqno3 **[36]**

Where, *sepn_direct* is the nitrate loading that goes through karst features for the day from the HRU, *ss* is the sinking stream nutrient partitioning coefficient, and *surqno3* is the amount of nitrate in surface runoff for the day from the HRU (kg N/ha). Nitrate lost from sinking streams is used in nitrate aquifer recharge loading calculations using Equation 33. The subroutine *virtual* calculates the amount of nitrate generated from the HRU entering the main channel. In this subroutine, nitrate lost from sinking streams is subtracted from the nitrate transported with surface runoff.

sub_no3 = (1-ss)*surqno3 * hru_dafr **[37]**

Where, *sub_no3* is the NO_3-N -N in surface runoff for the day in the subbasin (kg N/ha), *ss* is the sinking stream nutrient partitioning coefficient, *surqno3* is the amount of NO_3-N -N in surface runoff for the day from the HRU (kg N/ha), and *hru_dafr* is the fraction of watershed area in HRU.

4.3.3.1 Verification of model modifications

After the new variable *ss* was included in the new code, the SWAT model and the SWAT-karst were run in a monthly basis. The modified SWAT-karst was run to simulate sinking streams in a subbasin. Nitrate transported with surface runoff was partitioned. The model output confirmed that nitrate in transmission losses were included in baseflow calculations (Figure 22). The cumulative nitrate transported with baseflow increased eight percent in simulating sinking streams.

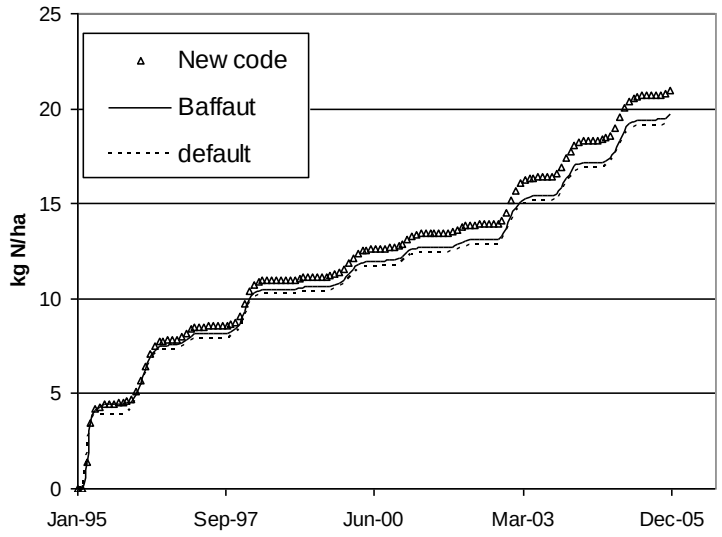

Figure 22. Cumulative NO_3 transported with baseflow when a sinking stream is simulated.

4.3.4 Springs

In karst regions, baseflow from a karst system usually returns to the surface through springs. Watersheds are defined by topographic boundaries; a groundwater basin for a karst spring (or group of springs) is defined by features such as sinking streams and cave streams, surveyed cave passages, and lithologic boundaries (White, 2002). The SWAT model itself cannot simulate a groundwater basin.

The first step in representing springs is to remove the amount of water that returns to the surface through a spring from the unconfined aquifer of the subbasin. The second step is to return the same amount of water as a point source where the spring is located. The amount of water removed is specified as the average daily water removal from the unconfined aquifer for each month of the year, and the water that is removed from the subbasin is considered lost from the system.

Point sources represent the loading of water and pollutants located at any point along the channel network. Point sources are used to represent water loadings from a spring feature and, at the

same time, return the water that is removed from the unconfined aquifer. Point sources are located near the subbasin outlet.

Chapter 5: Karst-influenced watershed simulation

5.1 Study area

The study site is the Opequon Creek watershed, located in the Potomac and Shenandoah River basin in Frederick and Clarke Counties in Virginia and Berkeley and Jefferson Counties in West Virginia (Figure 23). The Opequon River flows into the Potomac River northeast of Martinsburg, WV. The Opequon Creek watershed covers an area of 89,020 ha. According to the Opequon Creek Project Team (2008), nitrogen and phosphorus impairment indices developed in 2004 by the Potomac Tributary Stakeholder Team showed that Opequon Creek had the highest concentration for both nitrogen and phosphorus, more than any other West Virginia Potomac sub-watershed. These contaminants come from both point sources (wastewater treatment plants) and nonpoint sources (agricultural and suburban land uses).

5.2 Model input data

5.2.1 Elevation

The National Elevation Dataset (NED) 1/3 arc second resolution was downloaded from The National Map Seamless Server website (USGS, 2009a). The digital elevation model (DEM) coordinate system is GCS North American 1983 geographic coordinates. The DEM for the Opequon Creek watershed was projected using ArcGIS 9.2. The projected DEM coordinate system is NAD 1983 UTM zone 17N and the DEM has a 10 meter resolution (Figure 24). The mean elevation in the Opequon Creek watershed is 188 meters, with a maximum of 513 meters and a minimum of 45 meters (Figure 25). Using the latest version of SWAT model ArcView GIS interface (AVSWAT-X), the watershed and subbasin boundaries and topographic inputs were calculated with the 10-meter elevation data.

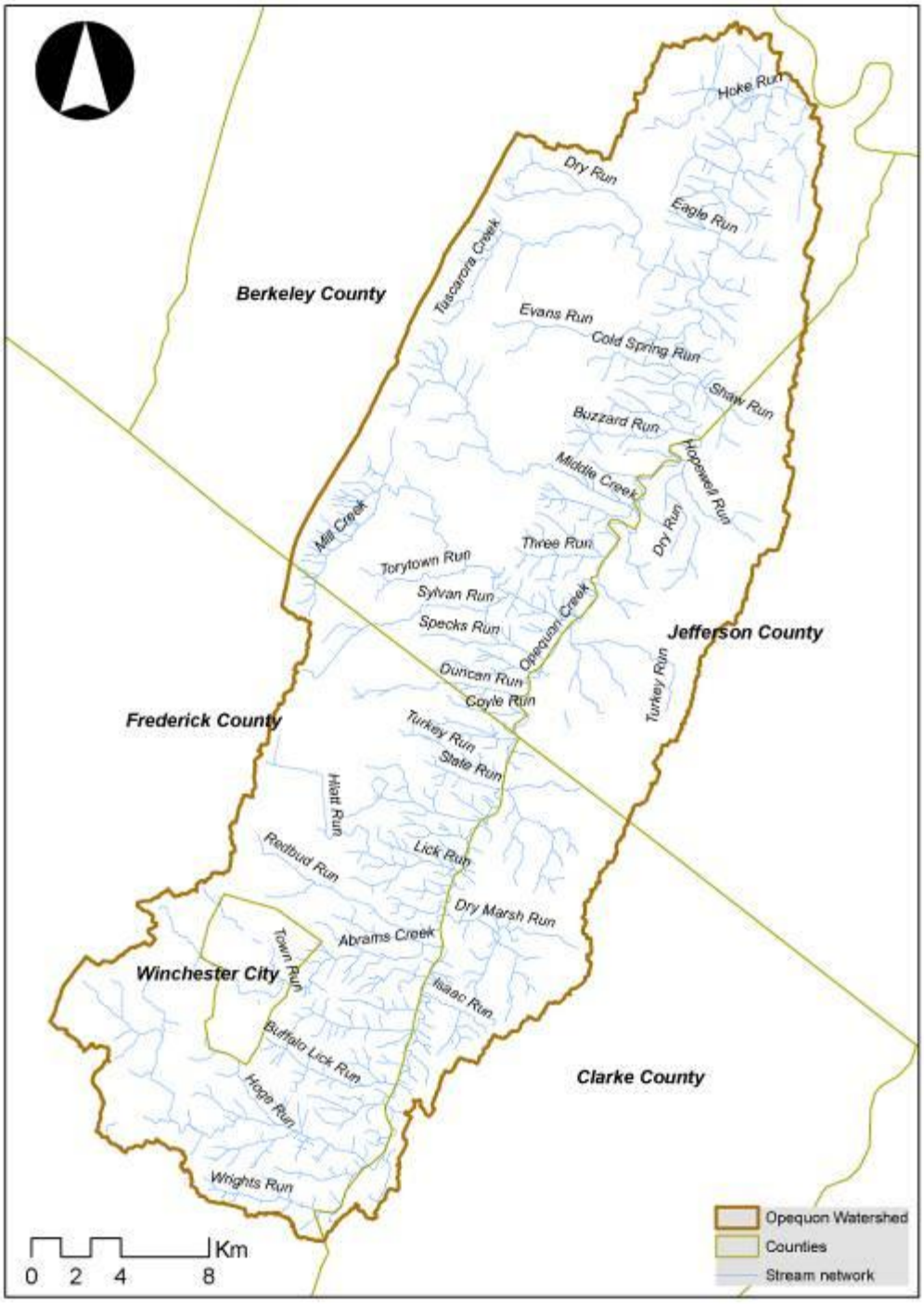

Figure 23. Opequon Creek Watershed.

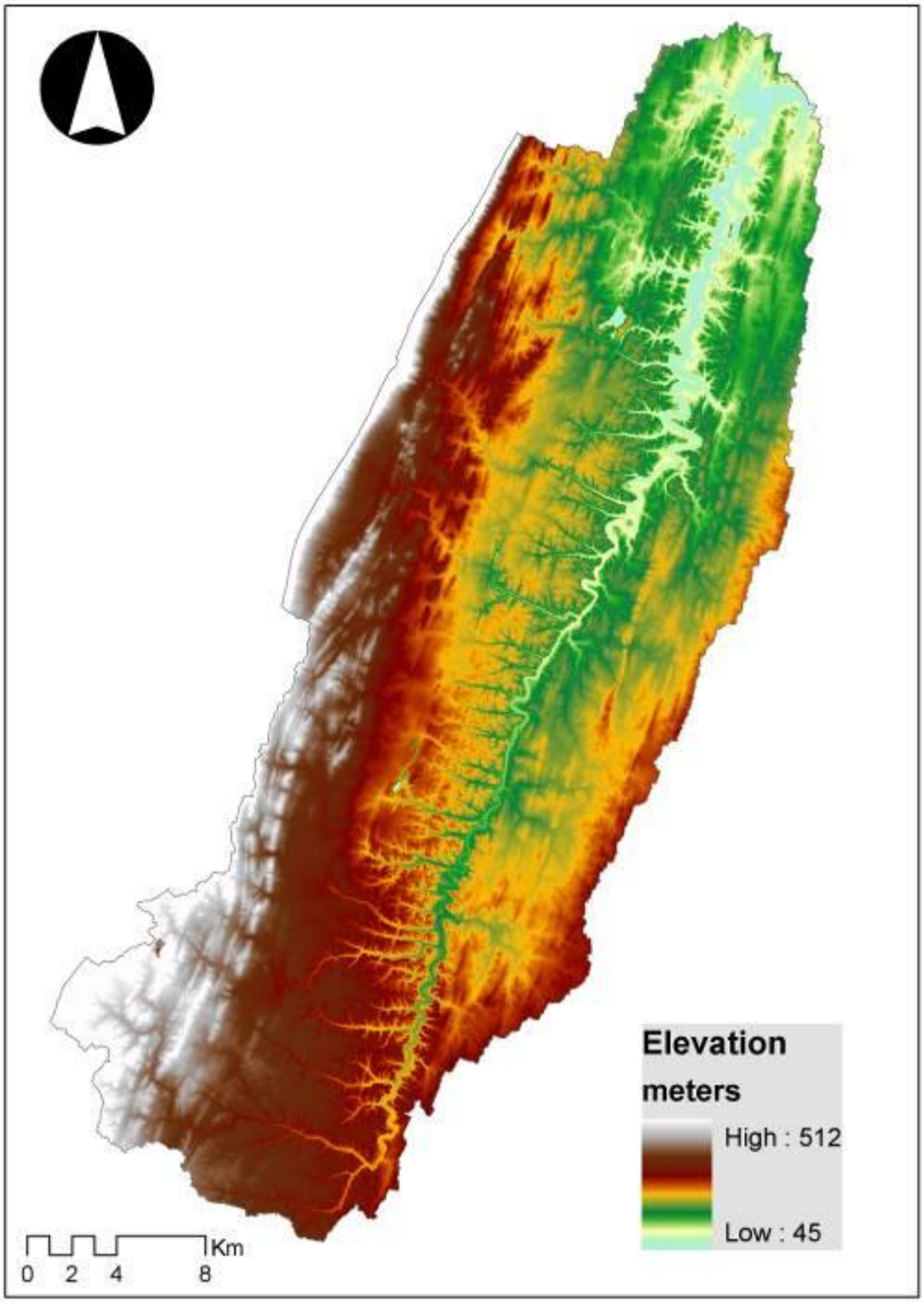

Figure 24. Data from the National Elevation Dataset for the Opequon Creek Watershed.

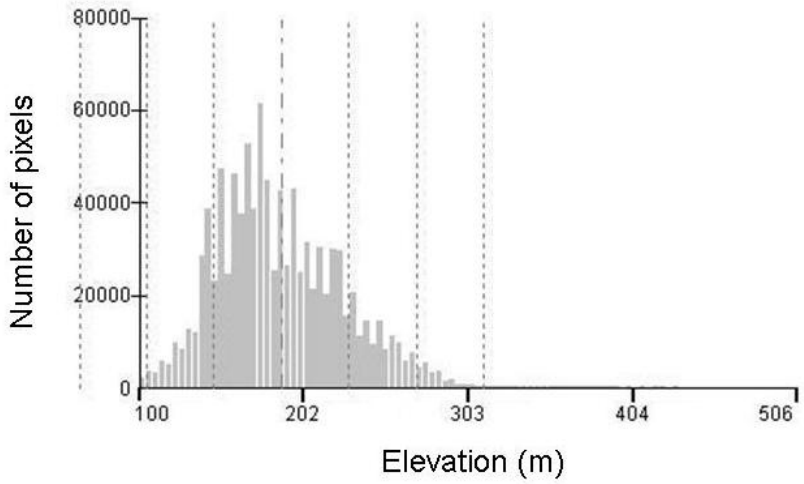

Figure 25. Opequon Creek Watershed elevation distribution.

5.2.2 Soil data

Soil information was obtained from the Soil Survey Geographic (SSURGO) Database and the State Soil Geographic (STATSGO) data set website (USDA-NRCS, 2009). The SSURGO database provides the highest level of soil detail on a county basis, while the STATSGO data set was originally intended for use on a state basis (Peschel et al., 2003). SSURGO data are available for the entire watershed except for the city of Winchester, VA. STATSGO data for the city of Winchester were used.

SSURGO Extension for AVSWAT-X (SEA) is an extension of the AVSWAT-X interface. The SEA tool is designed to download SSURGO data via the internet, to create digital soil maps, and to produce soil input parameters required by SWAT (Arnold et al., 2005). SEA could generate soil inputs only for Clarke County, Virginia. The data for the other counties were insufficient. Furthermore, SEA generated an error when creating the soil digital map because there are no SSURGO data for the city of Winchester.

The SSURGO SWAT 1.0 extension is a tool used in combination with the AVSWAT-X interface (Peschel, 2003). The tool prepares and incorporates SSURGO soil data sets into a format that the SWAT model can use. The SSURGO SWAT 1.0 extension successfully extracted

the soil data required by the model. In the Opequon Creek watershed, a total of 223 soil types were found (Figure 26). Water, pits, quarries, dams, and unsurveyed soils do not contain soil information. For those soils, the adjacent soil attributes were used. The soil data extracted from the SSURGO and STATSGO data provided the soil physical properties that control the movement of water and air through the soil profile within the HRU.

5.2.3 Landuse

Landuse information for the Opequon Creek Watershed was provided by Strager (2009) (Figure 27). The ten meter resolution land cover map was digitized by Strager and others using aerial photographs from the National Agriculture Imagery Program (NAIP). Seven land cover categories were identified in the watershed. Pasture areas represent almost forty percent of the total area of the watershed (Table 7). Using the AVSWAT-X interface, the SWAT land cover and plant growth database was linked to the landuse grid. This database supplies the information required to simulate plant growth in an HRU.

Table 7. Opequon Creek watershed landuse categories (Strager, 2009)

Category	Explanation	Area percentage
Open water	Larger lakes and rivers	0.2
Forest/woodland	Forested areas, wooded areas	37
Open/grassland/pasture	Includes open fields, sparsely forested areas, yards, open areas	38.1
Agriculture/row crops	Tilled or plowed fields, with or without crops	13.3
Urban/impervious	Urban or highly developed areas with a high degree of pavement or impervious surfaces	9.2
Barren	Bare earth	1.8
Wetland/small ponds	Wetlands, small ponds, marshes, swamps	0.4

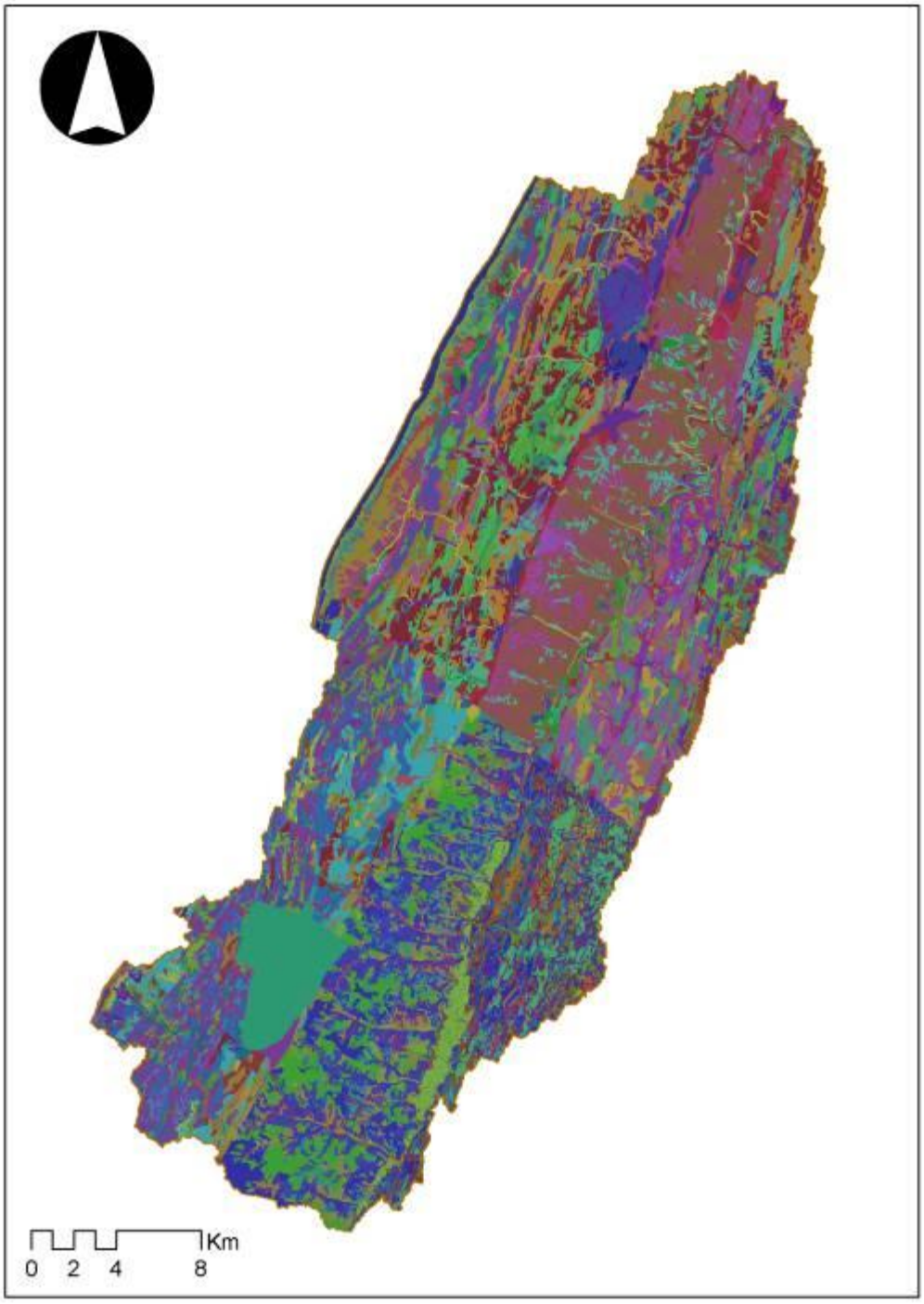

Figure 26. Soil survey geographic dataset (SSURGO) for the Opequon Creek watershed.

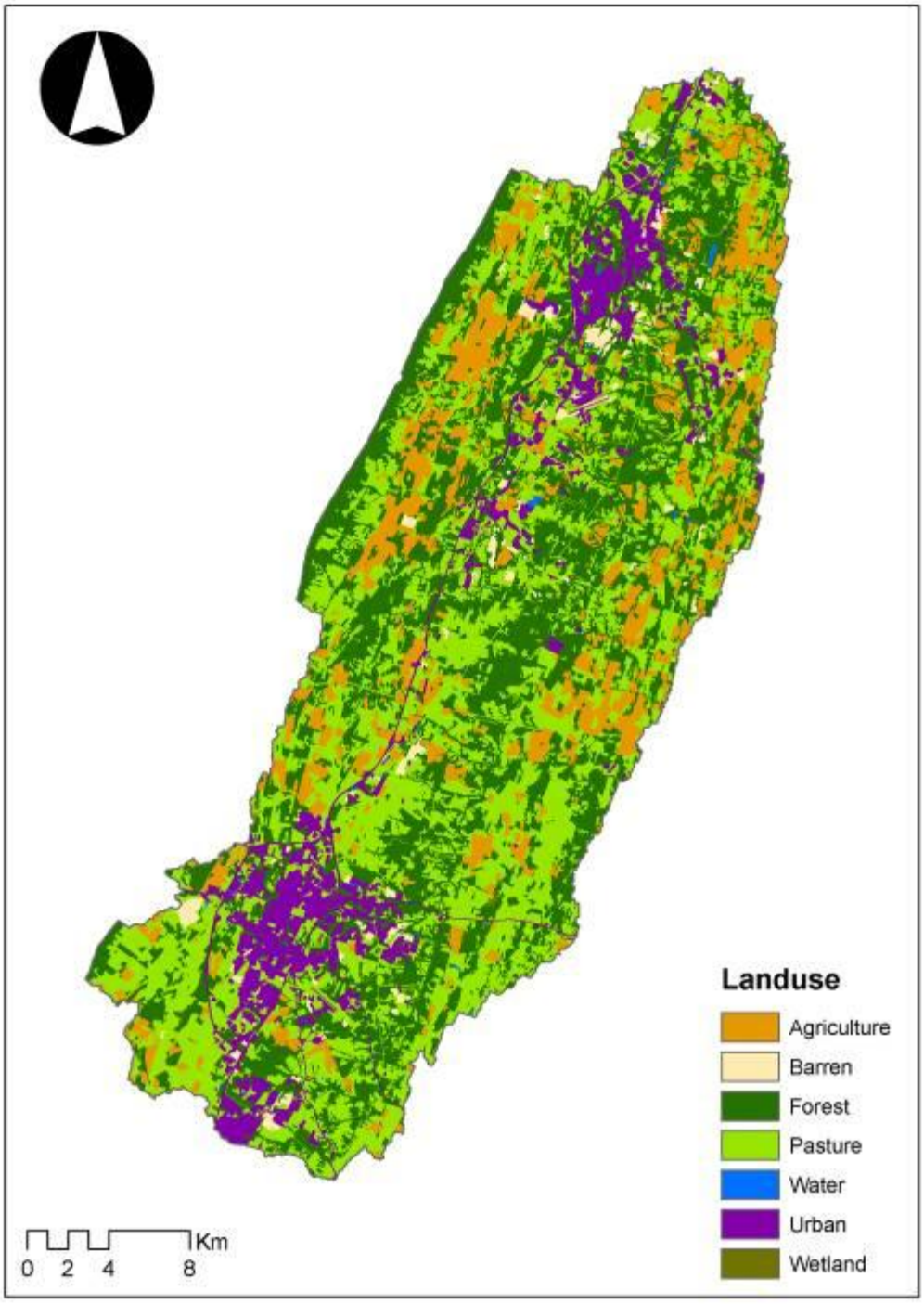

Figure 27. Ten meter resolution landuse map for the Opequon Creek Watershed using data from Strager (2009).

5.2.4 Climate Data

Climate data for Opequon Creek Watershed were downloaded from the NOAA Satellite and Information System website (NOAA, 2009). Daily precipitation and daily maximum and minimum temperature data were acquired for four weather stations from 1999 to 2009. Average daily wind speed and average daily dew point temperatures were from only one station from 2001 to 2009 (Table 8).

Table 8. Weather station locations.

Station Name	Latitude	Longitude	Data available
Star Tannery	39º 5′	-78º 26′	Daily precipitation and maximum and minimum temperature (1999-2009)
Winchester	39º 11′	-78º 9′	Daily precipitation and maximum and minimum temperature (1999-2009)
Winchester 7 Se	39º 11′	-78◦ 7′	Daily precipitation and maximum and minimum temperature (1999-2009)
Martinsburg E WV Rgnl Ap	39º 24′	-78º 59′	Daily precipitation and maximum and minimum temperature (1999-2009) Wind speed and dew point temperature (2001-2009)

The SWAT model requires daily precipitation, maximum and minimum temperature, solar radiation, wind speed, and relative humidity. Daily climate data can be read from observed data or can be generated. Daily climate data are generated when measured data are missing. The SWAT weather generator needs statistical parameters (Table 9) to generate the daily climate data.

Table 9. Statistical parameters required for daily weather data generation by the SWAT weather generator.

Parameters for the weather generator	Description
TMPMX(mon)	Average or mean daily maximum air temperature for month (ºC).
TMPMN(mon)	Average or mean daily minimum air temperature for month (ºC).
TMPSTDMX(mon)	Standard deviation for daily maximum air temperature in month (ºC).
TMPSTDMN(mon)	Standard deviation for daily minimum air temperature in month (ºC).
PCPMM(mon)	Average or mean total monthly precipitation (mm H_2O).
PCPSTD(mon)	Standard deviation for daily precipitation in month (mm H_2O /day).
PCPSKW(mon)	Skew coefficient for daily precipitation in month.
PR_W(1,mon)	Probability of a wet day following a dry day in the month.
PR_W(2,mon)	Probability of a wet day following a wet day in the month.
PCPD(mon)	Average number of days of precipitation in month.
RAINHHMX(mon)	Maximum 0.5 hour rainfall in entire period of record for month (mm H_2O).
SOLARAV(mon)	Average daily solar radiation for month (MJ/m^2/day).
DEWPT(mon)	Average daily dew point temperature in month (ºC).
WNDAV(mon)	Average daily wind speed in month (m/s).

Daily precipitation and daily maximum and minimum temperature records were used as inputs to the pcpSTAT program (Liersch, 2003) to compute the statistical parameters used by the weather generator of the SWAT model. The weather generator was used to generate daily data to replace missing daily precipitation and maximum and minimum temperature. Daily solar radiation, wind speed, and relative humidity were generated using the weather generator.

5.2.5 Opequon Creek Watershed Karst Features

Previous studies reported and depicted the location and characteristics of karst features providing information for this study. Jones (1997) depicted the results of dye trace studies conducted in

West Virginia through August 1997 and portrayed the location of karst features such as sinkholes and springs (Figure 28). Tracer tests represent only the dye injection point and the resurgence point (springs) rather than underground flow routes.

In Berkeley County, West Virginia, karst regions appear over about 40 percent of the county area (Jones, 1997). In the Shenandoah Valley karst region, the aquifer recharge is mostly autogenic. Jones (1997) reported that the annual groundwater recharge estimate of 254 mm is equivalent to the average discharge of the Shenandoah Valley karst region. In Jefferson County, West Virginia, karst regions appear over about 80 percent of the county area. In karst regions of this county, diffuse infiltration appears to be dominant and the average groundwater recharge was estimated at 241 mm per year (Jones, 1997).

Orndorff and Goggin (1994) plotted karst features such as sinkholes, caves, springs, and travertine deposits in the Shenandoah Valley (Figure 28). The sinkholes were identified from the USGS topographic quadrangle maps, some were mapped in the field, and others from previous studies. Orndorff and Goggin (1994) found that the most common karst features in the Shenandoah Valley were sinkholes.

The images from Jones (1997) and Orndorff and Goggin (1994) showing the locations of karst features were georeferenced using the georeferencing tool in ArcGis 9.2. Karst feature locations were digitized from the georeferenced images using the editor tool in ArcGis 9.2. The National Hydrography Dataset (USGS, 2009b) provided shape files containing springs locations, however, the information is not as detailed as the Orndorff and Goggin (1994) maps (Figure 28).

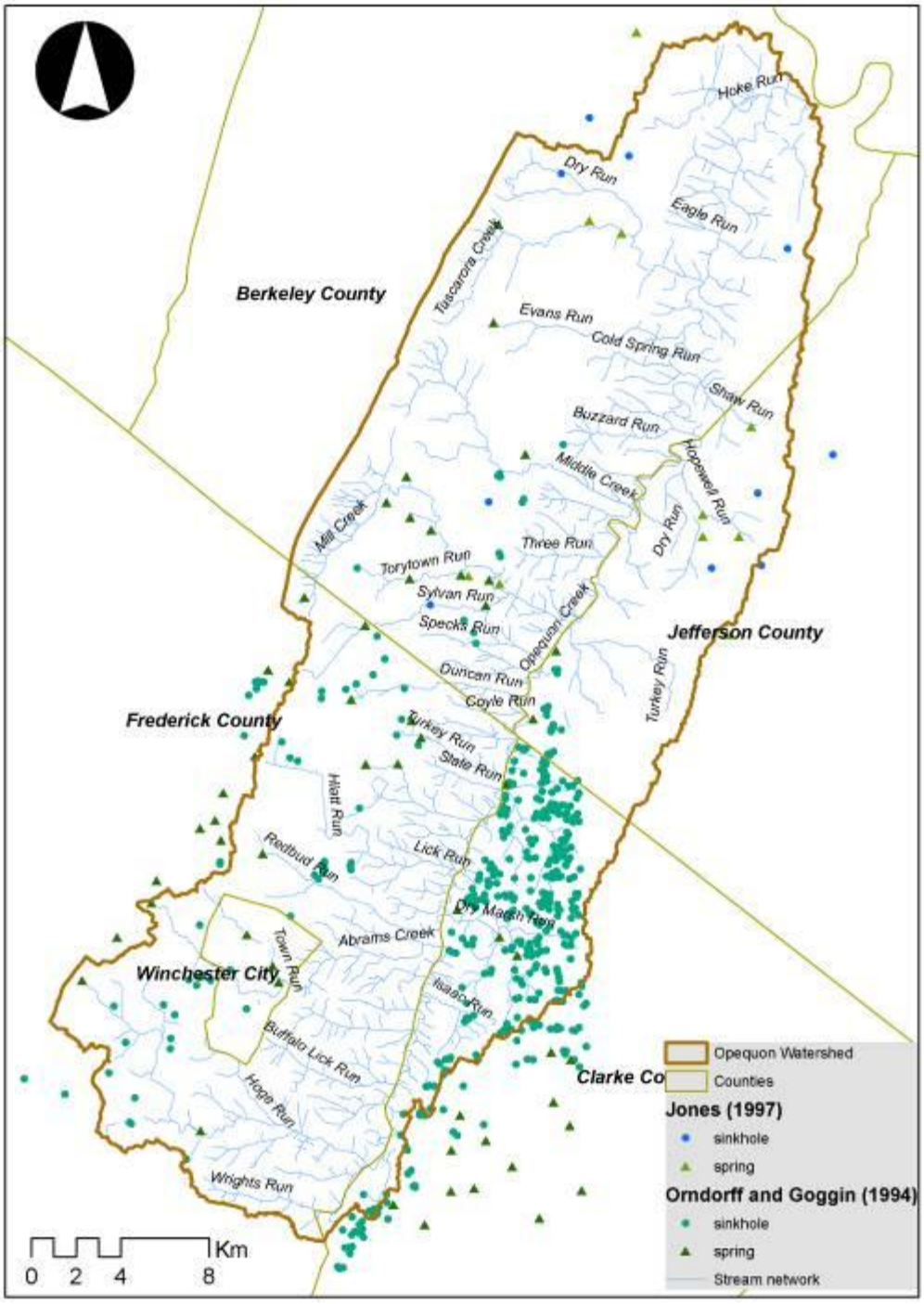

Figure 28. Opequon Creek Watershed springs and sinkhole locations, using data from Jones (1997) and Orndorff and Goggin (1994).

Jones (1997) and Orndorff and Goggin (1994) datasets only provide the location of sinkholes; they do not provide the area that contributes surface water to the sinkholes. In the Opequon Creek watershed, sinkhole regions were identified using the 10 meter resolution DEM obtained from the national elevation dataset. Using the spatial analysis tool in ArcGis 9.2, the elevation data were filled to eliminate depressions. Using raster calculator in ArcGis 9.2, the original elevation data were subtracted from the filled elevation to obtain sinkhole locations, area, and depth information (Figure 29 A). However, this process generated sinkholes in the streams. Using a buffer tool and a 60 meter buffer, those sinkhole regions were identified and eliminated (Figure 29 B). The remaining sinkhole regions represent 2.5 percent of the watershed area (2226 Ha).

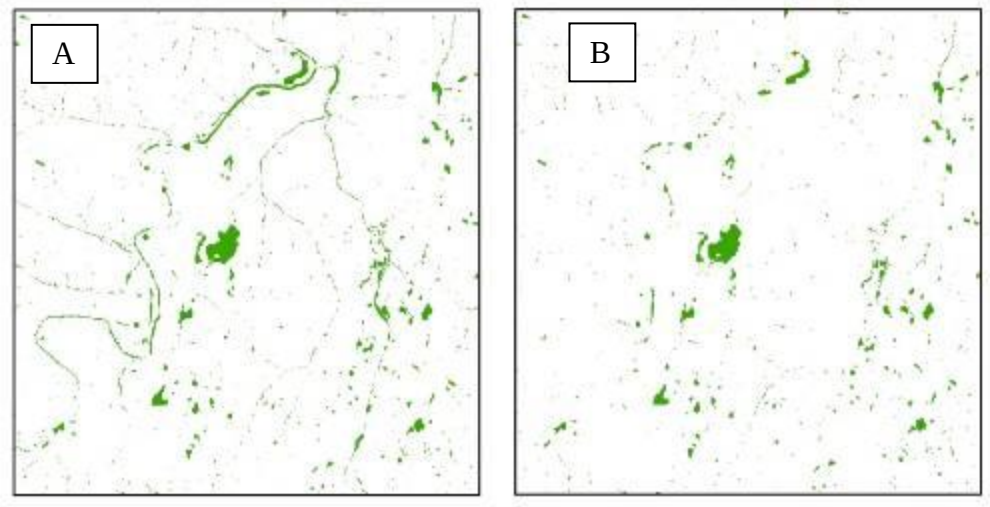

Figure 29. Depressions (A) and depressions with streams eliminated (B) in a portion of the Opequon Creek Watershed. Depressions with streams eliminated were considered as sinkholes for the simulation.

Identifying sinkhole locations using the DEM was not visually accurate when it was compared with Jones (1997) and Orndorff and Goggin (1994) datasets (Figure 30). In figure 30, sinkhole regions were close and sometimes in the same locations as the sinkhole location depicted by Jones (1997) and Orndorff and Goggin (1994), but in many instances, feature locations do not match. However, identifying sinkholes using a DEM was the only method that could provide sinkhole regions for the whole watershed.

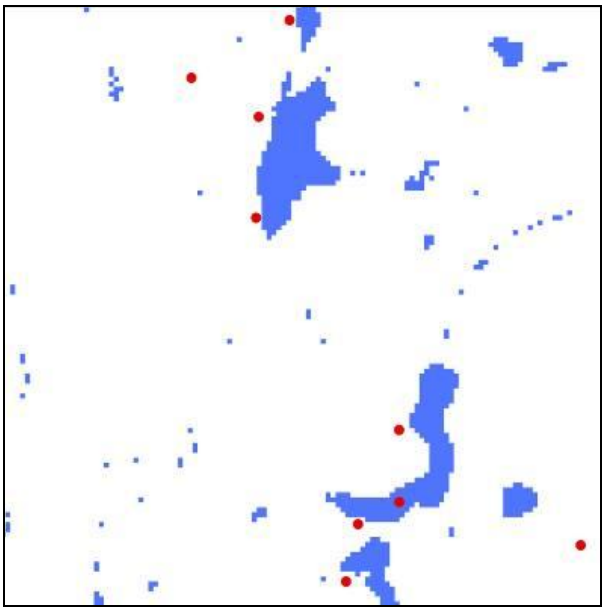

Figure 30. Sinkhole regions from a DEM and sinkhole points depicted by Jones (1997) and Orndorff and Goggin (1994) for a sample area of Opequon Creek watershed.

Evaldi and Paybins (2006) portrayed the locations of sinking streams and dry channel areas in the Opequon Creek watershed in West Virginia. Based on stream discharge measurements obtained at 69 sites, sinking stream regions were identified. Based on field experience of Lawrence (2009), sinking stream regions in the Virginia part of the Opequon Creek watershed were identified.

5.3 Karst-influenced watershed simulation

5.3.1 Watershed delineation

The National Elevation Dataset (NED) 10 meter resolution and streams network shape files downloaded from the National Hydrography Dataset (NHD) were used as inputs during the watershed delineation. The DEM was used to delineate all the subbasins and stream topographic parameters. The NHD stream network shape file was superimposed onto the DEM to define the location of the stream network and to improve the process of hydrographic segmentation.

SWAT requires the user to specify the minimum drainage area that contributes to the stream (threshold area). When delineating subbasins, the lower the threshold the more detail is obtained. In the Opequon Creek watershed, the threshold of 300 Ha, used during the delineation, captured the stream networks existing in the watershed. In addition, subbasins were located where spring measurements and USGS stations were located. A total of 96 subbasins were delineated (Figure 31).

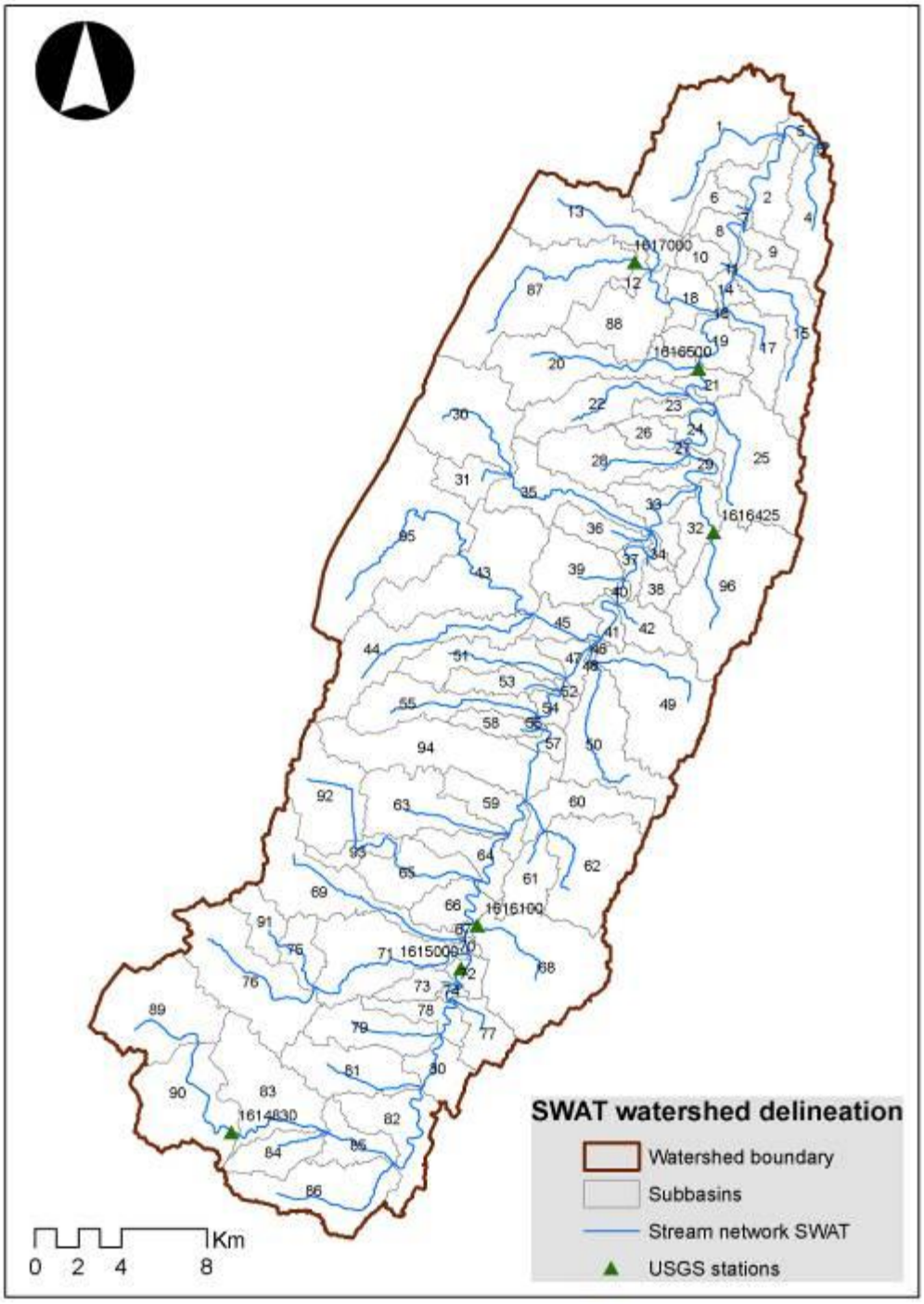

Figure 31. Opequon Creek watershed and subbasins delineation.

5.3.2 Hydrologic response units (HRUs)

There are two options to determine hydrologic response units (HRUs) in a subbasin. The dominant land use and soil option determines a single HRU for each subbasin based on the dominant landuse category and soil type within each subbasin. The multiple HRU option allocates multiple HRUs for each subbassin based on specified thresholds for the landuse and soil data. Land uses that cover a percentage of the subbasin area less than the threshold area are eliminated. The soil class threshold is used to eliminate minor soils within a land use area. The model developers recommend that a subbasin should have 1-10 HRUs (Neitsch et al., 2005). A landuse threshold of 20% and a soil class threshold of 10% are suitable. The developers also suggest that if more complexity is desired, the number of subbasins should be increased rather than the number of HRUs within a subbasin. If all the possible combinations of landuse and soil units per subbasin are simulated, a 0% landuse threshold and a 0% soil threshold are set.

Different numbers of HRUs were defined for different land use and soil class thresholds (Figure 32). The total number of HRUs in the watershed and the average number of HRUs within a subbasin are represented as bars and triangles in Figure 32, respectively. The recommended soil class threshold of 10% in the Opequon Creek watershed eliminated all the soils classes. In the Opequon Creek Watershed, a 20% landuse and a 5% soil class thresholds were selected because they yielded an average of 12 HRUs per subbasin, close to the maximum number of 10 per subbasin recommend by the model developers. Using that threshold combination resulted in 1196 HRUs.

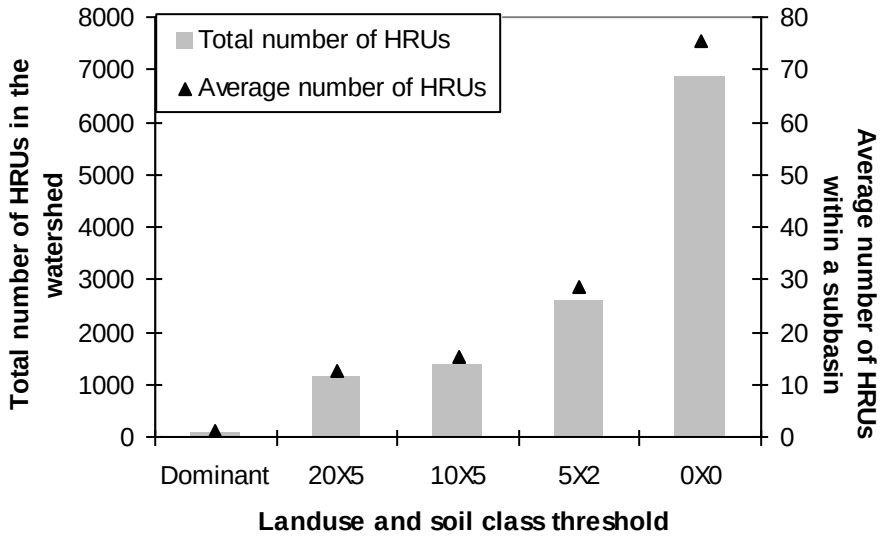

Figure 32. Total number of HRUs in the watershed and average number of HRUs within a subbasin using different thresholds.

The sinkhole regions obtained from the DEM and the landuse provided by Strager (2009) were overlapped using ArcGis 9.2, creating five new landuse categories. The new landuse categories have the unique characteristic that they are located in sinkhole regions. In the Opequon Creek watershed, less than 1% of each landuse is in a sinkhole region (Figure 33). The new landuse map was created to include sinkhole regions as an input in SWAT.

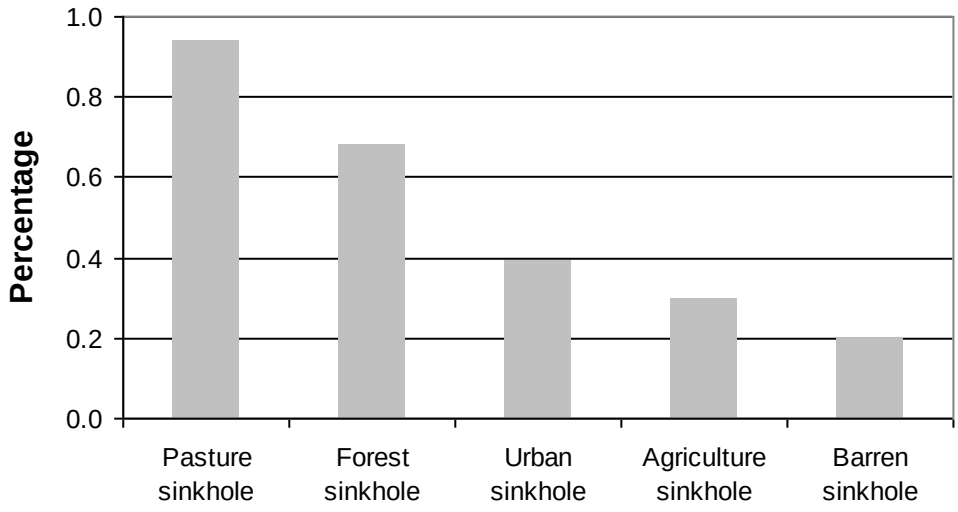

Figure 33. Percentages of landuses in sinkhole regions for the Opequon Creek Watershed.

Using the landuse dataset that includes sinkhole regions, different numbers of HRUs were defined for different land use and soil class thresholds (Figure 34). The total number of HRUs in the watershed and the average number of HRUs within a subbasin are represented as bars and triangles in Figure 34, respectively. In the Opequon Creek Watershed, setting the threshold to zero when a landuse category is lower than one percent generates an error. After applying the minimum threshold of 2% for both landuse and soil, SWAT could only capture 9 % of the total sinkhole regions of the watershed. Thus, this approach was not suitable for representing sinkholes in the Opequon Creek watershed.

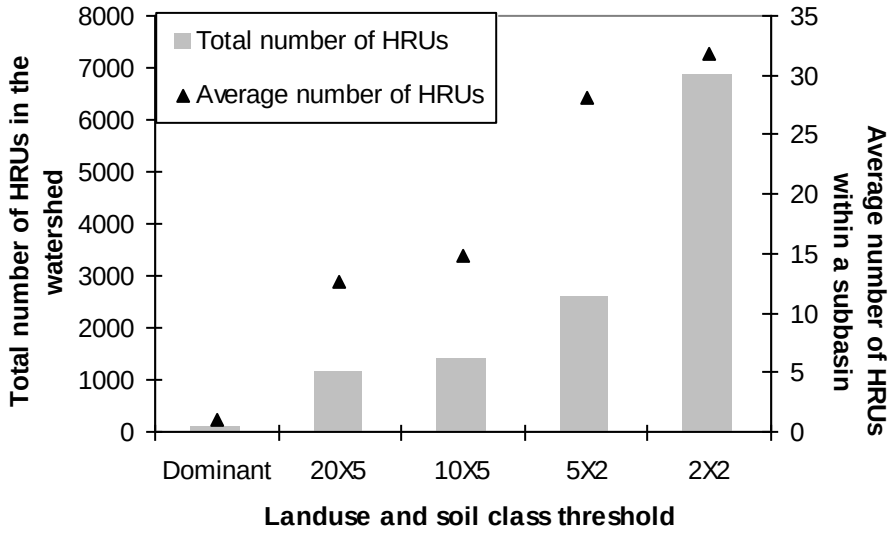

Figure 34. Total number of HRUs in the watershed and average number of HRUs within a subbasin including sinkhole regions using different thresholds.

5.4 Watershed simulation

The SWAT-B&B and SWAT-karst were run including sinkholes and sinking streams. Based on Evaldi and Paybins (2006) results, 13 subbasins were defined as sinking stream regions in West Virginia. Based on information provided by Lawrence (2009), another 13 subbasins were simulated as sinking stream regions in Virginia. In the Opequon Creek watershed, 26 subbasins were defined that contain sinking streams (Figure 34). In SWAT-karst and SWAT-B&B, sinking streams were simulated using high hydraulic conductivities in tributary channels. The same

hydraulic conductivity was used in all the identified sinking stream subbasins because no unique characteristics among sinking stream subbasins were found.

In SWAT-karst, HRUs were used to represent sinkholes. HRUs were selected to represent sinkholes based on the area of the sinkhole regions and the landuse where the sinkholes are located. In some cases, more than one HRU was used to simulate sinkholes in a subbasin. Sinkholes were simulated using the new parameter 'sink' (*sink*=1). In SWAT-B&B, sinkholes were represented as ponds by indicating the fraction of the subbasin that drains into the sinkhole region of the subbasin and specifying high hydraulic conductivities for the pond.

In karst regions, the delay time of 10 days was used to simulate the aquifer recharge from diffuse infiltration and the delay time of 1 day to simulate the aquifer recharge through sinkholes and sinking streams to represent the faster aquifer recharge through conduits. Baseflow was calculated using the maximum alpha factor (alpha=1). In non-karst regions, the SWAT default parameter values were used (Table 10). The simulations were performed for a period of 11 years from January 1999 to March 2009 with a daily time step.

Table 10. Parameters used in SWAT and SWAT-karst in the Opequon Creek watershed.

SWAT parameters	SWAT		SWAT B&B (2008)			SWAT-karst		
	Non-karst region	karst regions	Non-karst region	Karst region		Non-karst region	Karst region	
				Sinking stream	Sinkhole (Pond)		Sinking stream	Sinkhole (HRU)
Sink	-	-	-	-	-	0	0	1
Delay (days)	31	10	31	1	-	31	1	1
Alpha	0.048	1	0.048	1	-	0.048	1	1
Hydraulic conductivity (mm/hr)	0.05	0.05	0.05	250	100	0.05	250	0.05

∗The input value of the DELAY parameter is 10, which is then divided by 10 in the model, resulting in a delay time of 1 day.

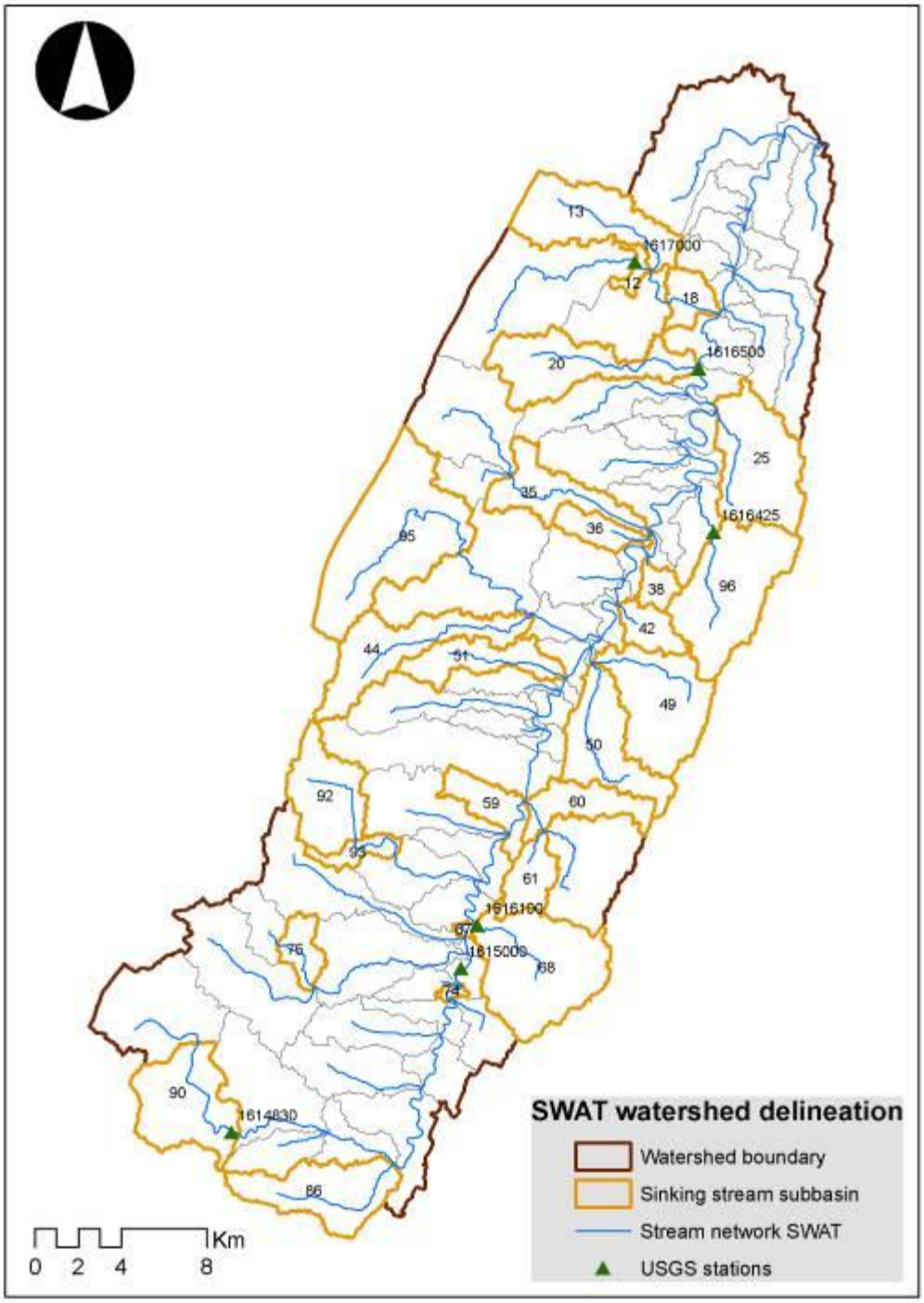

Figure 35. Sinking stream subbasins for the Opequon Creek watershed.

Nitrogen was applied to agricultural areas, grasslands, and urban areas at the rates shown in Table 11. The same amount of nitrogen was applied in the three models.

Table 11. Nitrogen applications in the Opequon Creek watershed

Landuse	Fertilizer Application Rates (kg/ha)	
	10-10-10	Urea
Agriculture/row crops	500	500
Pasture	250	-
Urban	50	-

5.5 Model evaluation

Models are often evaluated through calibration, which is the process of estimating model parameters by comparing model outputs for a given set of assumed conditions with observed data for the same conditions. In this study, no calibration was performed because it would disguise the strength of the new model for karst.

The SWAT, the SWAT-B&B, and the new SWAT-karst annual and monthly outputs were compared to evaluate the models' performance when simulating the Opequon Creek karst-influenced watershed. The model daily outputs for streamflow and stream nitrate concentrations were compared with observed data. A visual comparison between observed and simulated flow and nitrate concentrations showed the first overview of model performance. The next step was to calculate values for Nash-Sutcliffe efficiency (NSE), Percent bias (PBIAS), and RMSE-observations standard deviation ratio (RSR). With these values, model performance could be judged based on performance ratings for streamflow and nitrate. The general model evaluation guidelines for monthly results developed by Moriasi et al. (2007) were used in this study.

5.5.1 Annual output

For a period of 11 years from January 1999 to March 2009, SWAT-karst and SWAT-B&B average annual outputs were compared with the SWAT output to evaluate the annual water balance when representing the karst-influenced Opequon Creek watershed (Table 12). SWAT-karst and SWAT-B&B simulated 4% and 1%, respectively, less annual surface runoff depth than SWAT. SWAT-karst and SWAT-B&B simulated 12% and 10%, respectively, less annual surface runoff after transmission losses than SWAT (Figure 36).

Using SWAT-karst, the annual aquifer recharge depth increased 4%, and the annual baseflow depth increased 5%. Using SWAT-B&B, the annual aquifer recharge depth increased 3%, and the annual baseflow depth increased 3% (Figure 36). Transmission losses from sinking streams using SWAT-karst was 3 % less than the losses calculated using SWAT-B&B.

As a consequence of more surface water being lost through sinkholes in SWAT-karst than in SWAT-B&B, there is less surface runoff and less water being lost in sinking streams in SWAT-karst. Since the three models were run using the same parameters and input values, the only reason that SWAT-karst is calculating less runoff and more baseflow in the Opequon Creek watershed is the new capabilities introduced during model modification. SWAT-karst simulates the unique soil and landuse characteristics of sinkholes and the variability of sinkhole regions within the watershed. SWAT-B&B simulates sinkholes using a pond component to represent an average sinkhole in a subbasin, not capturing the unique characteristics of a sinkhole region.

SWAT-karst simulated a 5% increase in the annual nitrate loading transported with baseflow, while SWAT-B&B simulated a 1% increase. In SWAT-B&B, the nitrogen that is delivered to a pond is not transported to the aquifer when water seeps from the bottom of the pond.

Table 12. Opequon Creek watershed average annual predictions from a 10-year simulation by three versions of the SWAT model.

Average Annual Basin Values	SWAT	SWAT-B&B	SWAT-karst
Precipitation (mm)	981.20	979.50	979.50
Surface runoff (mm)	98.40	97.22	94.81
Surface runoff after transmission losses (mm)	97.65	88.21	86.09
Lateral flow (mm)	41.59	41.54	40.71
Percolation (mm)	233.10	232.13	232.13
Unconfined aquifer recharge (mm)	221.45	228.41	231.22
Confined aquifer recharge (mm)	11.65	12.02	12.17
Baseflow (mm)	210.30	217.24	220.22
Transmission losses (mm)	0.75	9.01	8.72
ET (mm)	601.40	601.90	601.90
PET (mm)	1311.30	1314.50	1314.50
NO_3 leached (kg/ha)	8.79	8.95	8.95
NO_3 baseflow (kg/ha)	7.41	7.44	7.75
Pond evaporation (mm)	0.00	0.01	0.00
Pond inflow water (mm)	0.00	7.90	0.00
Pond seepage (mm)	0.00	7.90	0.00
Pond outflow water (mm)	0.00	0.00	0.00

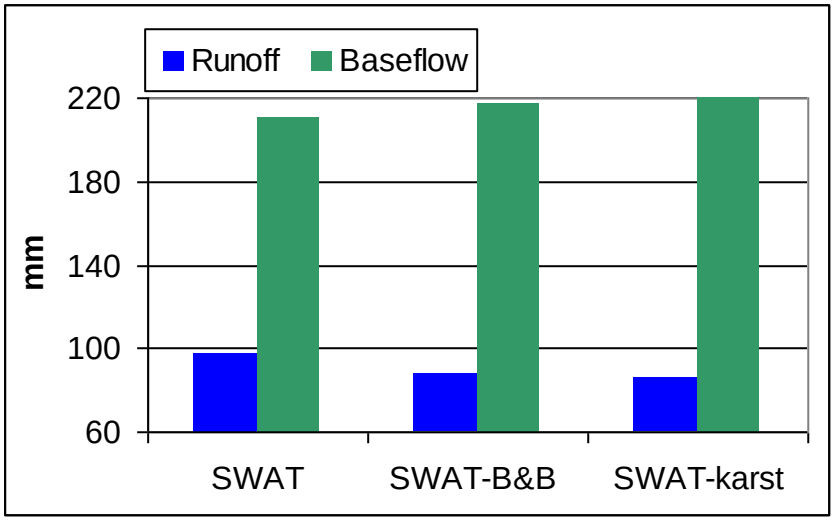

Figure 36. Average annual runoff and baseflow calculations from the Opequon Creek watershed.

The annual HRU output allowed evaluating how the models represent the HRU hydrology and nutrient transport related to a particular landuse (Table 13). In SWAT-karst and SWAT-B&B,

baseflow is the major contributor of water to the streams for all landuses, except in urban areas. SWAT-karst emphasizes the role of baseflow in the watershed hydrology due to sinkhole representation (Figure 37). In SWAT, surface runoff is the major contributor of water to the stream in agricultural and urban areas. The results from all three models showed the major average nitrate annual load to the streams occurred in urban and agricultural areas followed by pasture and forest areas.

Table 13. HRU average annual runoff, baseflow and nitrate loading from different landuses in the Opequon Creekwatershed.

	Surface runoff (mm)			Baseflow (mm)			Nitrate loading to the stream (kg/ha)		
Landuse	SWAT	SWAT-B&B	SWAT-karst	SWAT	SWAT-B&B	SWAT-karst	SWAT	SWAT-B&B	SWAT-karst
Agriculture	130.0	128.6	119.3	118.2	135.5	141.9	6.7	6.6	6.8
Urban	326.9	324.9	320.4	74.3	112.2	113.8	1.2	1.1	1.2
Forest	69.5	68.6	64.1	275.4	281.3	285.1	0.4	0.4	0.4
Pasture	94.9	93.2	87.4	295.4	303.5	309.0	0.6	0.6	0.6

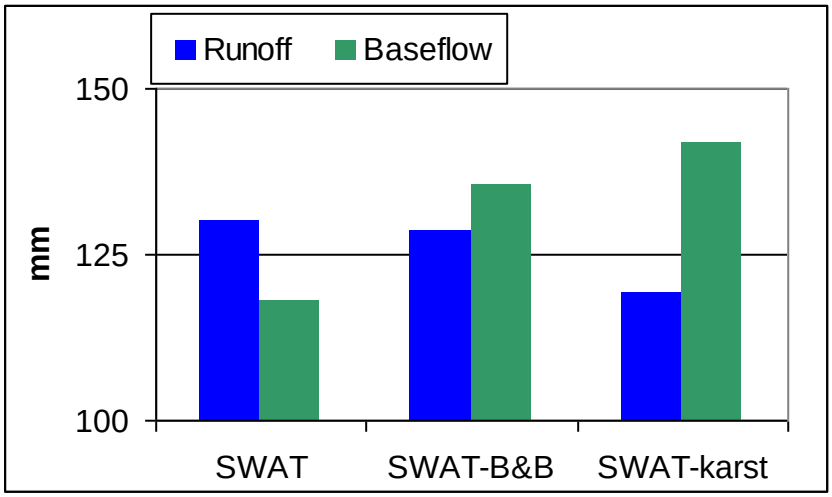

Figure 37. Average annual runoff and baseflow calculations from agricultural areas in the Opequon Creek watershed.

5.5.2 Daily output

5.5.2.1 Streamflow

Daily streamflow data are available for six USGS stations (Table 14). Figures 38 and 39 show a visual comparison of the daily observed and simulated streamflow at USGS 01615000 near

Berryville, VA and USGS 01616500 near Martinsburg, WV. The visual comparison shows that the three models overpredicted daily streamflow, however, the SWAT values for peak flows were higher than SWAT-karst and SWAT-B&B, for example May 2005 (Figure 40 A). The three models simulated flow values were closer to the observed values during lower flow periods, for example November 2004 (Figure 40 B).

Table 14. USGS stations with available daily flow data for the Opequon Creek watershed.

USGS station	Description	Daily discharge	
		Starting date	Ending date
01614830	Opequon Creek near Stephens City, VA	10/1/2006	3/31/2009
01615000	Opequon Creek near Berryville, VA	10/1/2002	6/18/2009
01616100	Dry Marsh Run near Berryville, VA	8/22/2002	6/18/2009
01616425	Hopewell Run At Leetown, WV	4/1/2003	3/31/2006
01616500	Opequon Creek near Martinsburg, WV	1/1/2001	3/31/2009
01617000	Tuscarora Creek above Martinsburg, WV	4/12/2006	9/30/2008

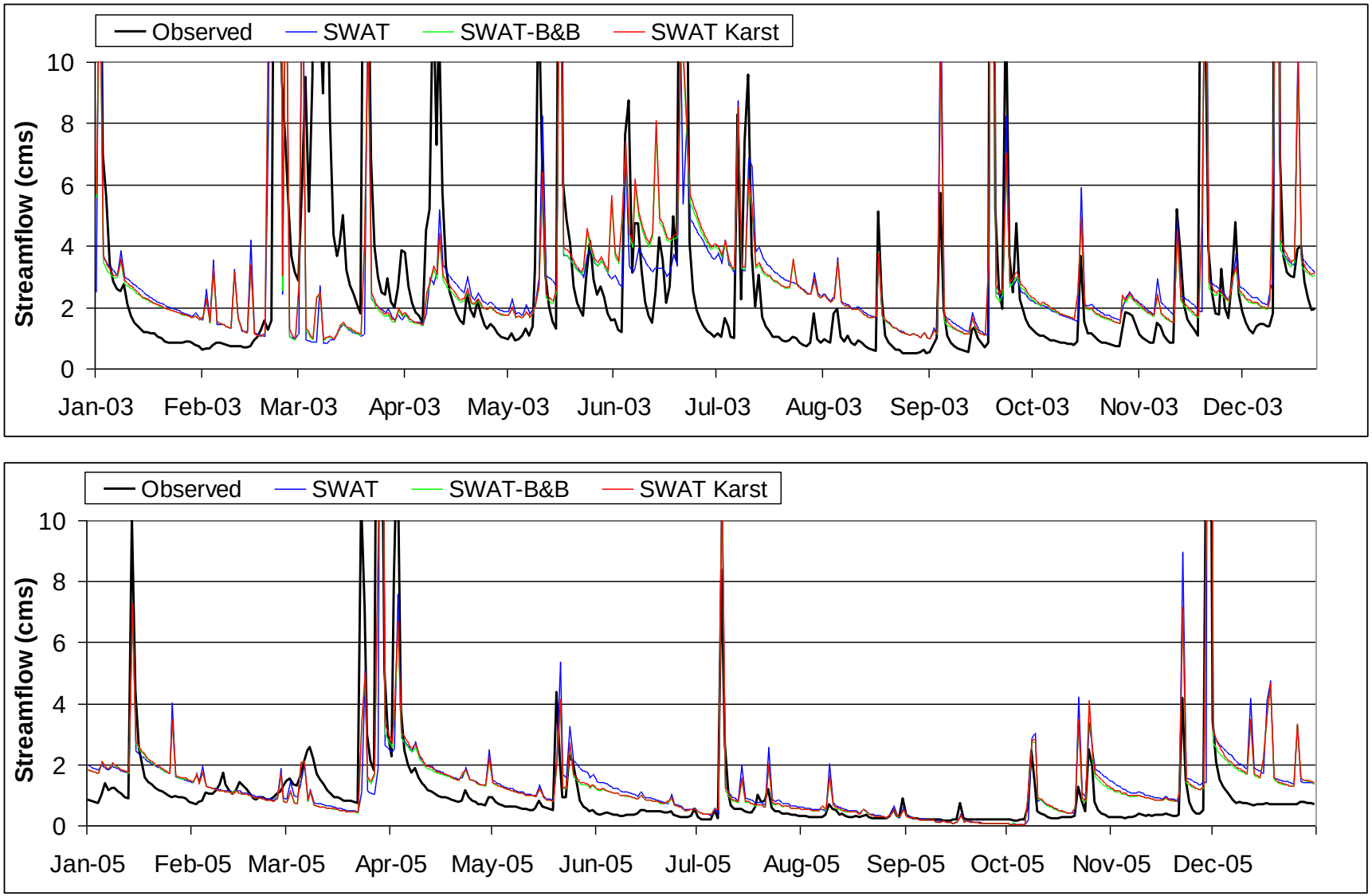

Figure 38. Observed and simulated daily streamflow for 2003 and 2006 in Opequon Creek near Berryville, VA (USGS 01615000).

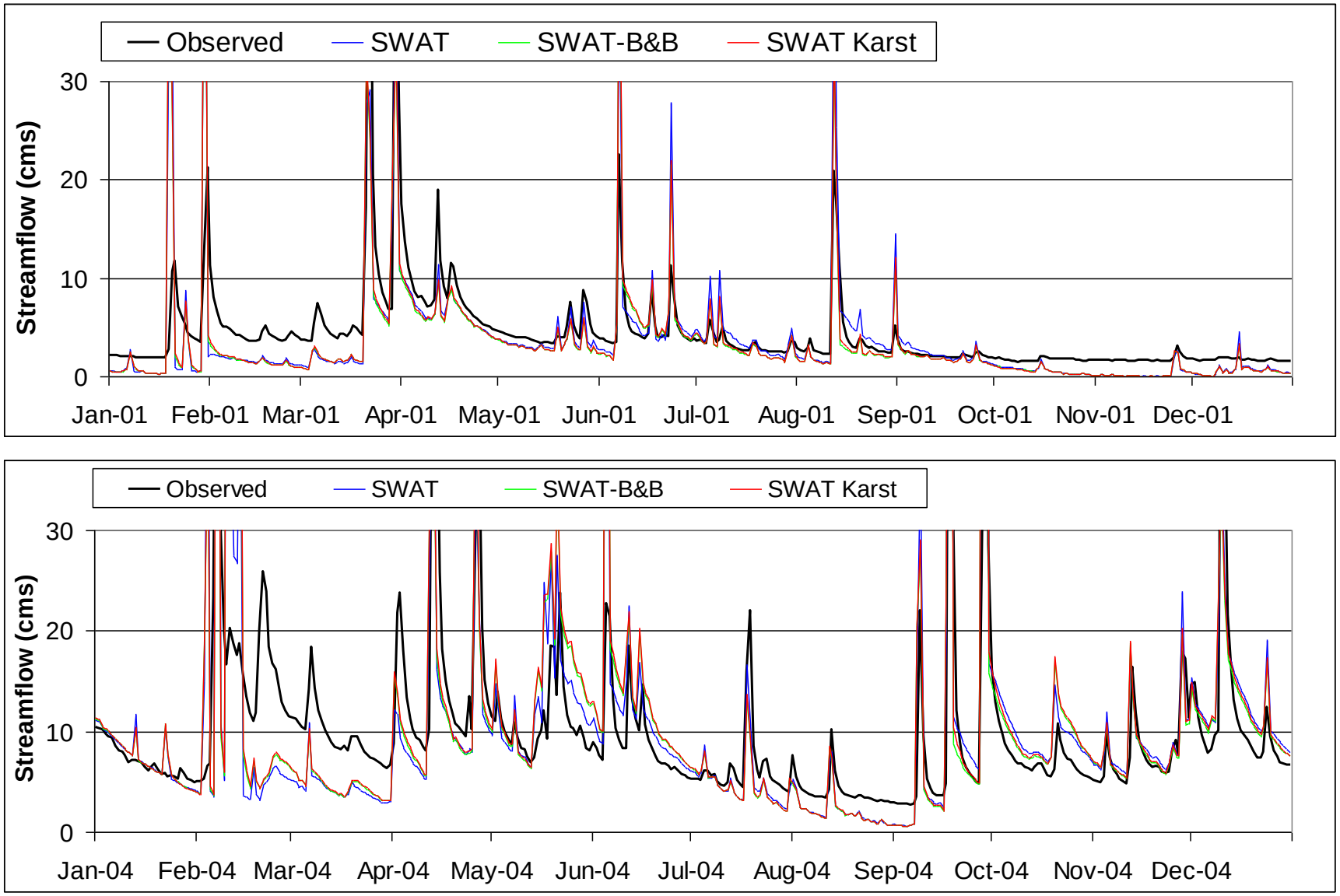

Figure 39. Observed and simulated daily streamflow for 2003 and 2006 in Opequon Creek near Martinsburg, WV (USGS 01616500).

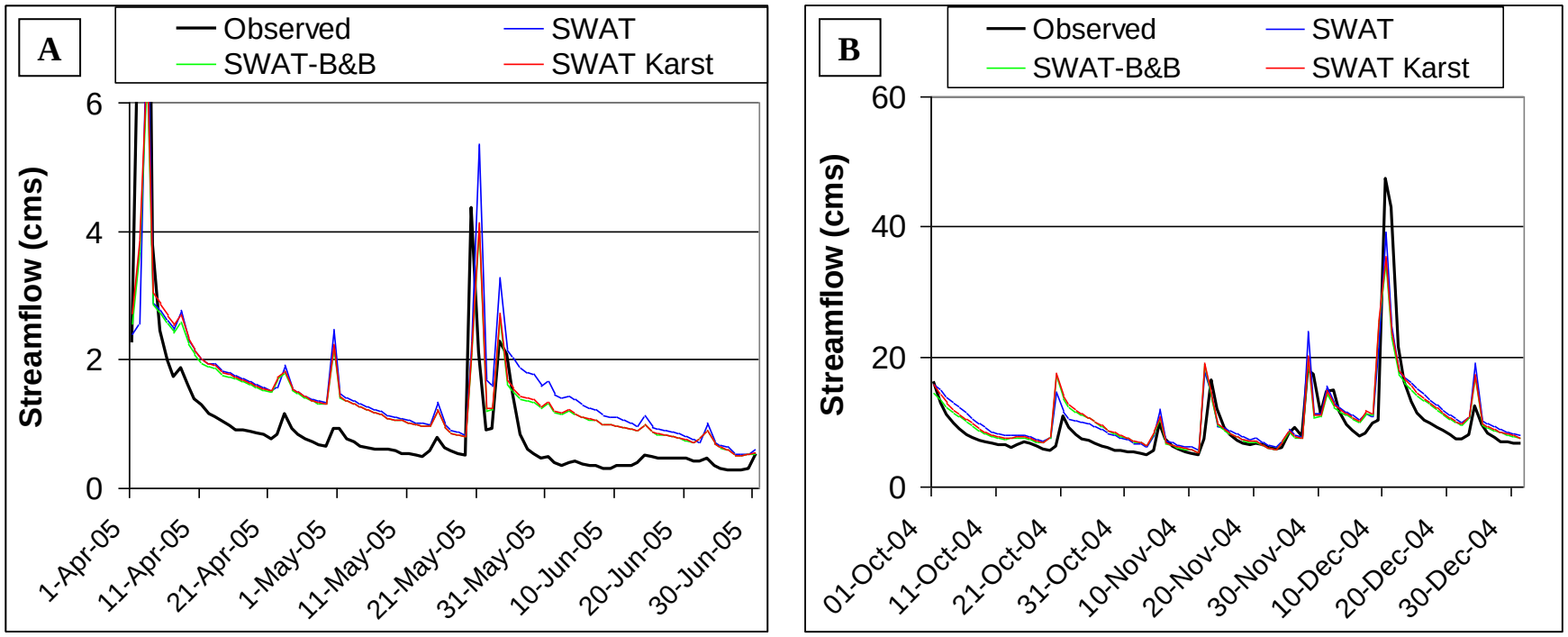

Figure 40. Observed and simulated lower flow periods and peak flows in Opequon Creek USGS 01615000 near Berryville, VA (A) and USGS 01616500 near Martinsburg, WV (B).

Moriasi et al. (2007) model evaluation guidelines were used to judge model performance of the three models on a daily time step, even though the recommendations are for monthly values. In general, the uncalibrated models performed unsatisfactorily (NSE<0.5) when simulating daily streamflow (Table 15). For all of the USGS stations, SWAT-karst and SWAT-B&B produced higher NSE values than SWAT. At USGS 01615000 near Berryville, VA, the models showed their best performance. For this station, SWAT-karst, SWAT-B&B, and SWAT obtained 0.37, 0.38, and 0.03 NSE values, respectively. For the rest of the stations, the NSE values were negative, meaning that the observed mean better predicted streamflow than the models did.

SWAT, SWAT-B&B, and SWAT-karst obtained negative PBIAS values at all subbasin outlets where the models were compared, specifically, the models overestimated streamflow. SWAT-karst and SWAT-B&B showed very good performance at USGS 1616425 Hopewell Run at Leetown, WV (PBIAS < ±10) and good performance (±10 < PBIAS < ±15) at USGS 1616500 Opequon Creek near Martinsburg, WV. At USGS 1616425 Hopewell Run at Leetown WV, SWAT showed very good performance. The three models obtained RSR values far from the optimal value of zero, indicating an unsatisfactory performance (RSR > 0.70). In the Opequon Creek watershed, the statistics showed that SWAT-karst and SWAT-B&B performed better than SWAT in predicting daily streamflow in a karst-influenced watershed.

It is unknown the amount of water that recharges the unconfined and confined aquifers in the watershed. Aquifer recharge from karst features can recharge other regions outside the watershed. This can be a reason why SWAT-karst is overestimating streamflow. The parameter *sink* can improve the model performance when simulating sinkholes. The parameter can be set to control the amount of water that recharges the unconfined and confined aquifers. For example, using *sink*=0.5, half of the water would recharge the unconfined aquifer and half would recharge an aquifer outside the watershed. The same concept can be applied for sinking streams using the deep aquifer percolation fraction parameter that controls the aquifer recharge into the unconfined aquifer recharge which contributes return flow to streams within the watershed, and confined aquifer recharge which contributes return flow to streams outside the watershed. In SWAT-karst, the new parameter *sink* can help to represent the process of losing water from the watershed and recharge an aquifer outside the watershed.

It is important to indicate that SWAT and SWAT-karst models obtained the same statistical values for 01617000 USGS station (Table 15). The reason is that no karst features were simulated in the subbasin that contributes water to the stream at that station. The statistics show that the model modifications apply only to karst conditions.

Table 15. Model evaluation statistics for daily streamflow for the Opequon Creek Watershed.

USGS Station		SWAT			SWAT-B&B			SWAT-karst		
		NSE	PBIAS	RSR	NSE	PBIAS	RSR	NSE	PBIAS	RSR
1614830	Opequon Creek near Stephens city, VA	-51.49	-247.13	7.25	-33.55	-237.94	5.88	-34.81	-242.86	5.98
1615000	Opequon Creek near Berryville, VA	0.03	-34.01	0.98	0.38	-30.47	0.79	0.37	-33.50	0.80
1616100	Dry Marsh Run near Berryville, VA	-4.07	-34.23	2.25	-2.69	-29.72	1.92	-2.63	-29.69	1.91
1616425	Hopewell Run at Leetown, WV	-4.59	-2.39	2.36	-3.97	-0.07	2.23	-4.09	-2.08	2.26
1616500	Opequon Creek near Martinsburg, WV	-0.04	-16.36	1.02	-0.02	-12.69	1.01	-0.04	-15.17	1.02
1617000	Tuscarora Creek above Martinsburg, WV	-1.22	-38.51	1.49	-1.22	-38.52	1.49	-1.22	-38.52	1.49

5.5.2.2 Nitrogen

Nitrate concentration data are available for three USGS stations (Table 16). The Opequon Targeted Watershed (OTW) project has 45 sample sites, and bi-weekly water quality data with regard to nitrogen (NO_3, NH_4) are available since May 2006. Figures 41, 42, and 43 show a visual comparison of the observed and simulated nitrate concentrations at USGS 01614830 near Stephens City, VA, USGS 01615000 near Berryville, VA, and USGS 01616500 near Martinsburg, WV. All the three models underestimated nitrate concentrations.

Table 16. USGS stations with available nitrate concentrations measurements for the Opequon Creek watershed.

USGS station	Description	Nitrate concentrations	
		Starting date	Ending date
01614830	Opequon Creek near Stephens city, VA	9/21/2006	12/10/2008
01615000	Opequon Creek near Berryville, VA	11/16/2006	12/10/2008
01616500	Opequon Creek near Martinsburg, WV	6/9/2005	6/17/2009

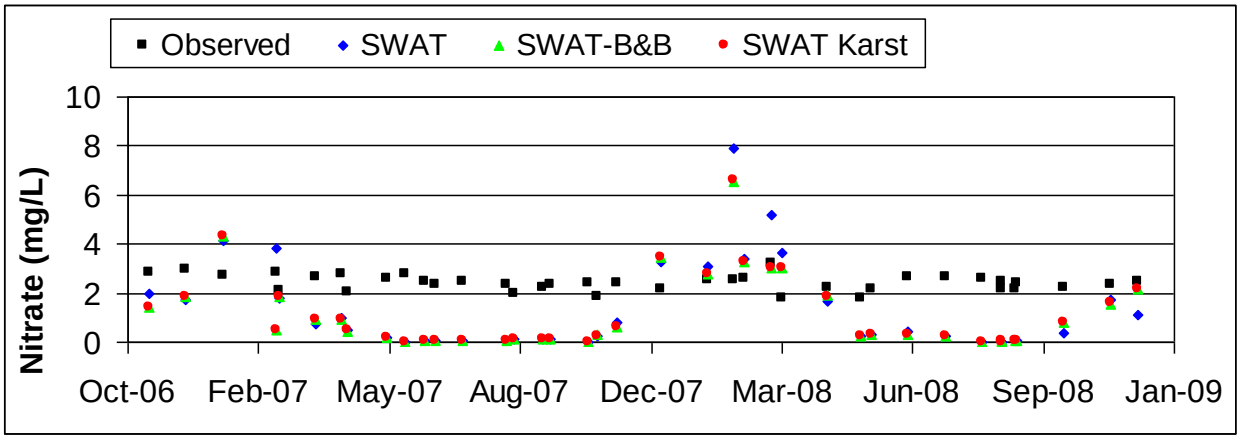

Figure 41. Observed and simulated daily nitrate concentrations in Opequon Creek near Stephens City, VA (USGS 01614830).

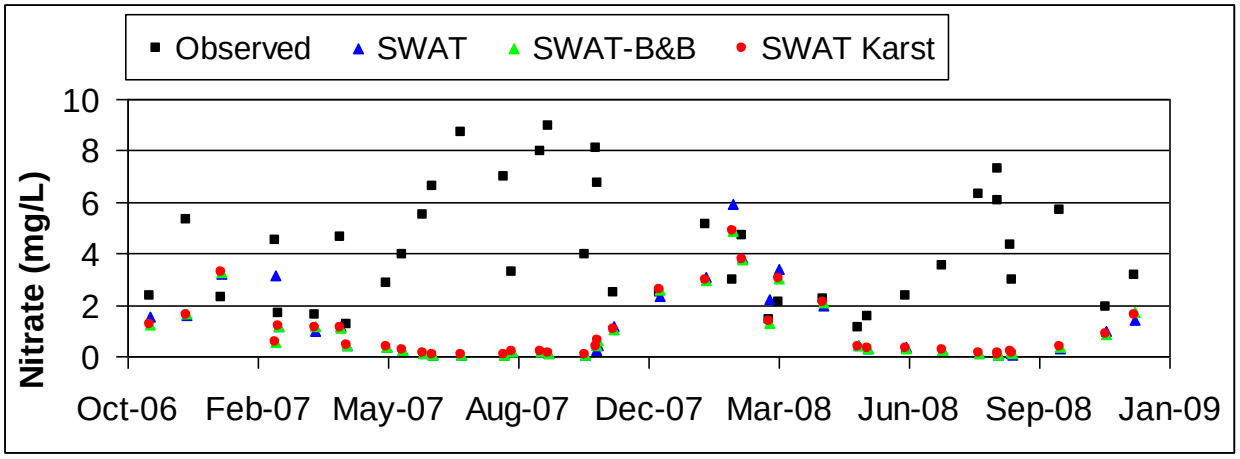

Figure 42. Observed and simulated daily nitrate concentrations in Opequon Creek near Berryville, VA (USGS 01615000).

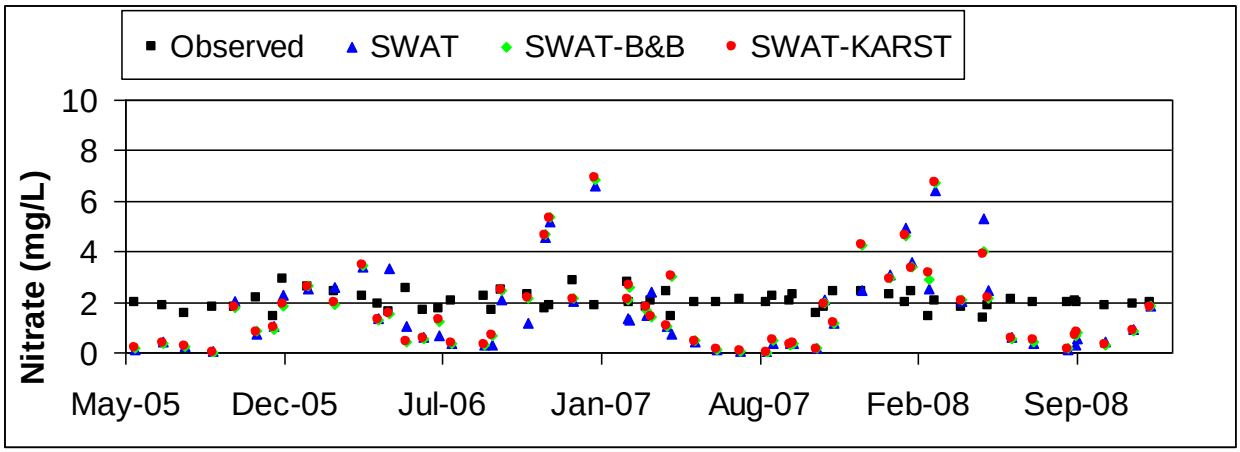

Figure 43. Observed and simulated daily nitrate concentrations in Opequon Creek near Martinsburg, WV (USGS 01616500).

The uncalibrated models performed unsatisfactorily (NSE<0.5) when simulating nitrate concentrations in the stream (Table 17). According to the PBIAS statistics results, the three models underestimated nitrate concentrations at all subbasin outlets where the models were compared (Table 16). SWAT and SWAT-karst models had RSR values far from the optimal value of zero, indicating an unsatisfactory performance. SWAT-karst and SWAT-B&B showed very good performance at USGS 1616500 Opequon Creek near Martinsburg, WV (PBIAS< ±25). At USGS 1616425 Hopewell Run at Leetown WV, SWAT showed very good performance. The three models obtained RSR values far from the optimal value of zero, indicating an unsatisfactory performance (RSR > 0.70).

Table 17. Model evaluation statistics for nitrate concentrations for the Opequon Creek Watershed.

USGS Station		SWAT			SWAT B&B			SWAT-karst		
		NSE	PBIAS	RSR	NSE	PBIAS	RSR	NSE	PBIAS	RSR
1614830	Opequon Creek near Stephens city, VA	-41.10	46.78	6.49	-37.13	53.67	6.17	-37.32	53.63	6.19
1615000	Opequon Creek near Berryville, VA	-2.64	73.64	1.91	-2.66	76.29	1.91	-2.66	76.43	1.91
1616500	Opequon Creek near Martinsburg, WV	-24.30	13.50	5.03	-23.92	10.70	4.99	-23.84	10.71	4.98

5.5.3 Karst features representation

5.5.3.1 Sinking stream subbasin

Subbasin 20 (Figure 34), located near Martinsburg, WV, is a subbasin characterized by sinking streams. The subbasin output was used to evaluate the model response when simulating sinking stream regions. For a period of 11 years, SWAT-karst simulated 28% less cumulative runoff than SWAT from January 1999 to March 2009 (Figure 44). SWAT-B&B simulated 25% less cumulative runoff than SWAT from January 1999 to March 2009 (Figure 44).

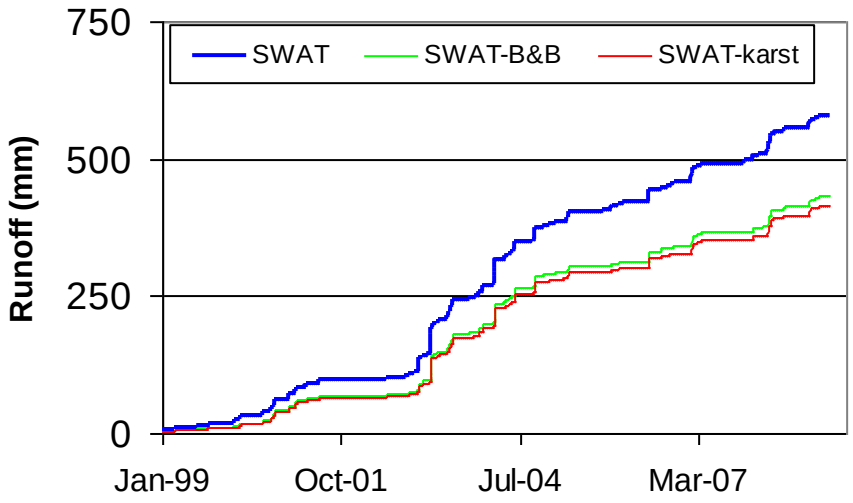

Figure 44. Cumulative runoff in a sinking stream subbasin near Martinsburg, WV.

In a sinking stream subbasin, SWAT-karst simulated 41% less cumulative nitrate transported with runoff than SWAT and SWAT-B&B (Figure 45). The results show the new capabilities of the SWAT-karst model to simulate nitrate transported with transmission losses. Nitrate losses from sinking streams are subtracted from nitrate transported with surface runoff (Figure 45)

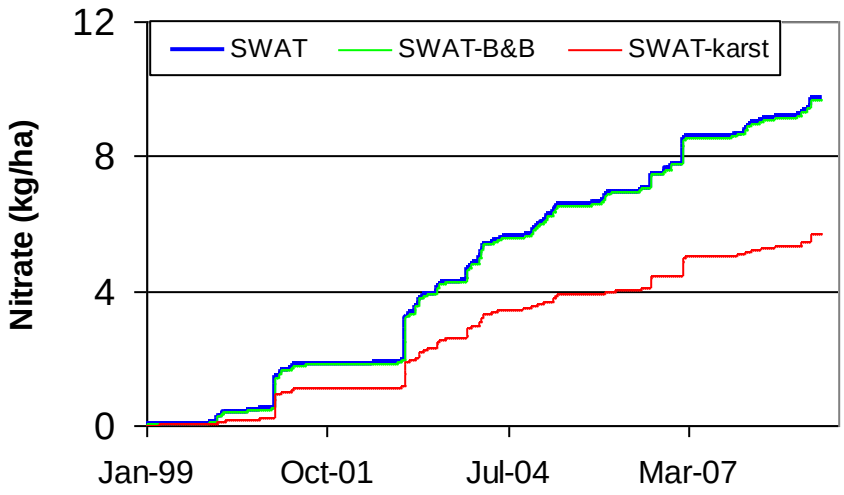

Figure 45. Cumulative nitrate transported with runoff in a sinking stream subbasin near Martinsburg, WV.

In a sinking stream subbasin, SWAT-karst simulated 9% more cumulative baseflow than SWAT and SWAT-B&B predicted 8% more cumulative baseflow than SWAT (Figure 46). SWAT-karst predicted 9% more cumulative nitrate loading transported with baseflow than SWAT and SWAT-B&B predicted 2% more cumulative nitrate transported with baseflow than SWAT (Figure 47). In a sinking stream subbasin, only SWAT-karst represented the nitrate transported from sinking streams (Figure 46).

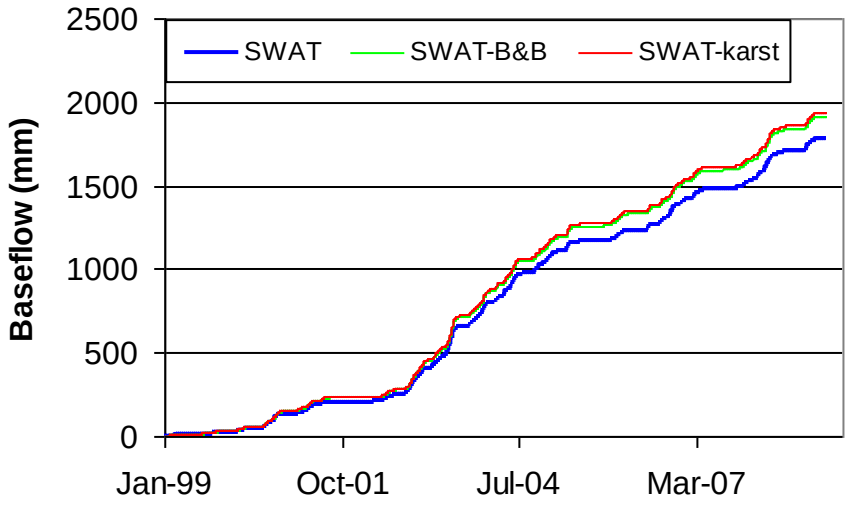

Figure 46. Cumulative baseflow in a sinking stream subbasin near Martinsburg, WV

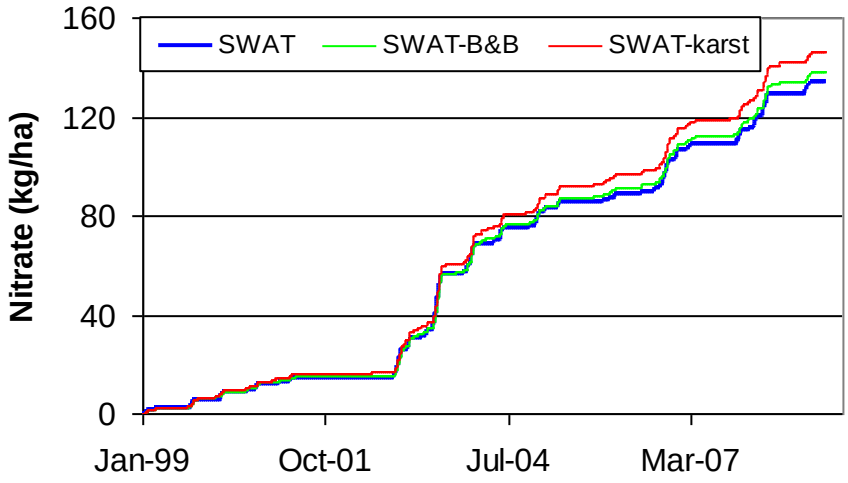

Figure 47. Cumulative nitrate transported with baseflow in a sinking stream subbasin near Martinsburg, WV.

5.5.3.2 Sinkholes

Subbasin 15 (Figure 30) is characterized by sinkholes. Sinkhole regions represent 8% of the total area of this subbasin. The subbasin output was used to evaluate the model response when simulating sinkholes as HRUs in a subbasin. SWAT-karst simulated 10% less runoff than SWAT in a subbasin characterized by sinkhole regions (Figure 48). SWAT-B&B simulated the same cumulative runoff as SWAT from January 1999 to March 2009 (Figure 48).

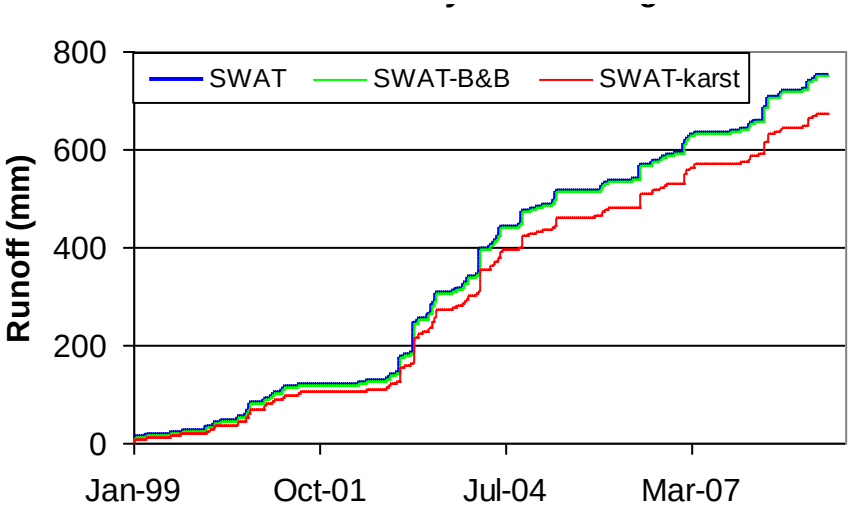

Figure 48. Cumulative runoff in a subbasin characterized by sinkholes.

In a subbasin characterized by sinkholes, SWAT-karst calculated 15% less nitrate transported with runoff than SWAT (Figure 49). SWAT-B&B, using ponds to simulate sinkholes, calculated 8% less nitrate transported with runoff than SWAT from January 1999 to March 2009 (Figure 49).

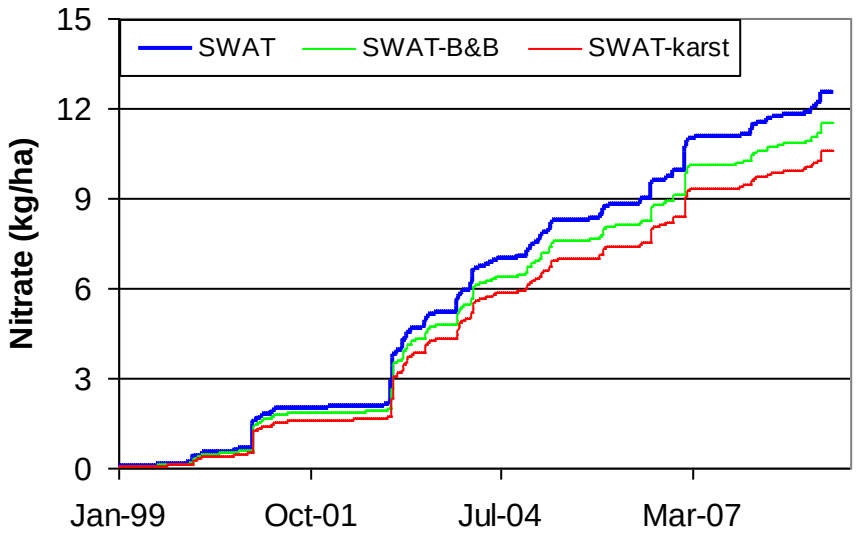

Figure 49. Cumulative nitrate transported with runoff in a subbasin characterized by sinkholes.

SWAT-karst simulated 5% more cumulative baseflow than SWAT in a subbasin characterized by sinkhole regions (Figure 50). SWAT-B&B simulated the same cumulative baseflow as SWAT in a subbasin characterized by sinkhole regions (Figure 50).

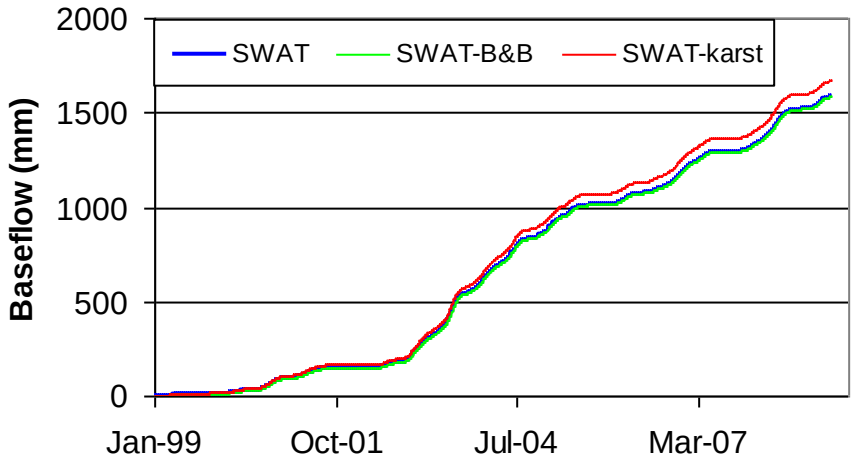

Figure 50. Cumulative baseflow in a subbasin characterized by sinkholes.

SWAT-karst calculated 3% more cumulative nitrate transported with baseflow than SWAT. SWAT-karst includes the nitrate that sinks into a sinkhole in the calculations of nitrate transported with baseflow (Figure 51). SWAT-B&B calculated 8% less cumulative nitrate transported with baseflow than SWAT. Using SWAT-B&B, the annual nitrate loading transported with baseflow decreased because nitrogen that is transported to a pond is not brought to the aquifer when water seeps through the bottom of the pond (Figure 51).

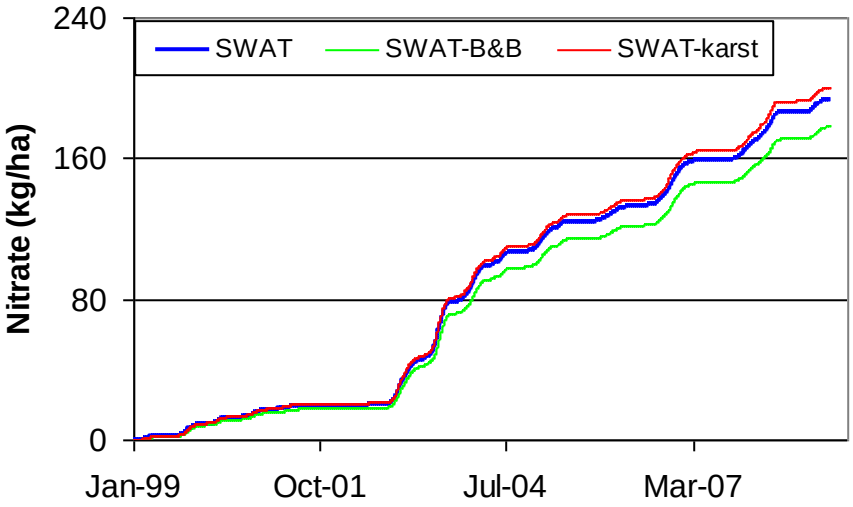

Figure 51. Cumulative nitrate transported with baseflow in a subbasin characterized by sinkholes.

5.6 Sensitivity analysis

The sensitivity of a model represents the change in a model output due to a change in the model input parameters. Sensitivity analysis results aid during model calibration providing valuable information when adjusting parameters is necessary. An analysis was conducted to determine SWAT-karst sensitivity to the key parameters used to represent karst features. The output variables of interest are runoff, baseflow, nitrate transported with runoff, nitrate transported with baseflow, streamflow and nitrate transported with streamflow. The parameters analyzed were channel effective hydraulic conductivity (sinking streams) and "*sink*" (sinkholes). A description of the parameters used for the sensitivity analysis is presented in table 18.

Table 18. Description of parameters of interest.

Parameter	Description	Range	Default
CH_K	Channel hydraulic conductivity (mm/hr)		0.5
Sink	Sinkhole partitioning coefficient	0-1	1

The baseline was defined using the parameters used in SWAT-karst. Changes in SWAT input parameters are presented in Table 19. The spatial unit selected for the sensitivity analysis was the hydrologic response unit (HRU). The HRU output was used because it is the smallest SWAT calculation unit, and HRU outputs are used to calculate the subbasin and watershed outputs. Two subbasins located in Opequon Creek watershed were used for the analysis. A single HRU was simulated in each subbasin. A sinking stream and a sinkhole were simulated in the two subbasins individually. The sensitivity analysis scenarios were defined based on karst feature representation.

Table 19. Baseline values and percentage of parameter change.

Variables	Range	Baseline	Parameter values				
CH_K (mm/hr)		0.5	10	100	200	500	1000
Sink	0-1	1	0.001	0.2	0.4	0.6	0.8

Sensitivity was calculated using the relative sensitivity (S_r). The greater the S_r, the more sensitive the model is to that particular parameter.

$$S_r = \frac{(O - O_b)P_b}{(P - P_b)O_b} \quad \textbf{[38]}$$

Where S_r is the relative sensitivity, O is the model output variable of interest, P is the parameter value, and b subscript represents the parameter values and output of the base scenario. Relative sensitivity scale developed by Storm et al. (1986) is used and described in table 20.

Table 20. Relative sensitivity scale developed by Storm et al. (1986).

Scale	Relative sensitivity (S_r)
Insensitive	Sr < |0.01|
Slightly sensitive	|0.01| <= Sr < |0.1|
Moderately sensitive	|0.1| <= Sr < |1|
Sensitive	|1| <= Sr< |2|
Extremely sensitive	Sr >= |2|

5.6.1 Sensitivity analysis results

The results of the sensitivity analysis with respect to the parameter *sink* for sinkholes are shown in Table 21. SWAT-karst predictions of baseflow and streamflow were moderately sensitive to the new parameter *sink*. The SWAT-karst model predictions of nitrate transported with baseflow and streamflow were slightly sensitive to the parameter *sink*.

Table 21. Relative sensitivity of the SWAT-karst model to the value of *sink*.

Sinkhole HRU	Parameter base	Output base	Value of *sink*	Output	Relative sensitivity	Scale
Streamflow (m^3)	1	0.4494	0.001	0.3766	0.16	Moderately sensitive
	1	0.4494	0.2	0.3911	0.16	Moderately sensitive
	1	0.4494	0.4	0.4056	0.16	Moderately sensitive
	1	0.4494	0.6	0.4202	0.16	Moderately sensitive
	1	0.4494	0.8	0.4348	0.16	Moderately sensitive
Nitrate transported with water out of reach kg/ha	1	31760	0.001	30480	0.04	Slightly sensitive
	1	31760	0.2	30780	0.04	Slightly sensitive
	1	31760	0.4	31030	0.04	Slightly sensitive
	1	31760	0.6	31340	0.03	Slightly sensitive
	1	31760	0.8	31540	0.03	Slightly sensitive
Baseflow	1	339.964	0.001	223.505	0.34	Moderately sensitive
	1	339.964	0.2	246.654	0.34	Moderately sensitive
	1	339.964	0.4	269.985	0.34	Moderately sensitive
	1	339.964	0.6	293.314	0.34	Moderately sensitive
	1	339.964	0.8	316.646	0.34	Moderately sensitive
NO_3 baseflow (kg/ha)	1	8.152	0.001	7.482	0.08	Slightly sensitive
	1	8.152	0.2	7.635	0.08	Slightly sensitive
	1	8.152	0.4	7.769	0.08	Slightly sensitive
	1	8.152	0.6	7.928	0.07	Slightly sensitive
	1	8.152	0.8	8.036	0.07	Slightly sensitive

The results of the sensitivity analysis of the SWAT-karst model with respect to hydraulic conductivity for sinking streams are shown in Table 22. SWAT-karst predictions of runoff, baseflow, streamflow, and nitrate transported with runoff, baseflow, and streamflow were insensitive to the hydraulic conductivity parameter.

Table 22. Relative sensitivity of the SWAT-karst model to the value of channel hydraulic conductivity.

Sinking streams Subbasin	Parameter base	Output base	Value of hydraulic conductivity	Output	Relative sensitivity	Scale
Streamflow (cms)	0.5	0.4534	10	0.4531	-0.000035	Insensitive
	0.5	0.4534	100	0.4521	-0.000014	Insensitive
	0.5	0.4534	200	0.4517	-0.000009	Insensitive
	0.5	0.4534	500	0.4514	-0.000004	Insensitive
	0.5	0.4534	1000	0.4512	-0.000002	Insensitive
Nitrate transported with streamflow kg/ha	0.5	31610	10	31640	0.000050	Insensitive
	0.5	31610	100	31720	0.000017	Insensitive
	0.5	31610	200	31730	0.000010	Insensitive
	0.5	31610	500	31740	0.000004	Insensitive
	0.5	31610	1000	31740	0.000002	Insensitive
Runoff	0.5	72.759	10	63.889	-0.006416	Insensitive
	0.5	72.759	100	36.415	-0.002510	Insensitive
	0.5	72.759	200	25.373	-0.001632	Insensitive
	0.5	72.759	500	13.649	-0.000813	Insensitive
	0.5	72.759	1000	6.039	-0.000459	Insensitive
Baseflow	0.5	224.233	10	232.604	0.001965	Insensitive
	0.5	224.233	100	258.557	0.000769	Insensitive
	0.5	224.233	200	269.037	0.000501	Insensitive
	0.5	224.233	500	280.171	0.000250	Insensitive
	0.5	224.233	1000	287.399	0.000141	Insensitive
NO_3 runoff (kg/ha)	0.5	0.243	10	0.206	-0.008014	Insensitive
	0.5	0.243	100	0.115	-0.002647	Insensitive
	0.5	0.243	200	0.084	-0.001640	Insensitive
	0.5	0.243	500	0.055	-0.000774	Insensitive
	0.5	0.243	1000	0.038	-0.000422	Insensitive
NO_3 baseflow (kg/ha)	0.5	7.487	10	7.54	0.000373	Insensitive
	0.5	7.487	100	7.674	0.000126	Insensitive
	0.5	7.487	200	7.708	0.000074	Insensitive
	0.5	7.487	500	7.74	0.000034	Insensitive
	0.5	7.487	1000	7.759	0.000018	Insensitive

SWAT-karst predictions of baseflow, nitrate transported with baseflow, and nitrate transported with streamflow have a direct relationship to the new parameter *sink* when representing sinkholes. SWAT-karst predictions of runoff, baseflow, and nitrate transported with streamflow have an inverse relationship with the hydraulic conductivity parameter when representing sinking streams.

SWAT-karst model modifications were confirmed during the sensitivity analysis. As the *sink* parameter is increased, more baseflow and more streamflow are calculated. In all the model runs

when a sinkhole was simulated (*sink*>0), all surface runoff sank into a sinkhole. The parameter *sink* can be used to sink surface water into a sinkhole and either recharge the unconfined aquifer using bigger sink values (*sink*=1) or recharge the confined aquifer in a region outside the watershed using lower sink values (*sink*=0.001).

Chapter 6: Summary and Conclusions

The first objective of the thesis research was to determine the appropriateness of existing models for simulating hydrologic processes and quantifying nitrogen concentrations in surface and ground water in a karst-influenced watershed. The second objective was to modify an existing model to simulate the hydrologic processes that drive nitrogen transport and to quantify nitrate concentrations in a karst basin. The final objective was to determine the major hydrologic contributor of nitrate to the stream in the Opequon Creek watershed.

Several existing watershed-scale models were evaluated to determine their appropriateness for use in a karst basin. The SWAT model was found to be appropriate to be modified and used in a karst basin due to its strength in simulating the hydrology and nutrient transport of a watershed compared to the other models.

The SWAT model was modified to simulate hydrologic processes and nitrogen transport in karst environments. The new SWAT-karst version includes two new parameters to simulate water and nitrate transport in karst features. The SWAT-karst model, using the new parameter *sink,* allows simulating the hydrology and nitrate transport in a sinkhole capturing its unique landuse and soil characteristics. Furthermore, in SWAT-karst, nitrate is transported with water that is lost from sinking streams using the new parameter *ss.*

Conceptually, SWAT-karst is an improvement and enables a better representation of water transport through sinkholes than SWAT and SWAT-B&B. In the Opequon Creek watershed, SWAT-karst using the HRU to represent sinkholes had a more notable impact in the watershed hydrology than SWAT-B&B using a pond to represent sinkholes. The difference might be related to SWAT-karst detailed representation of a sinkhole using an HRU over SWAT-B&B using an average representation of a sinkhole using a pond.

In the Opequon Creek watershed, model simulation statistics showed that SWAT-karst and SWAT-B&B performed better than SWAT in predicting streamflow in a karst-influenced watershed. Although SWAT-karst showed almost the same performance as SWAT-B&B, SWAT-karst model offers the flexibility to represent the unique relationship between surface and

ground water in karst features in an HRU. SWAT-karst uses an HRU to represent sinkholes thus can depict the associated variability of a karst landscape.

The new variables *sink* and *ss* provide a new and appropriate mechanism to represent the nutrient transport through sinkholes and sinking streams. The sensitivity analysis showed that SWAT-karst was moderately sensitive to the new parameter *sink.* The new parameter *sink* can be used for model calibration and to represent the water recharge and nutrient transport to aquifers outside the watershed boundary.

Although the model was not calibrated, in the Opequon Creek watershed, results of simulations from all three models show that baseflow from forest and pasture areas were identified as the major contributor of water to the streams. Agriculture and urban areas are the major landuse contributors of nitrate to the streams. Base on the simulations, the major hydrologic contributor of nitrate in the Opequon Creek watershed is baseflow.

The SWAT-karst model should be calibrated for the Opequon Creek watershed in order to provide more accurate results so that the code can be used as a research and decision-making tool. The SWAT-karst model should also be applied to a karst-influenced watershed where extensive field measurements specifically for karst features are available to evaluate the model. Also, further research is needed to evaluate other SWAT parameters, deep aquifer percolation and the baseflow threshold parameter, that can affect baseflow calculations in a karst-influenced watershed.

Chapter 7: References

1. Afinowicz, J., C. Munster, and P. Wilcox. 2005. Modeling effects of brush management on the rangeland water budget: Edwards Plateau, Texas. *JAWRA.* 41(1):181-193.
2. Arnold, J., M. Di Luzio, C. Green, and A. Saleh. 2005. AVSWAT - X short tutorial. Available at: http://www.brc.tamus.edu/swat/downloads/doc/swat2005/tutorial/Tutorial.pdf . Accessed 28 May 2009.
3. Bacchus, S. T. 2006. Nonmechanical dewatering of the regional floridan aquifer system. In *Perspectives on Karst Geomorphology, Hydrology, and Geochemistry – A Tribute Volume to Derek C. Ford and William B. White*. Boulder, Colorado: The Geological Society of America.
4. Baffaut, C. 2004. Upper Shoal Creek watershed water quality analysis. FAPRI-UMC Report 01-04.Columbia, MI: Food and Agricultural Policy Research Institute. Available at: http://www.fapri.missouri.edu/outreach/publications/2004/FAPRI_UMC_Report_01_04.pdf. Accessed 31 August 2008.
5. Baffaut, C. and V. Benson. 2008. Possibilities and challenges for modeling flow and pollutant transport in a karst watershed with SWAT. Paper No. 083933. St. Joseph, Mich.: *ASABE*.
6. Benham, B. L., C. Baffaut, R. W. Zeckoski, K. R. Mankin, Y. A.Pachepsky, A. M. Sadeghi, K. M.Brannan, M. L. Soupir, and M. J. Habersack. 2006. Modeling bacteria fate and transport in watersheds to support TMDLs. *Trans. ASABE* 49(4): 987−1002.
7. Bicknell, B.R., J.C. Imhoff, J.L. Kittle, A.S. Donigian, and R.C. Johanson. 1997. Hydrological Simulation Program - FORTRAN, user's manual for version 11: U.S. Environmental Protection Agency, National Exposure Research Laboratory. Available at: http://water.usgs.gov/software/HSPF/ Accessed 21 September 2008.
8. Borah, D. K., G. Yagow, A. Saleh, P. L. Barnes, W. Rosenthal, E. C. Krug, and L. M. Hauck. 2006. Sediment and nutrient modeling for TMDL development and implementation. *Trans. ASABE* 49(4): 967−986.

9. Bouraoui, F. and B. Grizzetti. 2007. An Integrated Modelling Framework to Estimate the Fate of Nutrients: Application to the Loire (France). *Ecological Modelling* 212 (2008) 450–459.
10. Cho, J. P. 2007. A comprehensive modeling approach for BMP impact assessment considering surface and ground water interaction. PhD diss. Blacksburg, VA. Virginia Polytechnic Institute and State University, Department of Biological Systems Engineering.
11. Coffey M. E., S. R. Workman, J. L. Taraba, and A. W. Fogle. 2004. Statistical procedures for evaluating daily and monthly hydrologic model predictions. *Trans. ASAE* 47(1): 59-68.
12. Evaldi, R. D. and K. S. Paybins. 2006. Channel Gains and Losses in the Opequon Creek Watershed of West Virginia, July 25–28, 2005. http://pubs.usgs.gov/ds/ds179/pdf/ds179.pdf
13. Fleury, P., Plagnes, V. and M. Bakalowicz. 2007. Modelling of the functioning of karst aquifers with a reservoir model: Application to Fontaine de Vaucluse (South of France). *Journal of Hydrology* 345, 38– 49.
14. Galbiati, L., F. Bouraoui, F. J. Elorza, and G. Bidoglio. 2005. Modeling diffuse pollution loading into a Mediterranean lagoon: development and application of an integrated surface–subsurface model tool. *Ecological Modelling* 193 (2006) 4–18.
15. Gassman, P. W., M. R. Reyes, C. H. Green, and J. G. Arnold. 2007. The soil and water assessment tool: historical development, applications, and future research directions. Iowa: Center for Agricultural and Rural Development Iowa State University Ames. Available at: http://www.card.iastate.edu/publications/DBS/PDFFiles/07wp443.pdf. Accessed 31 August 2008.
16. Haith, D. A., R. Mandel, and R. S. Wu. 1992. Generalized watershed loading functions - Version 2.0 User's manual. Available at: http://www.avgwlf.psu.edu/Downloads/GWLFManual.pdf. Accessed 15 December 2008.
17. Haith, D. A. 2008. GWLF: Generalized watershed loading functions. Available at: http://www.epa.gov/nrmrl/pubs/600r05149/600r05149gwlf.pdf. Accessed 15 December 2008.

18. Harbaugh, A.W., E.R. Banta, M.C. Hill, and M.G. McDonald. 2000. MODFLOW-2000, the U.S. Geological Survey modular groundwater model - user guide to modularization concepts and the groundwater flow process: U.S. Geological Survey Open-File Report 00-92, 121 p. Available at: http://water.usgs.gov/nrp/gwsoftware/modflow2000/ofr00-92.pdf. Accessed 21 September 2008.
19. Harmon, R., and C. Wicks. 2006. *Perspectives on Karst Geomorphology, Hydrology, and Geochemistry – A Tribute Volume to Derek C. Ford and William B. White*. Boulder, Colorado: The Geological Society of America.
20. Heatwole, C. 2009. Personal communication.
21. Jones, W. 1997. *Karst Hydrology Atlas of West Virginia*. Charles Town, WV: Karst Water Institute , Inc.
22. Kresic, N. 2007. *Hydrogeology and Groundwater Modeling.* Boca Raton, Florida: Taylor and Francis Group.
23. Lawrence, J. 2009. Personal communication.
24. Liersch, S. 2003. The program pcpSTAT user's manual. Available at: http://www.brc.tamus.edu/swat/manual_pcpSTAT.pdf. Accessed 16 July 2009.
25. Manguerra, H. B., and B. A. Engel. 1998. Hydrologic parameterization of watersheds for runoff prediction using SWAT. *JAWRA* 34(5): 1149-1162.
26. Migliaccio, K. W., and P. Srivastava. 2007. Hydrologic components of watershed-scale models. *Trans. ASABE* 50(5): 1695−1703.
27. Moriasi, D. N., J. G. Arnold, M. W.Van Liew, R. L. Bingner, R. D. Harmel, and T. L. Veith. 2007. Model evaluation guidelines for systematic quantification of accuracy in watershed simulations. *Trans. ASABE* 50(3): 885−900.
28. Neitsch, S.L., J.G. Arnold, J.R. Kiniry, and J.R. Williams. 2005. Soil and Water Assessment Tool Theoretical Documentation – Version 2005.
29. Neitsch, S.L., J.G. Arnold, J.R. Kiniry, R. Srinivasan, and J.R. Williams. 2005. Soil and Water Assessment Tool Input/Output File Documentation – Version 2005.
30. NOAA. 2009. NOAA Satellite and Information System. Available at http://noaasis.noaa.gov/NOAASIS. Accessed 11 July 2009.
31. Novotny, V. 2002. *Water Quality: Diffuse Pollution and Watershed Management.* 2nd ed. New York, N.Y.: John Wiley and Sons.

32. Opequon Team Project. 2008. Opequon Team Project. Available at: http://www.opequoncreek.org/. Accessed 23 September 2008.
33. Orndorff, R. C., and K.E. Goggin. 1994. Sinkholes and karst-related features of the Shenandoah Valley in the Winchester 30' X 60' quadrangle, Virginia and West Virginia. U.S.G.S. Available at: http://ngmdb.usgs.gov/Prodesc/proddesc_5881.htm. Accessed 28 May 2009.
34. Palmer, A. N. 2006. Digital modeling of karst aquifers – successes, failures, and promises. In *Perspectives on Karst Geomorphology, Hydrology, and Geochemistry – A Tribute Volume to Derek C. Ford and William B. White*. Boulder, Colorado: The Geological Society of America.
35. Peschel, J.M., P.K. Haan, and R.E. Lacey. 2003. A SSURGO pre-processing extension for the ArcView Soil and Water Assessment Tool. *ASAE* 032123.
36. Peschel, J.M. 2003. SSURGO SWAT 1.0 Installation & Instructions. Available at: http://lcluc.tamu.edu/ssurgo/instructions.pdf . Accessed 28 May 2009.
37. Saleh A., and B. Du. 2004. Evaluation of SWAT and HSPF within basins program for the upper North Bosque river watershed in central Texas. *Trans. ASABE* 47(4): 1039−1049.
38. Sangjun, I., K. M. Brannan, S. Mostaghimi, and S. M. Kim. 2007. Comparison of HSPF and SWAT models performance for runoff and sediment yield prediction. *Journal of Environmental Science and Health* 42**:** 1561–1570.
39. Sasowsky, I., and C. Wicks. 2000. *Ground water Flow and Contaminant Transport in Carbonate Aquifers*. Rotterdam, Netherlands: Balkema.
40. Singh, J. , H. V. Knapp, J.G. Arnold, and M. Demissie. 2005. Hydrological modeling of the Iroquois river watershed using HSPF and SWAT. *JAWRA* 41(2): 343-360.
41. Spruill, C., S. Workman, and J. Taraba. 2000. Simulation of daily and monthly stream discharge from small watersheds using the SWAT model. *Trans. ASAE* 43(6): 1431−1439.
42. Storm, D.E., T. A. Dillaha, and S. Mostaghimi. 1986. Modeling phosphorous transport in surface runoff. *Trans. ASAE* 31(1): 117-127.
43. Strager, M. 2009. Landuse map, Opequon Creek Watershed. Unpublished data. West Virginia University. Morgantown, WV.

44. Tzoraki, O., and N. P. Nikolaidis. 2007. A generalized framework for modeling the hydrologic and biogeochemical response of a mediterranean temporary river basin. *Journal of Hydrology* 346, 112– 121.
45. USDA-NRCS. 2009. Soil Survey Geographic (SSURGO) Database. Available at http://soils.usda.gov/survey/geography/. Accessed 4 June 2009.
46. USGS.1997. Modeling groundwater flow with MODFLOW and related programs. Available at: http://pubs.usgs.gov/fs/FS-121-97/fs-121-97.pdf . Accessed 1 November 2008.
47. USGS. 2002. Pesticides and nutrients in karst springs in the Green River Basin, Kentucky, May-September 2001. Available at: http://ky.water.usgs.gov/pubs/FAC_13301/pdf/FS-133-01.pdf. Accessed 31 August 2008.
48. USGS. 2008. Proposal for an Assessment of Water Resources in the Opequon Creek Watershed Using a Numerical Flow Model. Available at: http://va.water.usgs.gov/GreatValley/Proposal_Opequon_final.pdf. Accessed 23 September 2008.
49. USGS. 2009a. National Map Seamless Server. Available at http://seamless.usgs.gov/index.php. Accessed 13 July 2009.
50. USGS. 2009b. National Hydrography Dataset. Available at: http://nhd.usgs.gov/. Accessed 13 July 2009.
51. Walthman, T., F. Bell, and M. Culshaw. 2005. *Sinkholes and Subsidence – Karst and Cavernous Rocks in Engineering and Construction*. New York, N.Y.: Springer.
52. Ward, A. D. and S. W. Trimble. 2004. Environmental Hydrology. 2nd ed. Boca Raton, Fl.: Lewis Publishers.
53. Weight, W. 2008. Hydrogeology Field Manual. New York, N.Y.: Mc Graw Hill.
54. Westervelt, J. 2001. *Simulation Modeling for Watershed Management*. New York, N.Y.: Springer.
55. White, W. B. 2002. Karst hydrology: recent developments and open questions. *Engineering Geology* 65, 85- 105.
56. White, W. B. 1988. Geomorphology and Hydrology of Karst Terrains. New York, N.Y.: Oxford University Press.

57. Zheng, C., and P. P. Wang. 1999. MT3DMS a Modular Three - Dimensional Multispecies Transport Model. Available at: http://www.geology.wisc.edu/courses/g727/mt3dmanual.pdf. Accessed 15 December 2008.